

THESIS 2 3002

This is to certify that the

dissertation entitled

FEEDBACK STABILIZATION OF THE ROLLING SPHERE: AN INTRACTABLE NONHOLONOMIC SYSTEM

presented by

Tuhin Kumar Das

has been accepted towards fulfillment of the requirements for

Ph.D. degree in Mechanical Engineering

Date August 15, 2002

MSU is an Affirmative Action/Equal Opportunity Institution

0-12771

LIBRARY Michigan State University

PLACE IN RETURN BOX to remove this checkout from your record.

TO AVOID FINES return on or before date due.

MAY BE RECALLED with earlier due date if requested.

DATE DUE	DATE DUE	DATE DUE

6/01 c:/CIRC/DateDue.p65-p.15

FEEDBACK STABILIZATION OF THE ROLLING SPHERE: AN INTRACTABLE NONHOLONOMIC SYSTEM

By

Tuhin Kumar Das

A DISSERTATION

Submitted to

Michigan State University
in partial fulfillment of the requirements
for the degree of

DOCTOR OF PHILOSOPHY

Department of Mechanical Engineering

2002

ABSTRACT

FEEDBACK STABILIZATION OF THE ROLLING SPHERE: AN INTRACTABLE NONHOLONOMIC SYSTEM

By

Tuhin Kumar Das

A spherical rolling robot has several advantages over wheeled robots, such as enhanced mobility, orientational stability, compact and closed design, and capability of operations in hazardous environments. However, advances in the design and application of spherical mobile robots have been hindered due to complexity of their control problems. Of particular interest is the problem of feedback stabilization of a rolling sphere to an equilibrium configuration. The rolling sphere belongs to the class of nonholonomic systems which has been a popular area of research in the control systems community over the last decade. Although nonholonomic systems are usually controllable, they are not stabilizable to an equilibrium point using smooth static state feedback. This problem has been circumvented by development of techniques such as time-varying stabilization, discontinuous time-invariant stabilization, and hybrid stabilization. Nonetheless, the stabilization of a rolling sphere has remained an unsolved problem since its kinematic model cannot be reduced to the chained form; this renders all established nonholonomic motion planning and control algorithms inapplicable.

In this dissertation we present a feedback control law for stabilization of a rolling sphere to an equilibrium configuration. This control law, which to the best of our knowledge, is the first solution to the problem, stabilizes the sphere about an equilibrium point defined by the two Cartesian coordinates and three orientation coordinates of the sphere. In our formulation, the control inputs are two mutually perpendicular angular speeds in the moving reference frame of the sphere. These control actions individually cause the sphere to move in straight line and circular arc segments. Using an alternating sequence of these rudimentary maneuvers we achieve stabilization of the equilibrium configuration. We first develop an algorithm for partial reconfiguration of the sphere where evolution of one of the orientation coordinates is ignored. This algorithm, which we denote by the Sweep-Tuck algorithm, allows multiple solution trajectories of the sphere. We utilize this flexibility in achieving complete reconfiguration. In our discussion we first show the convergence of the configuration variables to the equilibrium under the proposed feedback law. Subsequently, we prove that the control algorithm stabilizes the equilibrium configuration of the sphere. Simulation results are presented to demonstrate the efficacy of the control strategy.

To my parents

ACKNOWLEDGMENTS

I sincerely thank all those who contributed to the completion of this research. I express my deepest gratitude for my major advisor, Dr. Ranjan Mukherjee, whose guidance, insight and encouragement has been an asset for me. I thank the members of my Ph.D. guidance committee: Dr. Hassan Khalil, Dr. Subhendra Mahanti and Dr. Steve Shaw, for all their suggestion and support.

I also thank all my fellow graduate students in the Dynamics and Controls Laboratory, for their camaraderie and cheerful disposition in the Lab.

I am specially grateful to my parents whose illimitable love and concern for me have always been my source of strength.

Tuhin Kumar Das

TABLE OF CONTENTS

Li	st of	Tables	viii
Li	st of	Figures	ix
1	Int	roduction	1
2	Bac	ekground	8
	2.1	Kinematic Model	8
	2.2	Alternate Kinematic Representation	10
	2.3	Control Actions	11
3	Par	tial Reconfiguration of the Sphere	14
	3.1	Problem Statement	14
	3.2	Sweep-Tuck Algorithm: The Basic Approach	15
	3.3	Sweep-Tuck Algorithm: Special Cases	23
	3.4	Simulations	25
4	Cor	nplete Reconfiguration: Convergence Studies for $n \in (1, \infty)$	28
	4.1	Problem Statement	28
	4.2	Analysis of Quadruple Sweep Options in Sweep-Tuck Algorithm	28
	4.3	Compensating and Restoring Sweep (CRS) Maneuver	31
	4.4	Inequality Condition for Convergence	36
	4.5	Range of ψ for Inequality Condition	40
	4.6	Preliminary Sweep Maneuver and Merging the Expanded Ranges	43
	4.7	Simulation Results	46
5	Cor	nplete Reconfiguration: Convergence Studies for $n \in (0,1)$	48
	5.1	Quadruple Sweep Options	48
	5.2	CRS Maneuvers and Inequality Condition for Convergence	49
	5.3	Range of ψ for Inequality Condition	52
	5.4	Preliminary Sweep Maneuver and Merging the Expanded Ranges	54
	5.5	Simulations	55

6	Tuc	k-Out	Maneuver and Special Cases	58
	6.1	Tuck-	Out Maneuver	58
	6.2	Specia	al Cases	63
		6.2.1	Case: $n = 1 \dots \dots \dots \dots \dots \dots \dots \dots \dots \dots$	63
		6.2.2	Case: $n = \infty$	66
		6.2.3	Case: $n = 0$	67
		6.2.4	Case: n undefined	68
		6.2.5	Case: $\theta_0 > \left(\frac{\pi}{2} - \epsilon\right)$	68
	6.3	Comp	lete Reconfiguration Algorithm	69
	6.4	Simul	ations	73
		6.4.1	Tuck-Out Maneuver	73
		6.4.2	Special Cases	74
7	Stal	bility A	Analysis	80
7.1 Modified Governing Equations			ied Governing Equations	80
	7.2	Stabil	ity of Equilibrium under PPS followed by CRS-DPT sequence .	83
	7.3	Stabil	ity of Equilibrium under TO Maneuver	88
	7.4 Stability Analysis for the Special Cases		90	
		7.4.1	Case: $n = 1 \dots \dots \dots \dots \dots \dots \dots \dots \dots \dots$	90
		7.4.2	Case: $n = \infty$	92
		7.4.3	Case: $n=0$	93
		7.4.4	$Case: \ n = undefined \ \ldots \ldots \ldots \ldots \ldots \ldots \ldots$	94
		7.4.5	Case: $\theta_0 > \left(\frac{\pi}{2} - \epsilon\right)$	94
	7.5	Stabil	ity of Equilibrium under Complete Reconfiguration Algorithm .	95
8	Con	clusio	n	98
Appendix			102	
	A. Proof of Inequality 3.21			
Bi	bliog	graphy		105

LIST OF TABLES

4.1	Quadruple RS maneuvers starting from $P_{\psi'}$ configuration: $n \in (1, \infty)$	30
4.2	Quadruple RS maneuvers starting from $N_{\psi'}$ configuration: $n \in (0,1)$.	31
4.3	CRS maneuvers for different values of β_k for starting $P_{\psi'}$ configuration	37
4.4	CRS maneuvers for different values of β_k for starting $N_{\psi'}$ configuration	38
4.5	Numerical values of Ψ for various $n \in (1, \infty)$	42
5.1	Numerical values of Ψ for various $n \in (0,1) \dots \dots \dots$	53

LIST OF FIGURES

2.1	Initial and final configurations of sphere	9
2.2	Motion of the sphere under control actions (A) and (B)	12
3.1	An arbitrary configuration of the sphere	15
3.2	Dual-point theorem: The $C-C'$ pair for $n>1$ and $n<1$ cases	17
3.3	RS and DPT maneuvers for $n > 1$ and $n < 1$ cases	21
3.4	The special cases: $n = 0$, $n = 1$, and $n = \infty$	24
3.5	Simulation results for $n \in (1, \infty)$	26
3.6	Simulation results for $n \in (0,1)$	27
4.1	Quadruple sweep options: $n \in (1, \infty)$	29
4.2	Range of β_k for starting $P_{\psi'}$ configuration	33
4.3	Expanded range of β_k for starting $P_{\psi'}$ configuration	34
4.4	Range of β_k for starting $N_{\psi'}$ configuration $\ldots \ldots \ldots \ldots$	35
4.5	Expanded range of β_k for starting $N_{\psi'}$ configuration	36
4.6	Angle Ψ for various values of $n \in (1, \infty)$	42
4.7	Convergence of β in Sweep-Tuck algorithm	45
4.8	Complete reconfiguration: simulation results for $n \in (1, \infty)$	47
5.1	Quadruple sweep options: $n \in (0,1) \ldots \ldots \ldots \ldots$	49
5.2	Angle Ψ for various values of $n \in (0,1)$	54
5.3	Complete reconfiguration: simulation results for $n \in (0,1)$	56
6.1	The tuck-out maneuver	60
6.2	Convergence of β following the TO maneuver	62
6.3	Preliminary control action (B) for $n = 1 \ldots \ldots \ldots$	65
6.4	Preliminary control action (A) for $n = \infty \ldots \ldots \ldots$	66
6.5	Preliminary control action (A) for $n = 0 \ldots \ldots \ldots$	67
6.6	Preliminary control action (A) when n is undefined	68
6.7	Configuration of sphere showing the case when $\theta_0 > (\frac{\pi}{2} - \epsilon)$	69
6.8	Flow diagram of the complete reconfiguration algorithm	70
6.9	Diagram illustrating possible transitions from any initial configuration	
	set to the equilibrium	72
6.10	Tuck-Out maneuver and complete reconfiguration	74
6.11	Complete reconfiguration from the special case of undefined n	75
6.12	Complete reconfiguration from the special case of $n = 0 \dots \dots$	77

6.13	Complete reconfiguration from the special case of $n = \infty$	78
7.1	Typical configuration of sphere used to illustrate the triangle inequality	
	for $\triangle OCQ$	83
7.2	Variation of OC during a DPT maneuver	84
7.3	Triangle inequality on $\triangle OQQ'$: TO maneuver	89
7.4	The constant K 's associated with each transition \dots	98

CHAPTER 1

Introduction

Mobile robots are typically designed with wheels, likely due to our kinship with automobiles. Relying on traditional use of the wheel as a quasi-static device, mobility and stability of the robots are enhanced using multiple wheels, large wheels, multi-wheel drives, broad wheel bases, traction enhancing devices, articulated body configurations, etc. The single-wheel robot proposed by Brown and Xu [10] represents a paradigm shift in mobile robot design. This robot, known as the Gyrover, exploits gyroscopic forces for steering and stability, and has certain advantages over traditional designs. Similar to the Gyrover, which differs from traditional quasi-static models, a few designs have been proposed for spherical wheels with internal mechanisms for propulsion (Koshiyama and Yamafuji, [25]; Halme, et al., [21]; Bicchi, et al., [4]; Camicia, et al., [12]; Bhattacharya and Agrawal, [3]; Mukherjee, et al., [30]). The robot designed by Halme, et al. [21] incorporates a single-wheeled device constrained inside the spherical wheel; the device generates motion by creating unbalance and changes heading by turning the wheel axis. The design by Bicchi, et al. [4]) and Camicia, et al. [12] is similar but employs a four-wheeled car to generate the unbalance. The omnidirectional robot by Koshiyama and Yamafuji [25] has a limited range of lateral roll due to its arch-shaped body. Naturally, it fails to completely exploit the maneuverability associated with spherical exo-skeletons. The propulsion

mechanism by Bhattacharya and Agrawal [3] generates motion by angular momentum conservation utilizing two perpendicular spinning rotors placed inside the sphere. The mechanism can be easily modeled, however propulsion is limited in the presence of external opposing torques or motions requiring constant acceleration.

We are independently engaged in research and development of a spherical mobile robot. The propulsion mechanism proposed by Mukherjee, et al. in [30] is fixed to the exo-skeleton. The mechanism consists of masses reciprocating along spokes fixed to the exo-skeleton. The advantages of this mechanism are easy routing of sensory information from the surface to the processor housed inside, availability of space inside the robot for housing the processor, power supply, structural robustness due to the presence of an internal truss formed by the spokes carrying the unbalanced weights, etc. A detailed dynamic analysis of the proposed mechanism has been performed by Das [14]. Two different spatial arrangement of spokes has been considered for the proposed propulsion mechanism. In the first configuration, the spokes form a regular tetrahedral structure with its center coinciding with the center of the sphere. In the second configuration, the spokes are along the non-intersecting sides of an imaginary cube centered at the center of the sphere. The dynamic analysis of the motion of the spherical robot was preceded by a detailed study of the dynamics of a rolling disk with unbalance masses, Das and Mukherjee [15]. This is a simpler, two dimensional version of the motion of the rolling sphere and gave interesting results in terms of bounded trajectories of unbalance masses while tracking acceleration profiles of the disk and led to important theoretical insight into the dynamics of the rolling sphere.

The geometry of rotations is central to the analysis of diverse problems in mechanics involving rolling motion and the rolling sphere epitomizes the profundity of the control problems of many of these systems. The rolling sphere is a classical example of a nonholonomic mechanical system and is characterized by nonintegrable differential constraints of motion [18]. Due to the nonintegrable nature of the con-

straints, it is possible to reconfigure nonholonomic systems in a space that has higher dimension than the number of degrees of freedom of the system. In the case of the sphere, the nonintegrable constraints provide the scope for reconfiguration of its two Cartesian and three orientation coordinates using rolling motion corresponding to its two degrees of freedom.

In comparison to holonomic systems, nonholonomic systems can access a larger dimensional configuration space but the problems of motion planning and feedback stabilization pose unique challenges. A majority of papers on stabilization of nonholonomic systems deal with wheeled mobile robots and the rigid spacecraft with two actuators. Here we summarize the results briefly but the references cited are not extensive. A more extensive literature survey can be found in the review paper by Kolmanovsky and McClamroch [24]. For nonholonomic systems, standard nonlinear control methods do not lend themselves well for the common objective of stabilization to an equilibrium state. This follows from Brockett's theorem [9] which establishes that there exists no smooth static state feedback which renders the equilibrium state of the closed loop system asymptotically stable. To circumvent this problem, researchers have developed strategies that may be classified under smooth time-varying stabilization, piecewise-smooth time-invariant stabilization, and hybrid stabilization. The work on time-varying stabilization was initiated by Samson [38] and a constructive approach based on Lyapunov's direct method was first developed by Pomet [35]. Smooth time-varying controllers suffer from slow rates of convergence [20] and faster convergence can be achieved through the design of non-smooth controllers. The existence of a piecewise smooth stabilizing controller for nonholonomic systems was shown by Sussmann [42], but the development of such control methods was initiated by Bloch, et al. [7]. Subsequently, exponentially stable non-smooth controllers were developed by Canudas de Wit and Sordalen [13] and Sordalen and Wichlund [41]. Other non-smooth control designs include the work by Aicardi, et al. [1], Astolfi [2],

Mukherjee and Kamon [29], Bloch and Drakunov [6], and Guldner and Utkin [19]. Hybrid controllers are based on switchings at discrete time instants between various low level continuous time controllers and have been proposed by a few authors such as Bloch, et al. [8] and Sordalen, et al. [40].

An important class of nonholonomic systems is the class of two-input nilpotentizable systems that can be transformed into a special form known as the "chained form" [33]. The necessary and sufficient conditions for existence of a feedback transformation to chained-form was provided by Murray [32] and an algorithm for finding the coordinate transformation was presented by Tilbury et al. [43]. An extension of the chained-form to nonholonomic system with more than two inputs was later presented by Bushnell et al. [11] and Walsh and Bushnell [44]. The chained-form, by its very structure and construction, lends itself well to the development of motion planning and control algorithms and researchers have therefore largely focused their efforts on such systems. Incidentally, chained-form system are differentially flat [17] and therefore the methods developed by Rouchon, et al. [36] for differentially flat systems can be profitably applied to chained-form systems. The nonholonomic systems that cannot be converted to chained-form have intrinsic difficulties associated with design of stabilization strategies and render regimented control algorithms developed for chained-form systems inapplicable. Such systems, often referred to as "defective" or "intractable", require stabilization strategies to be custom designed a good example is the work on planar space robots by Mukherjee and Kamon [29]. The kinematic model of the rolling sphere does not satisfy the necessary and sufficient conditions for flatness [17] and hence cannot be converted to chained-form [28]. Therefore, similar to the space robot, the rolling sphere requires motion planning and stabilization strategies to be custom designed.

The motion planning problem for the rolling sphere, a simpler problem than the stabilization problem, has seen a few solutions till date. Li and Canny [27] used

differential-geometric tools to ascertain controllability of the sphere and proposed a three-step algorithm. The position coordinates of the sphere are converged to their desired values in the first step of the algorithm. In the second step, two of the three orientation coordinates are converged using Lie Bracket-like motion. Such motion generates an equatorial spherical triangle on the surface of the sphere. The third step uses a polhode to converge the last orientation coordinate. Bicchi, et al. [5] proposed a control input transformation to obtain a kinematic model of the rolling sphere with a triangular structure. This structure simplifies integration of the state equations for alternating inputs and arrives at a system of nonlinear equations that can be solved by taking additional criteria into account, such as workspace limits and path length. Their iterative solution however demands excessive computational time and may also fail because of extremals encountered along the path. An optimal solution, which minimizes the integral of the kinetic energy of the sphere along the path, was proposed by Jurdjevic [23]. The results indicate that the optimal trajectories have a closedform solution described by elliptic functions. Mukherjee, et al. [30] recently proposed two computationally efficient motion planning algorithms for the sphere. The first algorithm is similar to the third step of Li and Canny's algorithm [27] but is more general and can reconfigure the sphere in fewer steps. The second algorithm is similar to the second step of Li and Canny's algorithm [27] but uses general spherical triangles as opposed to equatorial triangles. The Gauss-Bonet theorem of parallel transport [26] provides a basis for the second algorithm but the basis can be independently established using spherical trigonometry [31].

Although many researchers have investigated control problems associated with the dynamics of rolling contact, [22], [39] for example, the nonholonomic control problem of the rolling sphere has been addressed only by a few researchers. Date, et al., [16] used the time-state control form [37] to design a controller for the ball-plate system described by eight states and three inputs. Although the controller was shown to

converge all states of the system to the equilibrium state, the stability property of the equilibrium was not adequately investigated. Oriolo and Vendittelli [34] recently showed that the equilibrium point of the sphere, modeled by five states and two inputs, can be stabilized through iterative application of an appropriate open-loop control law designed for the nilpotent approximation of the system. In the first phase, they proposed steering three states of the sphere, which conform to chained-form, to their desired coordinates. In the second phase, they proposed closed trajectories of the three states to steer the other two states closer to their desired coordinates. The algorithm relies on repeated application of closed trajectories of the three states such that the remaining two states are converged to their desired values. In the presence of perturbations, both the first and second phases of their controller have to be repeated. This is significantly more complex than repeated application of alternate inputs, as required by our stabilizing controller.

In this dissertation we develop a stabilizing feedback control algorithm for a sphere rolling without slipping on a horizontal plane with the objective of completely reconfiguring the sphere from an arbitrary location and orientation to an equilibrium configuration. In chapter 2, we introduce the kinematic model of the sphere in section 2.1. The states in the kinematic model are the two Cartesian coordinates of the center of the sphere and the three Euler angles representing the orientation of the sphere. The two control inputs are angular speeds applied in mutually perpendicular directions on the horizontal plane. An alternate kinematic representation that helps in posing the complete reconfiguration problem is given in section 2.2. The effect of the individual control inputs on the motion of the sphere is shown in section 2.3. We establish that while one control action causes linear motion of the sphere, the other causes the sphere to roll in a circular arc.

In chapter 3 we develop an algorithm for partial reconfiguration of the sphere.

In partial reconfiguration, while the Cartesian coordinates of the sphere are driven

to the origin, the orientation coordinates are not all reconfigured. Following the problem statement in section 3.1, we present the Sweep-Tuck algorithm for partial reconfiguration in section 3.2. The Sweep-Tuck algorithm forms the basis of complete reconfiguration of the sphere presented in the later chapters. Special cases arising from certain unique configurations of the sphere are discussed in section 3.3, and simulation results corroborating the Sweep-Tuck algorithm are given in section 3.4.

The complete reconfiguration algorithm is discussed for the two general categories of n > 1 and n < 1 separately in chapters 4 and 5 respectively. The parameter n, a ratio arising from the initial condition of the sphere, is an important element of the Sweep-Tuck algorithm. The general categories and special cases are distinguished based on the value of n. Discussions for the general categories of n > 1 and n < 1 are similar, however they are presented separately for clarity and for highlighting the differences between them. Chapters 4 and 5 investigate the flexibility in the Sweep-Tuck algorithm and exploit the same in arriving at a scheme for complete reconfiguration. Simulation results are presented for both categories

The necessary conditions for applying the Sweep-tuck algorithm are established in chapters 4 and 5. These conditions can be satisfied by applying certain initial control actions depending on the initial configuration of the sphere. Also, the special cases are transformed, by certain initial control actions such as the Tuck-Out maneuver, to the general categories of n > 1 or n < 1 before the Sweep-Tuck algorithm is applied. These initial control actions are discussed in chapters 6. The stability analysis of the entire control strategy, consisting of the Sweep-Tuck algorithm, the Tuck-Out maneuver, and the initial control actions for th special cases, are detailed in chapter 7. This is followed by the concluding remarks in chapter 8 and finally the appendices which give details of certain mathematical derivations.

CHAPTER 2

Background

2.1 Kinematic Model

The configuration of a sphere is best described by the two Cartesian coordinates of its center and three coordinates that describe its orientation. In Figure 2.1(a), we define the center of the sphere by point Q and orientation of the sphere by points P and R; P is an arbitrary point on the surface of the sphere and R is an arbitrary point on the equatorial circle defined with P in the vertically top position. Since P and R together require three independent coordinates for description, they constitute a valid choice of points that define the orientation of the sphere. With the position and orientation of the sphere defined by points P, Q, and R, the task of complete reconfiguration can be accomplished by converging Q to the origin of the Cartesian coordinate frame, P to the vertically top position, and R on the positive x axis. This configuration is shown in Figure 2.1(b).

To obtain a kinematic model of the sphere, we denote the Cartesian coordinates of the sphere center by $Q \equiv (x, y)$. We adopt the z-y-z Euler angle sequence (α, θ, ϕ) to represent the orientation of the sphere. We first translate the xyz frame to the center of the sphere and rotate it about the positive z axis by angle α , $-\pi \leq \alpha \leq \pi$, to obtain frame $x_1y_1z_1$. We rotate frame $x_1y_1z_1$ about the y_1 axis by angle θ , $0 \leq \theta \leq \pi$,

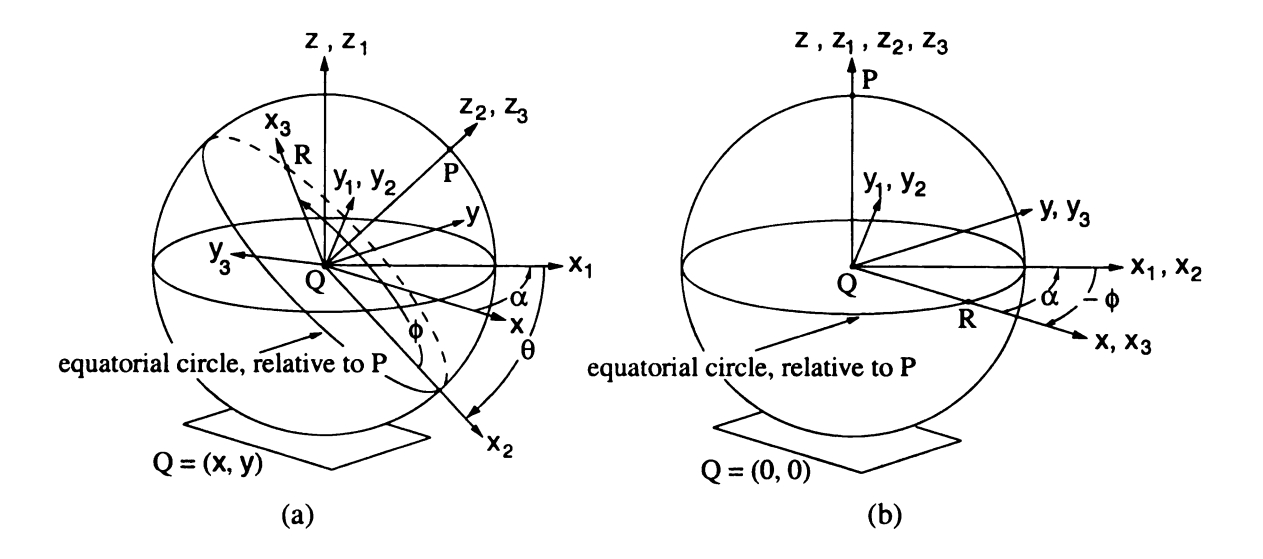


Figure 2.1. Initial and final configurations of sphere

to obtain frame $x_2y_2z_2$. The point P is located at the intersection point of the z_2 axis with the sphere surface. The $x_2y_2z_2$ frame is rotated about the z_2 axis by angle ϕ to obtain frame $x_3y_3z_3$. The point R is located at the intersection point of the x_3 axis and the sphere surface. The frames xyz, $x_1y_1z_1$, $x_2y_2z_2$, $x_3y_3z_3$, and z-y-z Euler angles (α, θ, ϕ) are all shown in Figure 2.1(a). Assuming the sphere to have unity radius without any loss of generality, and denoting the angular velocities of the sphere about the x_1 , y_1 , z_1 axes as ω_x^1 , ω_y^1 , ω_z^1 , respectively, the state equations for $\omega_z^1 = 0$ can be written as

$$\dot{x} = \omega_y^1 \cos \alpha + \omega_x^1 \sin \alpha \tag{2.1}$$

$$\dot{y} = \omega_y^1 \sin \alpha - \omega_x^1 \cos \alpha \tag{2.2}$$

$$\dot{ heta} = \omega_y^1$$
 (2.3)

$$\dot{\alpha} = -\omega_x^1 \cot \theta \tag{2.4}$$

$$\dot{\phi} = \omega_x^1 \csc \theta \tag{2.5}$$

In the model above, the first three equations can be derived simply. The expression for $\dot{\alpha}$ can be obtained from the relative velocity of P with respect to Q, when the sphere rotates with angular velocity ω_x^1 . The angular velocity $\dot{\phi}$ is simply the vector sum of the angular velocities $\dot{\alpha}$ and ω_x^1 . Alternatively, Eqs. (2.3), (2.4), and (2.5), can be derived from the relation between the z-y-z Euler angle rates $\dot{\alpha}$, $\dot{\theta}$, $\dot{\phi}$, and the angular velocities ω_x^1 , ω_y^1 , ω_z^1 , subject to the constraint $\omega_z^1 = 0$.

The reorientation of the sphere refers to the task of bringing P to the vertically upright position, and R, which then lies on the diametrical circle in the xy plane, to lie on the positive x axis. Indeed, this results in $x_3y_3z_3$, the body-fixed axes, to coincide with the inertially fixed axes xyz. This can be achieved with $\theta = 0$, and $\alpha + \phi = 0$, irrespective of the individual values of α and ϕ , as shown in Figure 2.1(b). Therefore, the sphere can be completely reconfigured by satisfying

$$x = 0, \quad y = 0, \quad \theta = 0, \quad \alpha + \phi = 0$$
 (2.6)

The above equation may create the false impression that our objective is to converge the sphere to a configuration manifold. However, it can be verified from Figure 2.1(b) that Eq. (2.6) represents a unique configuration of the sphere.

2.2 Alternate Kinematic Representation

The last condition for complete reconfiguration of the sphere, given in Eq. (2.6) depends on the sum of α and ϕ and not on their individual values. We therefore define the new variable β

$$\beta = \alpha + \phi \tag{2.7}$$

Thus, from Eqs. (2.4) and (2.5),

$$\dot{\beta} = \omega_x^1 \tan \frac{\theta}{2} \tag{2.8}$$

We now write an alternate kinematic formulation in which we replace Eq. (2.5) by the equation of motion in the new state variable β . We have the following alternate kinematic representation

$$\dot{x} = \omega_y^1 \cos \alpha + \omega_x^1 \sin \alpha \tag{2.9}$$

$$\dot{y} = \omega_y^1 \sin \alpha - \omega_x^1 \cos \alpha \tag{2.10}$$

$$\dot{\theta} = \omega_y^1 \tag{2.11}$$

$$\dot{\alpha} = -\omega_x^1 \cot \theta \tag{2.12}$$

$$\dot{\beta} = \omega_x^1 \tan \frac{\theta}{2} \tag{2.13}$$

Using this kinematic model, complete reconfiguration is achieved by satisfying

$$x = 0, \quad y = 0, \quad \theta = 0, \quad \beta = 0$$
 (2.14)

2.3 Control Actions

Consider the motion of the sphere, described by the kinematic model in Eqs. (2.9), (2.10), (2.11), (2.12), (2.13), for the individual control actions

(A)
$$\omega_y^1 \neq 0$$
, $\omega_x^1 = 0$

(B)
$$\omega_x^1 \neq 0$$
, $\omega_y^1 = 0$, $\theta \neq 0$

The motion of the sphere for these actions are explained with the help of Figure 2.2. For action (A), the sphere moves along straight line CF as θ changes. Let F be the

point on this straight line where the sphere would have $\theta = 0$. Since the sphere rolls without slipping, this point remains invariant under control action (A). For control action (B), the instantaneous radius of the path traced by the sphere on the xy plane can be computed using Eqs. (2.9) through (2.12) as follows

$$\rho = \left| \frac{(\dot{x}^2 + \dot{y}^2)^{3/2}}{\dot{x} \, \ddot{y} - \dot{y} \, \ddot{x}} \right| = \tan \theta \tag{2.15}$$

Since $\omega_y^1 = 0$, θ is maintained constant. This implies that the contact point of

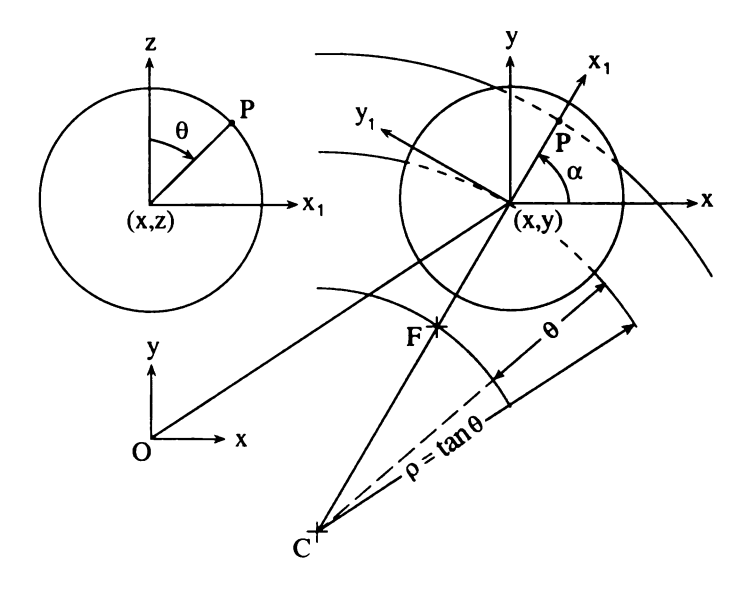


Figure 2.2. Motion of the sphere under control actions (A) and (B)

the sphere moves along a circular path; the center of this circle is located at C in Figure 2.2. Along with the contact point, points P and F also move along circular paths; the center of these paths lie on the vertical axis that passes through C. The point C remains fixed under control action (B), but under control action (A) it moves away from F, as θ increases, and converges to F, as θ converges to zero.

The variables α , ϕ , and β in Eqs. (2.4), (2.5), and (2.13) change during control action (B) but remain invariant during control action (A). During control action (B), the change in variable β is given by the expression

$$\Delta \beta = \Delta \alpha + \Delta \phi = \Delta \alpha (1 - \sec \theta) \tag{2.16}$$

This indicates that $\Delta\beta$ will be always opposite in sign to $\Delta\alpha$ for $0 < \theta < \pi/2$.

CHAPTER 3

Partial Reconfiguration of the Sphere

3.1 Problem Statement

In this section we develop a simple algorithm for partial reconfiguration of the sphere. This algorithm will provide the basis for the stabilizing controller for complete reconfiguration, which we will design over the next few sections. Our objective for partial reconfiguration is to converge the sphere from any initial configuration to a configuration that satisfies

$$x = 0, \quad y = 0, \quad \theta = 0 \tag{3.1}$$

Clearly, the goal of partial reconfiguration is to converge the center of the sphere, Q, to the origin of the Cartesian coordinate frame and the point P to the vertically top position. This leaves the sphere with only one degree-of-freedom that allows R to be have an arbitrary orientation on the equatorial circle. In the context of the kinematic model in section 2.2, this corresponds to arbitrary value of β in the final configuration.

3.2 Sweep-Tuck Algorithm: The Basic Approach

In this section we present an algorithm for partial reconfiguration of the rolling sphere. The control actions (A) and (B) form the basic elements of the reconfiguration strategy. Control actions (A) and (B) are applied repeatedly in pair and the process leads to convergence of the states x, y, θ to zero. For simplicity, we develop our algorithm under the assumption that θ satisfies $0 < \theta < \pi/2$ at the initial time. We will remove this restriction later when we develop the stabilizing controller for complete reconfiguration. Now, consider an arbitrary configuration of the sphere as shown in Figure 3.1, with the configuration defined only by the variables x, y, θ , and α . The points C and F in Figure 3.1 were defined earlier in section 2.3 using Figure 2.2.

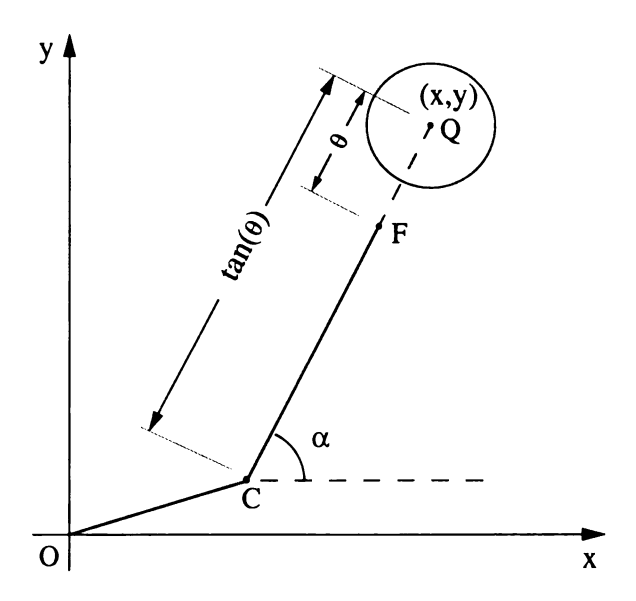


Figure 3.1. An arbitrary configuration of the sphere

The Cartesian coordinates of C, namely, C_x , C_y , are related to the Cartesian

coordinates of Q, namely x, y, as follows

$$C_x = x - \tan \theta \cos \alpha \implies x = C_x + \tan \theta \cos \alpha$$

 $C_y = y - \tan \theta \sin \alpha \implies y = C_y + \tan \theta \sin \alpha$ (3.2)

Also, the distances CO and CF are given by the relations

$$CO = \left(C_x^2 + C_y^2\right)^{1/2} \qquad CF = \tan \theta - \theta \qquad (3.3)$$

where $(\tan \theta - \theta)$ is a monotonically increasing function of θ and equal to zero only when $\theta = 0$. It readily follows from Eqs. (3.2) and (3.3) that

$$(CF, CO) \equiv (0,0) \iff (x,y,\theta) \equiv (0,0,0) \tag{3.4}$$

The above result is summarized in the following remark.

Remark 3.1 The sphere in Figure 3.1, defined by points C, F, and Q, will be partially reconfigured in the sense of Eq. (3.1) if and only if (CF, CO) converge to (0,0).

For partial reconfiguration of the sphere, we will therefore design an algorithm that will converge both points C and F in Figure 3.1 to the origin O. The basis for our algorithm lies in the theorem presented next with the help of Figure 3.2.

Theorem 3.1 (Dual-Point Theorem) Let C and F be two points in the xy coordinate frame that has its origin at O and suppose $\psi = \angle OCF$ is an acute angle. Let the ratio of CF and CO be denoted by n = (CF/CO). If ψ satisfies the condition

$$0 \le \psi < \cos^{-1}(1/n) \quad for \quad n \in (1, \infty)$$

$$0 \le \psi < \cos^{-1}(n) \quad for \quad n \in (0, 1)$$
(3.5)

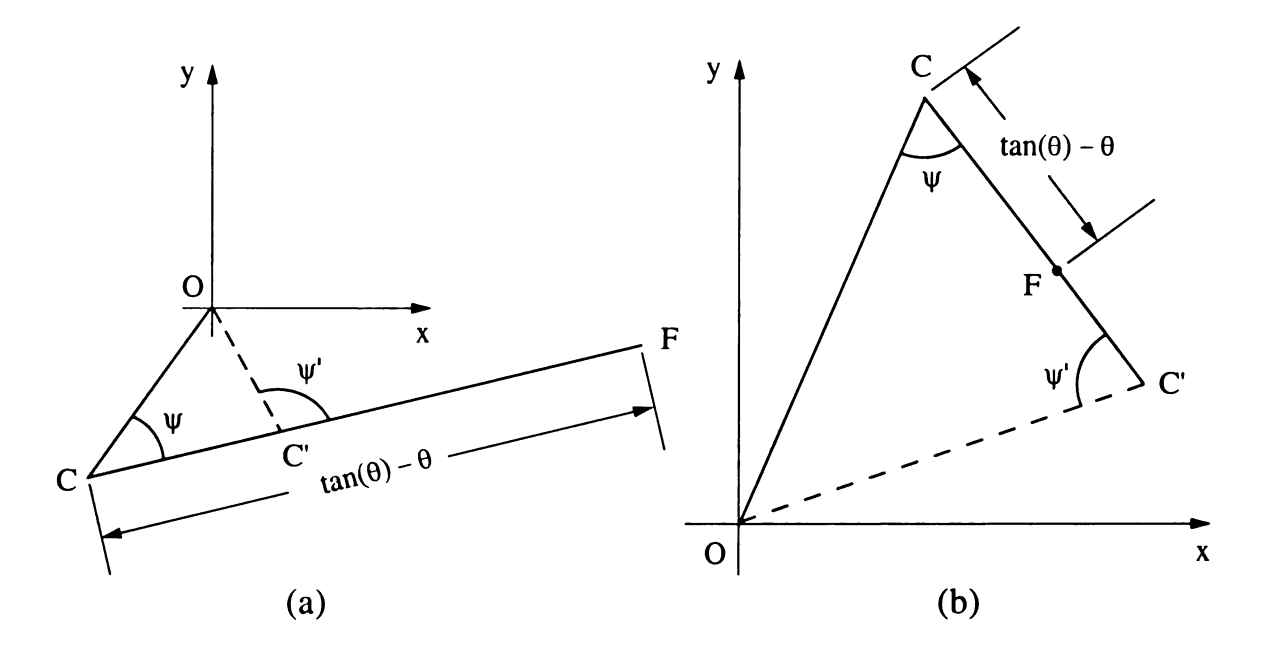


Figure 3.2. Dual-point theorem: The C-C' pair for n>1 and n<1 cases

then there exists a point C' on the extended line CF such that for $\psi' = \angle OC'F$, $0 \le \psi' \le \pi$,

$$(C'F/C'O) = n,$$

$$0 < (C'O/CO) < 1$$

$$\psi' > \psi,$$

$$(3.6)$$

Proof: Since ψ is acute and we seek a point C' that will satisfy C'O < CO, C' can only be located between C and F, as in Figure 3.2(a), or beyond F as shown in Figure 3.2(b). For both cases, OC' satisfies

$$OC'^{2} = OC^{2} + CC'^{2} - 2OC.CC'\cos\psi$$
(3.7)

For the two cases in Figures 3.2(a) and 3.2(b), the expression for CC' is different and

is given below by Eqs. (3.8) and (3.9), respectively

$$CC' = CF - C'F \implies CC' = nCO - C'F$$
 (3.8)

$$CC' = CF + C'F \implies CC' = nCO + C'F$$
 (3.9)

Let us now assume (C'F/C'O) = n. Substituting this in Eqs.(3.8) and (3.9), we get

$$nC'O = (nCO - CC') \tag{3.10}$$

$$nC'O = -(nCO - CC') \tag{3.11}$$

Using Eq.(3.10) or Eq.(3.11) with Eq.(3.5) we eliminate C'O to obtain the following non-trivial solution for CC'

$$CC' = \frac{2n \, CO \, (n \cos \psi - 1)}{(n^2 - 1)} \tag{3.12}$$

When $n \in (1, \infty)$, we have $(n^2 - 1) > 0$ and we can show from Eq.(3.5) that $(n \cos \psi - 1) > 0$. Therefore, CC' in Eq.(3.12) is positive. When $n \in (0, 1)$, we have $(n^2 - 1) < 0$ and $\cos \psi < 1 < (1/n)$. This again implies that CC' is positive. Since CC' is always positive, our assumption (C'F/C'O) = n is correct. $\diamond \diamond \diamond$

To prove the second assertion, we make use of the following inequality

$$(n - \cos \psi)^2 + \sin^2 \psi > 0 \implies 2(n \cos \psi - 1) < (n^2 - 1)$$
 (3.13)

which is true for all n and ψ . Therefore, for $n \in (1, \infty)$ we can claim

$$\frac{2(n\cos\psi - 1)}{(n^2 - 1)} < 1 \quad \Longrightarrow \quad CC' < nCO = CF \tag{3.14}$$

Thus Figure 3.2(a), and Eqs.(3.8) and (3.10), correspond to the case $n \in (1, \infty)$,

where C' lies between C and F. When $n \in (0,1)$, it follows from Eq.(3.12)

$$\frac{2(n\cos\psi - 1)}{(n^2 - 1)} > 1 \quad \Longrightarrow \quad CC' > nCO = CF \tag{3.15}$$

Thus Figure 3.2(b), and Eqs.(3.9) and (3.11) correspond to $n \in (0,1)$, where C' lies beyond F. Using Eqs.(3.8), (3.9), (3.12), and the relation C'F = n C'O, which we have already established, we can show

$$\frac{C'O}{CO} = \begin{cases} [1 - 2(n\cos\psi - 1)/(n^2 - 1)] & \text{for } n \in (1, \infty) \\ -[1 - 2(n\cos\psi - 1)/(n^2 - 1)] & \text{for } n \in (0, 1) \end{cases}$$
(3.16)

From Eqs.(3.14), (3.15), and (3.16), we can directly show that C'O/CO > 0 for both $n \in (1, \infty)$ and $n \in (0, 1)$. For $n \in (1, \infty)$ we have already shown that $(n\cos\psi - 1)/(n^2 - 1) > 0$ and hence 0 < (C'O/CO) < 1. The same holds true for $n \in (0, 1)$ since $\cos\psi > n \Rightarrow n\cos\psi > n^2 \Rightarrow 2(n\cos\psi - 1)/(n^2 - 1) < 2$. $\diamond \diamond \diamond$

From both Figures 3.2(a) and 3.2(b) we can write

$$C'O\sin\psi' = CO\sin\psi \tag{3.17}$$

This implies $\sin \psi' > \sin \psi$ because C'O < CO. Since ψ is an acute angle, it follows that $\psi' > \psi$. $\diamond \diamond \diamond$

We now derive an expression for the intermediate angle ψ' in our Dual-Point Theorem. From $\triangle OCC'$ in Figures 3.2(a) and 3.2(b) we can write

$$CO\cos\psi = CC' + C'O\cos\psi'$$
 for $n \in (1, \infty)$
 $CO\cos\psi = CC' - C'O\cos\psi'$ for $n \in (0, 1)$

Using Eqs. (3.12), (3.17), and (3.18) we get

$$\tan \psi' = \frac{-|1 - n^2| \sin \psi}{(1 + n^2) \cos \psi - 2n} \qquad n \in (0, 1) \cup (1, \infty)$$
 (3.19)

It can verified from Eq.(3.19) that

$$0 \le \psi < \cos^{-1}\left(\frac{1}{n}\right) \implies \cos^{-1}\left(\frac{1}{n}\right) < \psi' \le \pi \qquad \text{for } n \in (1, \infty)$$

$$0 \le \psi < \cos^{-1}(n) \implies \cos^{-1}(n) < \psi' \le \pi \qquad \text{for } n \in (0, 1)$$

$$(3.20)$$

Since ψ' depends only on the values of n and ψ , it attains the same value prior to each intermediate RS-DPT maneuver pair. An important inequality which will be later useful in our analysis is

$$\psi + \psi' \le \pi \qquad \qquad n \in (0,1) \cup (1,\infty) \tag{3.21}$$

The proof of this inequality is provided in Appendix A.

Consider Figures 3.3(a) and 3.3(b) where C and F define arbitrary configurations of the sphere for the cases $n \in (1, \infty)$ and $n \in (0, 1)$, respectively, and suppose $\psi = \angle OCF$ satisfies the conditions in Eq.(3.5). From Theorem 3.1, we know that there exists a point C' along the line CF that satisfies the conditions in Eq.(3.6). Let C' in Figures 3.3(a) and 3.3(b) be this point. We are now ready to define two specific maneuvers of the sphere.

Definition 3.1 (DPT Manuever) In reference to Figures 3.3(a) and 3.3(b), we define a "Dual-Point Tuck" (DPT) Maneuver as control action (A) that moves the sphere such that point C moves to C'.

From Theorem 3.1 we know that a DPT maneuver results in $\psi' > \psi$. For both cases $n \in (1, \infty)$ and $n \in (0, 1)$, ψ' can therefore be restored to the value ψ in one of two ways as shown in Figure 3.3. This motivates the next definition.

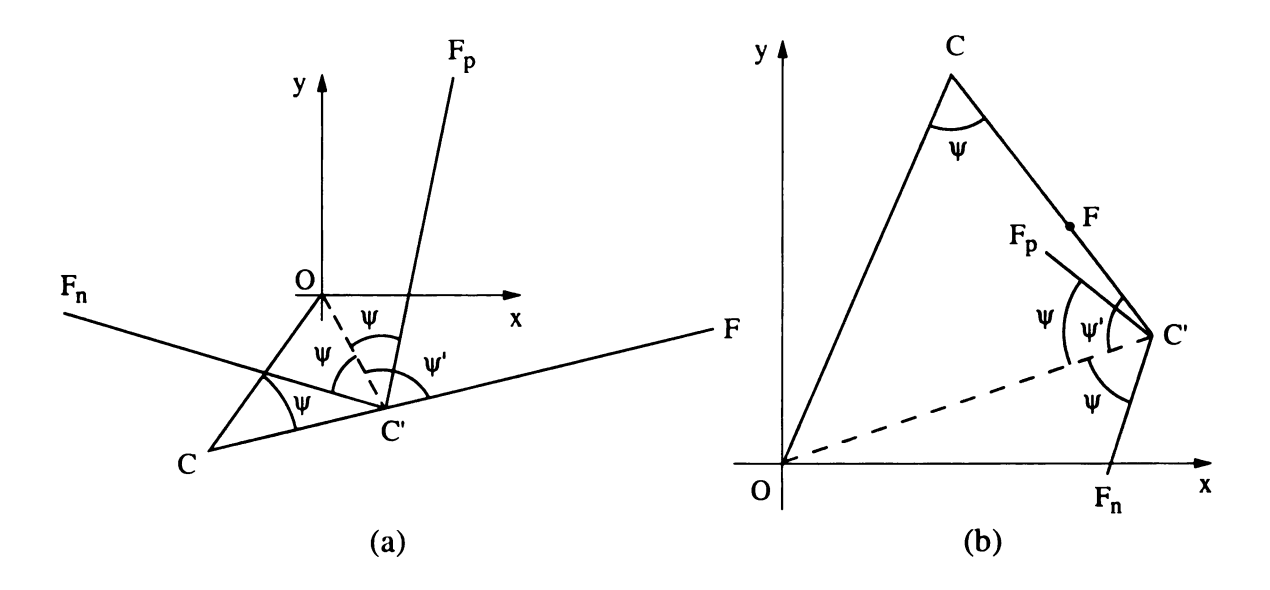


Figure 3.3. RS and DPT maneuvers for n > 1 and n < 1 cases

Definition 3.2 (RS Manuever) Following a DPT maneuver, a control action (B) that moves the sphere to restore ψ' to ψ is defined as a "Restoring-Sweep" (RS) Maneuver.

In the sequel, we will prove that a series of alternate RS and DPT maneuvers can partially reconfigure the sphere. However, since the initial configuration of the sphere may not satisfy $\angle OCF = \psi'$, we define one additional maneuver.

Definition 3.3 (PS Manuever) A control action (B) that moves the sphere at the initial time to bring $\angle OCF$ to ψ' is defined as a "Preliminary-Sweep" (PS) Maneuver.

We now present the "Sweep-Tuck" algorithm with the help of the following theorem.

Theorem 3.2 (Sweep-Tuck Algorithm) Consider a sphere whose partial configuration (x, y, θ) is defined by the location of the points C and F. Suppose at the initial time, $0 < \theta < \pi/2$ and $(CF/CO) = n \in (0,1) \cup (1,\infty)$. Depending on whether n

is greater or lesser than unity, choose ψ in accordance with Eq.(3.5). Then, partial reconfiguration of the sphere in the sense of Eq.(3.1) can be achieved through a PS maneuver followed by repeated application of RS-DPT maneuvers.

Proof: The application of a PS maneuver at the initial time results in $\angle OCF = \psi'$. This sets the stage for repeated application of RS-DPT maneuvers. The application of an RS maneuver does not alter the values of CF and CO but sweeps F about C (in one of two ways for both cases $n \in (1, \infty)$ and $n \in (0, 1)$, as shown in Figure 3.3 to bring $\angle OCF$ to the value ψ , which was earlier chosen in accordance with Eq.(3.5). At the end of the RS maneuver, the new point F_p or F_n is simply renamed F. Using Theorem 3.1 we can show that a subsequent DPT maneuver results in

$$0 < \frac{C'O}{CO} = \frac{C'F}{CF} = r < 1 \qquad r \triangleq \left| 1 - \frac{2(n\cos\psi - 1)}{(n^2 - 1)} \right|$$
 (3.22)

and change of $\angle OCF = \psi$ to $\angle OC'F = \psi' > \psi$, as shown in Figures 3.2 and 3.3. By renaming C' as C, we can again execute the RS-DPT pair of maneuvers. Each pair simply reduces the values of both CF and CO in geometric progression and from Eq.(3.22) it can be readily shown that $CF, CO \rightarrow 0$ as $N \rightarrow \infty$, where N is the number of RS-DPT pairs. From Remark 3.1 it simply follows that repeated application of RS-DPT maneuvers results in partial reconfiguration of the sphere.

Remark 3.2 From Eqs.(3.14) and (3.15) we know that CC' < CF for $n \in (1, \infty)$ and CC' > CF for $n \in (0,1)$. This implies that α does not change its value for a DPT maneuver with $n \in (1,\infty)$ but for $n \in (0,1)$ it undergoes a discontinuous change in value by π as the sphere goes through the configuration where $\theta = 0$. This is consistent with the adopted convention that Euler angle θ is positive.

000

22

Corollary 3.1 The sequence of values assumed by θ at the end of every DPT maneuver of the Sweep-Tuck algorithm decreases monotonically and converges to zero.

Proof: Since θ remains constant during RS maneuvers, its change can be attributed to the DPT maneuvers. From Theorem 3.2 we know that DPT maneuvers cause CF to decrease in geometric progression and converge to zero. Since $(\tan \theta - \theta)$ is a monotonically increasing function of θ and equal to zero only when $\theta = 0$, we claim that the sequence of values assumed by θ at the end of every DPT maneuver decreases monotonically and converges to zero. $\diamond \diamond \diamond$

Remark 3.3 It can be seen from both Figures 3.3(a) and 3.3(b) that the RS maneuver is not unique. To restore $\angle OCF$ to ψ , the RS maneuver can sweep F to the location F_p or F_n . Furthermore, F can be taken to both F_p and F_n via a clockwise (cw) or a counter-clockwise (ccw) rotation about C. Although the partial reconfiguration problem is not affected by the particular choice of F_p or F_n and cw or ccw direction of rotation since r in Eq.(26) is the same for all four choices, the flexibility will be necessary for complete reconfiguration of the sphere. The complete reconfiguration problem will be discussed over the next few sections.

3.3 Sweep-Tuck Algorithm: Special Cases

The Sweep-Tuck algorithm in Theorem 3.2 is applicable for $n \in (0,1) \cup (1,\infty)$ but inapplicable for the special cases where n=0, n=1, and $n=\infty$. In this section we discuss initial maneuvers that revert the special cases back to $n \in (0,1) \cup (1,\infty)$ such that the sweep-tuck algorithm can be directly applied.

The special case n=0 occurs when $CF=0 \Longrightarrow \theta=0$. In this configuration, shown in Figure 3.4(a), both control action (B) and angle ψ are undefined and the sweep-tuck algorithm is inapplicable. The problem is remedied by changing the value of n using control action (A). Since $\theta=0$, α is arbitrary and point C can be made to

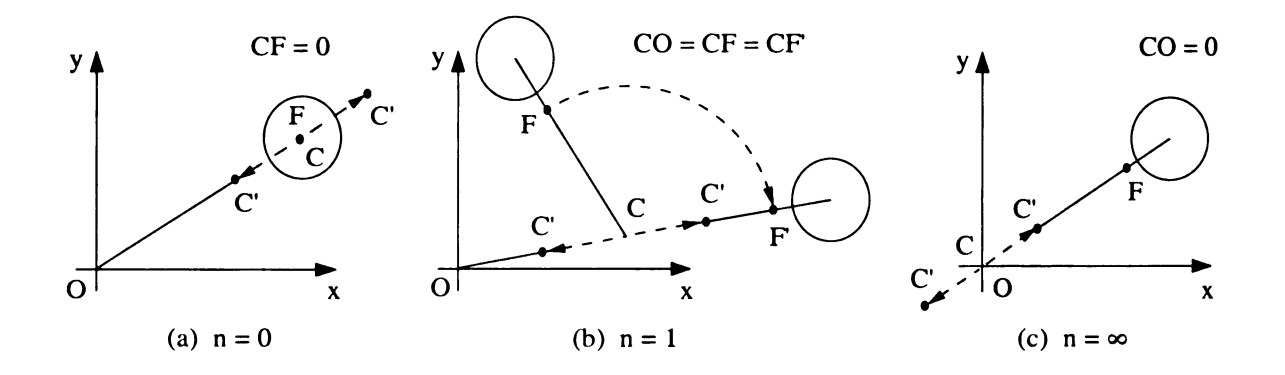


Figure 3.4. The special cases: n = 0, n = 1, and $n = \infty$

move in any arbitrary direction away from F. We choose to move C along the line OF, towards or away from O, since this gives us the maximum flexibility in choosing any value of n from the set $(0,1) \cup (1,\infty)$.

The special case n=1 occurs when CF=CO, as illustrated in Figure 3.4(b). From Eq.(3.22) it can be verified that $r=\infty$ when n=1. Since this violates the condition 0 < r < 1, the Sweep-Tuck algorithm is not applicable. The sphere can be partially reconfigured by first applying control action (B) such that F converges to the origin and then applying control action (A) such that F converges to the origin. These two maneuvers are however not the same as the RS and DPT maneuvers. If it is desired that the Sweep-Tuck algorithm be used, control action (B) should be used to sweep F onto line F0, but not at F1, as shown in Figure 3.4(b). The value of F2 should then be changed to any value in the set F3, using control action (A).

When C lies at the origin O, we have the special case $n = \infty$. It can be shown from Eq.(3.22) that the condition 0 < r < 1 is violated when $n = \infty$ since r = 0. The problem is remedied using control action (A), as shown in Figure 3.4(c), such that $n = \infty$ can have any value in the set $(0,1) \cup (1,\infty)$. This enables us to subsequently apply the Sweep-Tuck algorithm.

Remark 3.4 In this section we presented the Sweep-Tuck algorithm for partial reconfiguration of the sphere and discussed maneuvers that render the algorithm applicable to special cases where it is inapplicable otherwise. We proved asymptotic convergence of the configuration variables $(x,y,\theta) \to (0,0,0)$ but did not show stability of the equilibrium. We will prove asymptotic stability of the equilibrium as well as remove the restriction on the initial condition, namely $0 < \theta < \pi/2$, when we address the complete reconfiguration problem.

3.4 Simulations

We present simulation results of partial reconfiguration, one each for the two cases $n \in (1, \infty)$ and $n \in (0, 1)$. The initial configuration of the sphere for these cases were taken as follows

$$x = 3.0$$
 $y = 3.0$ $\theta = 1.35$ $\alpha = 1.05$ (3.23)

$$x = 10.0$$
 $y = 5.0$ $\theta = 1.40$ $\alpha = 0.52$ (3.24)

where the units are meters and radians. Using the definition of n in Theorem 3.1 and Eqs.(3.2) and (3.3) we can show that the initial conditions in Eqs.(3.23) and (3.24) correspond to n = 2.691 and n = 0.816, respectively. To satisfy the constraints in Eq.(3.5), we chose ψ for the two cases to lie at 40% and 50% of their permissible range, respectively. Among the four possible options for the RS maneuvers, we chose ccw sweep to the P_{ψ} configuration for both cases. The simulation results are shown in Figures 3.5 and 3.6. Figures 3.5(a), 3.5(b), and 3.5(c) show the trajectories of points C and F in the x-y plane, trajectory of point Q in the x-y plane, and evolution of θ in time, respectively, for n = 2.691. The corresponding trajectories for n = 0.816 are shown in Figure 3.6.

Both Figures 3.5(c) and 3.6(c) indicate that θ remains constant for certain intervals

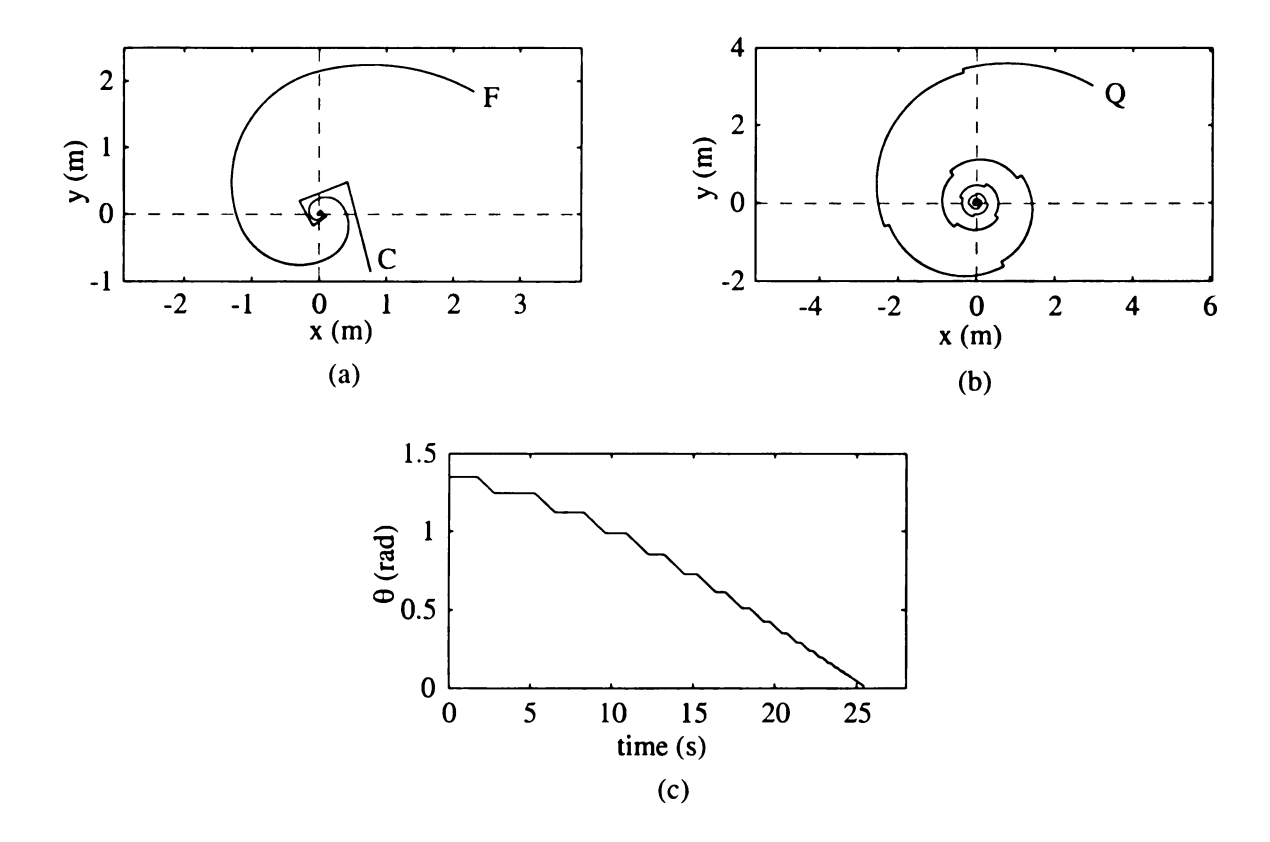


Figure 3.5. Simulation results for $n \in (1, \infty)$

of time - these intervals correspond to RS maneuvers. The value of θ changes during the DPT maneuvers and in agreement with Corollary 3.1, value of θ at the end of each DPT maneuver is less than its value at start. The difference in the trajectories of θ in Figures 3.5(c) and 3.6(c) during the DPT maneuvers can be explained with Remark 3.2.

It was discussed in Remark 3.2 that α discontinuously changes its value during DPT maneuvers for $n \in (0,1)$. This explains the discontinuities in the derivative of the trajectory of F in Figure 3.6(a). In comparison, the trajectory of F in Figure 3.5(a) has continuous derivatives since CC' < CF for DPT maneuvers with $n \in (1,\infty)$, and CC' < CF ensures a constant value of α . The DPT maneuvers in Figures 3.5(a) and 3.6(a) correspond to the straight line trajectory segments of C.

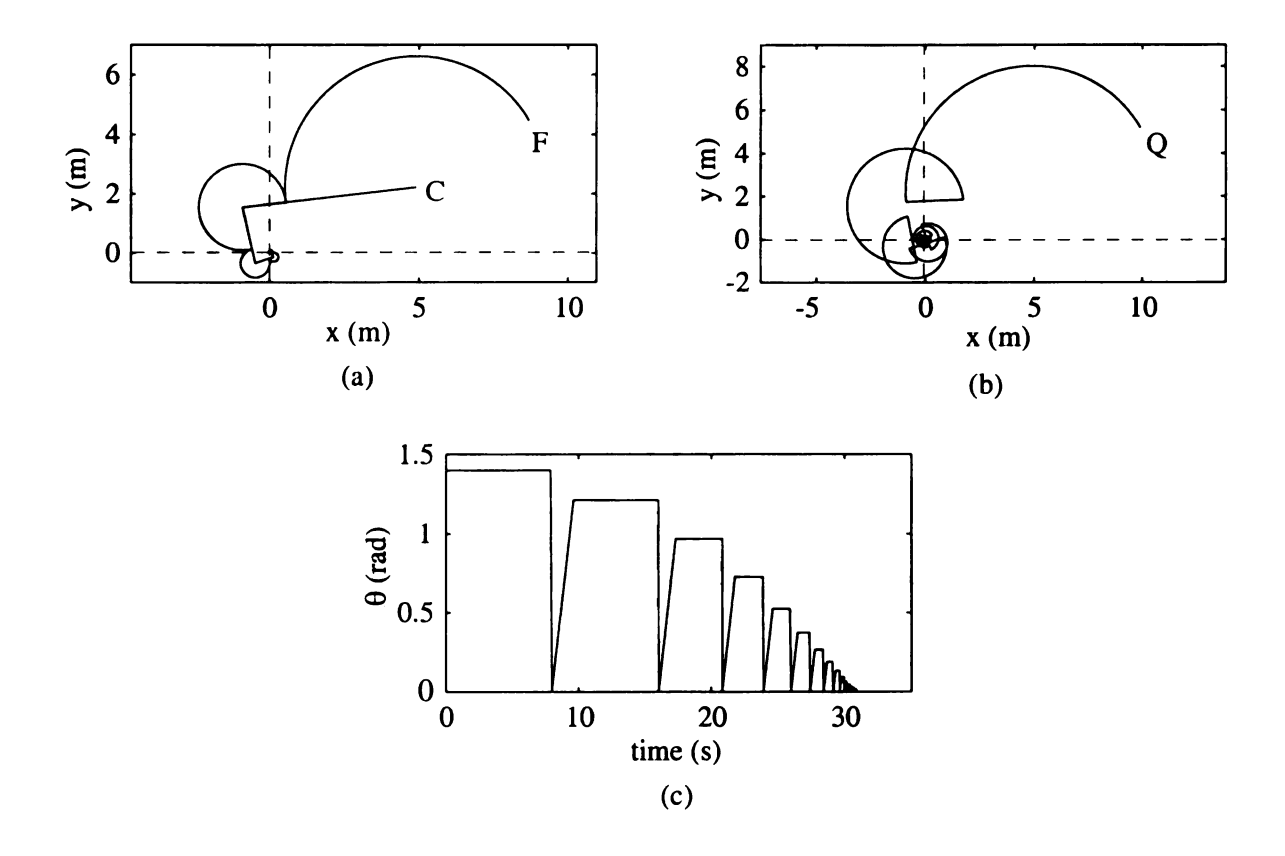


Figure 3.6. Simulation results for $n \in (0,1)$

Both the RS and DPT maneuvers are also obvious from the motion of the center of the sphere, shown in Figure 3.5(b) and 3.6(b). The trajectory of Q in Figure 3.6(b) is however self-intersecting unlike in Figure 3.5(b). Once again, this can be attributed to the discontinuous change in α during DPT maneuvers for $n \in (0, 1)$.

CHAPTER 4

Complete Reconfiguration:

Convergence Studies for $n \in (1, \infty)$

4.1 Problem Statement

For the kinematic model of the sphere described by Eqs.(2.9) through (2.13), complete reconfiguration refers to the task of converging $(x, y, \theta, \beta) \to (0, 0, 0, 0)$, as shown in Eq.(2.14). In chapter 3 we developed the Sweep-Tuck algorithm to converge $(x, y, \theta) \to (0, 0, 0)$ and in this section we will extend it to converge $\beta \to 0$ for the case $n \in (1, \infty)$. As in chapter 3, the convergence algorithm in this section will be developed under the restriction $0 < \theta < \pi/2$. In chapter 5 we will address the complete reconfiguration problem for $n \in (0, 1)$.

4.2 Analysis of Quadruple Sweep Options in Sweep-Tuck Algorithm

It was discussed in Remark 3.3 that the RS maneuver is not unique; it can sweep point F to the location F_p or F_n in a cw or ccw manner. Although all four choices of sweep

have the same effect on the partial reconfiguration problem, they result in different values of β , the additional variable we need to converge for complete reconfiguration. To investigate the change in β for the four sweep options in a systematic manner, we resort to the following definitions.

Definition 4.1 (P_{ψ} Configuration) The partial configuration of a sphere defined by the pair $\{C, F\}$ is a P_{ψ} configuration if $\vec{CF} \times \vec{CO} > 0$ and $\cos \angle OCF = \cos \psi$.

Definition 4.2 (N_{ψ} Configuration) The partial configuration of a sphere defined by the pair $\{C, F\}$ is a N_{ψ} configuration if $\vec{CF} \times \vec{CO} < 0$ and $\cos \angle OCF = \cos \psi$.

According to Definitions 4.1 and 4.2, $\{C, F\}$ and $\{C', F_p\}$ are P_{ψ} configurations in Figure 4.1(a), $\{C', F\}$ is a $P_{\psi'}$ configuration and $\{C', F_n\}$ is a N_{ψ} configuration.

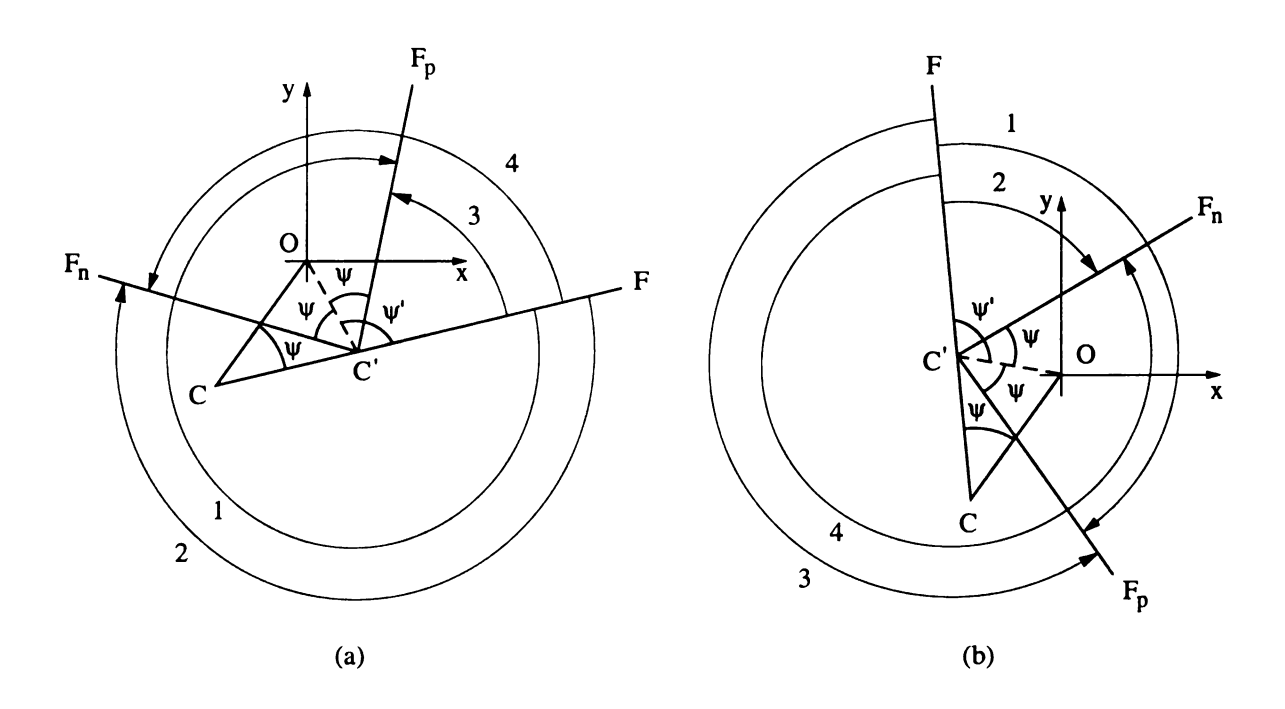


Figure 4.1. Quadruple sweep options: $n \in (1, \infty)$

We now investigate the change in β for the four RS maneuvers that are possible

Starting From $P_{\psi'}$ Configuration									
Ending at Direction Sweep angle $ \Delta \alpha $ $\Delta \beta$ Value									
P_{ψ}	cw	$-(2\pi-\psi'+\psi)$	Δeta_1	$-(2\pi-\psi'+\psi)(1-\sec\theta)$					
$N_{m{\psi}}$	cw	$-(2\pi-\psi'-\psi)$	Δeta_2	$-(2\pi-\psi'-\psi)(1-\sec\theta)$					
P_{ψ}	ccw	$\psi' - \psi$	Δeta_{3}	$(\psi' - \psi)(1 - \sec \theta)$					
$N_{oldsymbol{\psi}}$	ccw	$\psi' + \psi$	Δeta_{4}	$(\psi' + \psi)(1 - \sec \theta)$					

Table 4.1. Quadruple RS maneuvers starting from $P_{\psi'}$ configuration: $n \in (1, \infty)$

starting from $P_{\psi'}$: $\{C', F\}$ in Figure 4.1(a). These maneuvers, marked 1, 2, 3, and 4, respectively, correspond to

- 1. a cw sweep ending at P_{ψ} : $\{C', F_p\}$,
- 2. a cw sweep ending at N_{ψ} : $\{C', F_n\}$,
- 3. a ccw sweep ending at P_{ψ} : $\{C', F_p\}$, and
- 4. a ccw sweep ending at N_{ψ} : $\{C', F_n\}$

It can be verified from Figure 2.2 that the angle of sweep during an RS maneuver is equal to $\Delta \alpha$. For the above maneuvers $\Delta \beta$ can therefore be computed using Eq.(2.16); the results are summarized in Table 4.1 below. The results in Table 1 correspond to the start configuration $P_{\psi'}$: $\{C', F\}$. When the start configuration is $N_{\psi'}$: $\{C', F\}$, as shown in Figure 4.1(b), the change in β for the four different RS maneuvers can be summarized by Table 4.2.

It was established in Theorem 3.1 that $\psi' > \psi$ for $n \in (1, \infty) \cup (0, 1)$. Furthermore we know from Eq.(3.21) that $\psi + \psi' \leq \pi$. Using these results we can establish the following relations between the four possible sweep angles given in Table 4.1

$$-(2\pi - \psi' + \psi) \le -(2\pi - \psi' - \psi) \le 0 \le (\psi' - \psi) \le (\psi' + \psi) \tag{4.1}$$

Starting From $N_{\psi'}$ Configuration										
Ending at $ $ Direction $ $ Sweep angle $ $ $ $ $ $ $ $ Value $ $ Value										
$P_{m{\psi}}$	cw	$-(\psi'+\psi)$	Δeta_1	$-(\psi'+\psi)(1-\sec\theta)$						
N_{ψ}	cw	$-(\psi'-\psi)$	Δeta_2	$-(\psi'-\psi)(1-\sec\theta)$						
P_{ψ}	ccw	$2\pi-\psi'-\psi$	Δeta_3	$(2\pi - \psi' - \psi)(1 - \sec \theta)$						
N_{ψ}	ccw	$2\pi - \psi' + \psi$	Δeta_{4}	$(2\pi - \psi' + \psi)(1 - \sec \theta)$						

Table 4.2. Quadruple RS maneuvers starting from $N_{\psi'}$ configuration: $n \in (0,1)$

Similarly, the sweep angles in Table 4.2 satisfy the relationship

$$-(\psi' + \psi) \le -(\psi' - \psi) \le 0 \le (2\pi - \psi' - \psi) \le (2\pi - \psi' + \psi) \tag{4.2}$$

4.3 Compensating and Restoring Sweep (CRS) Maneuver

Consider partial reconfiguration of the sphere based on the Sweep-Tuck algorithm. Let the configuration variables of the sphere at the initial time be $(x_0, y_0, \theta_0, \alpha_0, \beta_0)$. A PS maneuver is first invoked to set $\angle OCF = \psi'$. Suppose $(x_1, y_1, \theta_1, \alpha_1, \beta_1)$ are the configuration variables at the end of the PS maneuver. Now denote all configuration variables prior to the k-th RS-DPT pair using subscript k. Then $(x_1, y_1, \theta_1, \alpha_1, \beta_1)$ denote the configuration variables prior to application of the first RS-DPT pair. The change in β during the k-th RS-DPT pair can be expressed as

$$\beta_{k+1} = \beta_k + \Delta\beta \tag{4.3}$$

where $\Delta\beta$ takes the values in Tables 4.1 and 4.2 for start configurations $P_{\psi'}$ and $N_{\psi'}$, respectively, based on the direction of sweep (cw or ccw) and type of end configuration $(P_{\psi} \text{ or } N_{\psi})$. From the entries in Tables 4.1 and 4.2 it is clear that $\Delta\beta$ is a function of

 θ_k , and parameters of the Sweep-Tuck algorithm, namely ψ and ψ' , or n and ψ . We now define the Compensating and Restoring Sweep (CRS) maneuver.

Definition 4.3 (CRS Maneuver) Among the four choices for an RS maneuver in a sweep-tuck sequence, the Compensating and Restoring Sweep (CRS) maneuver is the one that minimizes the absolute value of β .

Remark 4.1 Mathematically, for $n \in (1, \infty)$, the k-th RS maneuver $(k \ge 1)$ of a sweep-tuck sequence is a CRS maneuver if

$$\beta_{k+1} = \min_{\Delta \beta \in S} |\beta_k + \Delta \beta|, \qquad S = \{\Delta \beta_1, \Delta \beta_2, \Delta \beta_3, \Delta \beta_4\}$$
(4.4)

where $\Delta\beta_1$, $\Delta\beta_2$, $\Delta\beta_3$, and $\Delta\beta_4$ are the entries in Table 4.1 or Table 4.2 depending on whether the configuration variables, x_k , y_k , θ_k , α_k , define a $P_{\psi'}$ or an $N_{\psi'}$ configuration, respectively.

We now investigate the effect of a CRS maneuver for a $P_{\psi'}$ start configuration. The entries of S in Eq.(4.4) are taken from Table 4.1 and shown in Figure 4.2 in their relative order of magnitude, which was established in Eq.(4.1). The range of the set is found to be

$$(\psi + \psi') (1 - \sec \theta_k) \le S \le -(2\pi - \psi' + \psi) (1 - \sec \theta_k) \tag{4.5}$$

Suppose β_k lies in the range that is a mirror image of the range of S in Eq.(4.5). This implies

$$(2\pi - \psi' + \psi) \left(1 - \sec \theta_k\right) \le \beta_k \le -(\psi + \psi') \left(1 - \sec \theta_k\right) \tag{4.6}$$

Using Eqs.(4.5) and (4.6), the range of β_{k+1} can be obtained from Eq.(4.4). This range, shown in Figure 4.3(a), reveals that $\beta_{k+1} = 0$ when $\beta_k = -\Delta \beta_i$, i = 1, 2, 3, 4.

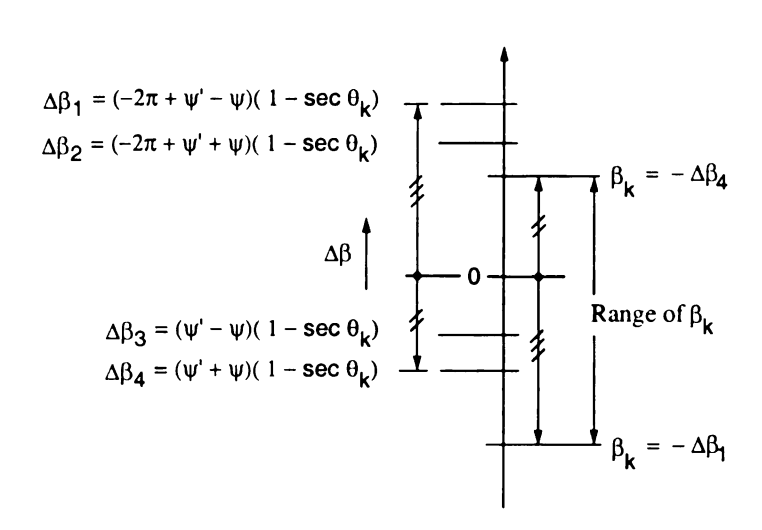


Figure 4.2. Range of β_k for starting $P_{\psi'}$ configuration

For other values of β_k in the range given by Eq.(4.6), β_{k+1} mostly varies linearly and $|\beta_{k+1}|$ reaches a local maxima of $-\psi$ $(1 - \sec \theta_k)$ when $\beta_k = (-\Delta \beta_1 - \Delta \beta_2)/2$ and $\beta_k = (-\Delta \beta_3 - \Delta \beta_4)/2$, and the global maxima of $(\psi - \pi)(1 - \sec \theta_k)$ when $\beta_k = (-\Delta \beta_2 - \Delta \beta_3)/2$. Since the global maxima of $|\beta_{k+1}|$ is $(\psi - \pi)(1 - \sec \theta_k)$, we can reduce the conservatism of the range of β_k in Eq.(4.6) by expanding it by $(\psi - \pi)(1 - \sec \theta_k)$ on both sides. The expanded range, deduced from Figure 4.3(a), is shown graphically in Figure 4.3(b). Mathematically, the expanded range can be expressed as follows

$$(3\pi - \psi')\left(1 - \sec \theta_k\right) \le \beta_k \le -(\pi + \psi')\left(1 - \sec \theta_k\right) \tag{4.7}$$

and it guarantees

$$|\beta_{k+1}| \le (\pi - \psi) \left(1 - \sec \theta_k\right) \tag{4.8}$$

The extended range of β_k in Eq.(4.7) pertains to a CRS maneuver with $P_{\psi'}$ start configuration. If the CRS maneuver has a $N_{\psi'}$ configuration, a similar set of results can be deduced. To obtain these results, the entries of S in Eq.(4.4) are first taken

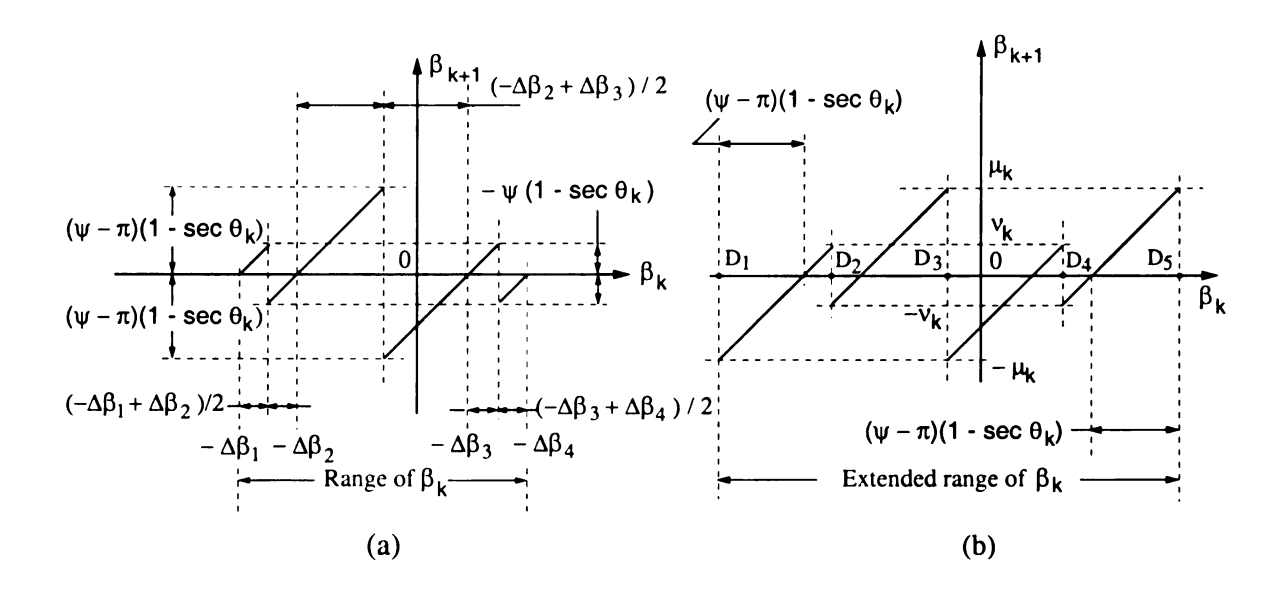


Figure 4.3. Expanded range of β_k for starting $P_{\psi'}$ configuration

from Table 4.2 and plotted in Figure 4.4 in their relative order of magnitude using Eq.(4.2). The range of the set is found to be

$$(2\pi - \psi' + \psi) (1 - \sec \theta_k) < S < -(\psi + \psi') (1 - \sec \theta_k)$$
(4.9)

As in the previous case, we again assume β_k to lie in the range that is a mirror image of the range of S in Eq.(4.9). This implies

$$(\psi + \psi') \left(1 - \sec \theta_k\right) \le \beta_k \le -(2\pi - \psi' + \psi) \left(1 - \sec \theta_k\right) \tag{4.10}$$

The application of Eq.(4.4) gives us the range of β_{k+1} when β_k is in the range given by Eq.(4.10). This range, shown in Figure 4.5(a), indicates that Eq.(4.8) holds good for $N_{\psi'}$ start configurations as well. The expanded range of β_k , shown in Figure 4.5(b), is obtained by increasing the range in Eq.(4.10) by $(\psi - \pi)(1 - \sec \theta_k)$ on both sides.

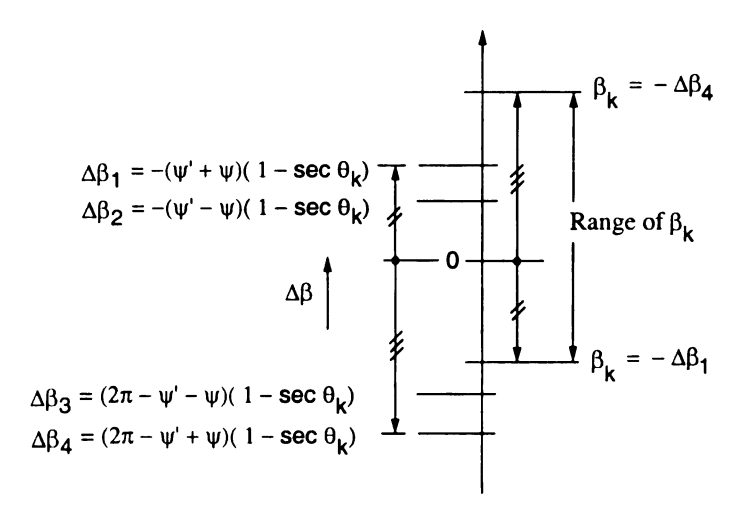


Figure 4.4. Range of β_k for starting $N_{\psi'}$ configuration

The expanded range of β_k for the $N_{\psi'}$ configuration is thus obtained as

$$(\pi + \psi') (1 - \sec \theta_k) \le \beta_k \le -(3\pi - \psi') (1 - \sec \theta_k)$$
 (4.11)

We are now summarize the results obtained above with the help of the following lemma.

Lemma 4.1 Consider a sweep-tuck sequence where the k-th RS maneuver $(k \ge 1)$ is a CRS maneuver. Then, if the configuration variables $(x_k, y_k, \theta_k, \alpha_k, \beta_k)$, define a $P_{\psi'}$ configuration and satisfy Eq. (4.7), or define a $N_{\psi'}$ configuration and satisfy Eq. (4.11), β_{k+1} will be bounded according to the relation given in Eq. (4.8).

Proof: The proof follows directly from the derivation above. $\diamond \diamond \diamond$

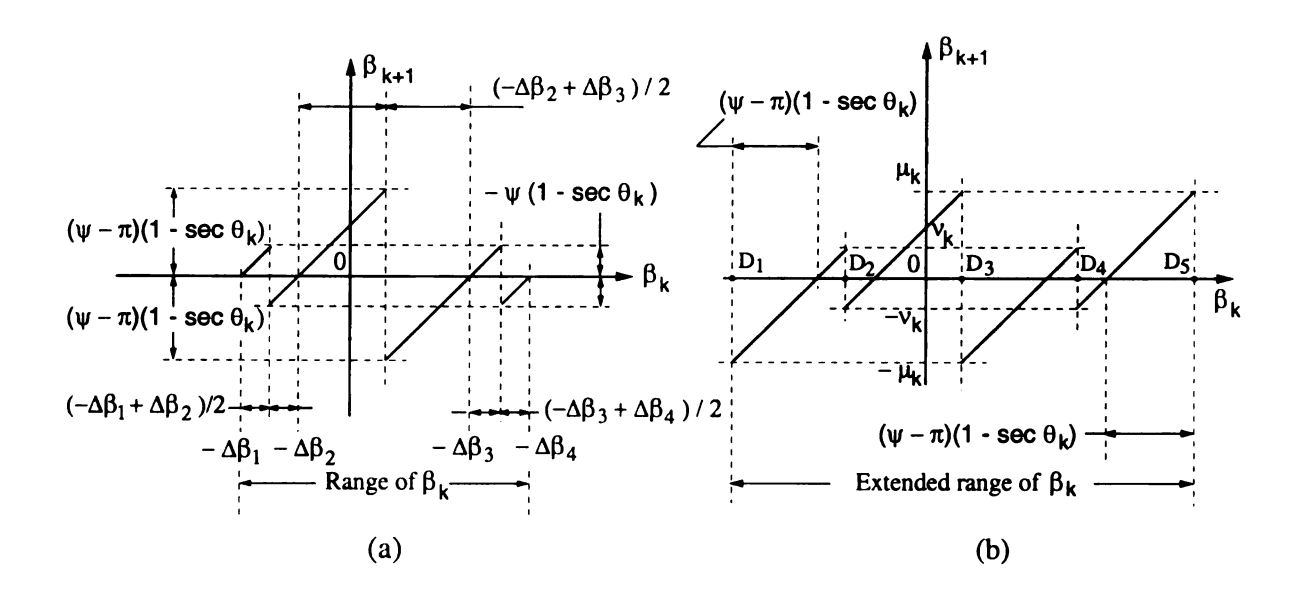


Figure 4.5. Expanded range of β_k for starting $N_{\psi'}$ configuration

4.4 Inequality Condition for Convergence

The bounds on β_{k+1} in Eq.(4.8) are valid for the expanded range of β_k in Eqs.(4.7) and (4.11) for $P_{\psi'}$ and $N_{\psi'}$ start configurations, respectively. Instead of considering the entire expanded range, we now consider the sub-intervals of β , D_1 - D_2 , D_2 - D_3 , D_3 - D_4 , and D_4 - D_5 , in Figures 4.3(b) and 4.5(b). The bounds on β_{k+1} for these sub-intervals are shown in Tables 4.3 and 4.4 for $P_{\psi'}$ and $N_{\psi'}$ start configurations. The values of μ_k and ν_k in Figures 4.3(b) and 4.5(b) and Tables 4.3 and 4.4 are as follows

$$\mu_k = (\psi - \pi) \left(1 - \sec \theta_k \right), \qquad \nu_k = -\psi \left(1 - \sec \theta_k \right) \tag{4.12}$$

Our next result is stated in Lemma 4.2, which is an extension of Lemma 4.1.

Lemma 4.2 Consider a sweep-tuck sequence where the k-th RS maneuver $(k \ge 1)$ is a CRS maneuver. Then, if the configuration variables $(x_k, y_k, \theta_k, \alpha_k, \beta_k)$, define a $P_{\psi'}$ configuration and satisfy Eq. (4.7), or define a $N_{\psi'}$ configuration and satisfy Eq. (4.11),

Starting From $P_{\psi'}$ Configuration										
Expanded	Expanded Range of β_k : $(3\pi - \psi')(1 - \sec \theta_k) \le \beta_k \le -(\pi + \psi')(1 - \sec \theta_k)$									
Sub-range	Compensating Final Direction Range of β_{k+1}									
of β_k	Δeta	Form								
$D_1 - D_2$	$-(2\pi - \psi' + \psi)(1 - \sec \theta_k)$	P_{ψ}	cw	$-\mu_k \le \beta_{k+1} \le \nu_k$						
$D_2 - D_3$	$-(2\pi - \psi' - \psi)(1 - \sec \theta_k)$	N_{ψ}	cw	$-\nu_k \le \beta_{k+1} \le \mu_k$						
$D_3 - D4$	$(\psi'-\psi)(1-\sec heta_k)$	P_{ψ}	ccw	$-\mu_k \le \beta_{k+1} \le \nu_k$						
D_4-D_5	$(\psi' + \psi)(1 - \sec \theta_k)$	N_{ψ}	ccw	$-\nu_k \le \beta_{k+1} \le \mu_k$						

Table 4.3. CRS maneuvers for different values of β_k for starting $P_{\psi'}$ configuration

 β_{k+1} will be bounded according to the relation

$$-\mu_k \le \beta_{k+1} \le \nu_k \tag{4.13}$$

if the CRS maneuver ends in a P_{ψ} configuration, and according to the relation

$$-\nu_k \le \beta_{k+1} \le \mu_k \tag{4.14}$$

if the CRS maneuver ends in a N_{ψ} configuration.

Proof: The proof follows directly from the entries in Tables 4.3 and 4.4. $\diamond \diamond \diamond$

Theorem 4.1 (First Reconfiguration Theorem) Consider the Sweep-Tuck algorithm for $n \in (1, \infty)$ and ψ satisfying Eq.(3.5). Assume $0 < \theta < \pi/2$ at the initial time, as required by the Sweep-Tuck algorithm. Let $k, k \geq 1$, be any integer for which the configuration variables $(x_k, y_k, \theta_k, \alpha_k, \beta_k)$ define a $P_{\psi'}$ configuration and satisfy Eq.(4.7) or define a $N_{\psi'}$ configuration and satisfy Eq.(4.11). If for all integer values of $j, j \geq k$, the j-th RS maneuver is a CRS maneuver and the inequality

$$\frac{(1 - \sec \theta_j)}{(1 - \sec \theta_{j+1})} \le \frac{(\pi + \psi')}{(\pi - \psi)} \tag{4.15}$$

Starting From $N_{\psi'}$ Configuration										
Expanded	Expanded Range of β_k : $(\pi + \psi')(1 - \sec \theta_k) \le \beta_k \le -(3\pi - \psi')(1 - \sec \theta_k)$									
Sub-range	Sub-range Compensating Final Direction Range of β_{k+1}									
of β_k	Δeta	Form	:							
$D_1 - D_2$	$-(\psi'+\psi)(1-\sec\theta_k)$	P_{ψ}	cw	$-\mu_k \le \beta_{k+1} \le \nu_k$						
$D_2 - D_3$	$-(\psi'-\psi)(1-\sec\theta_k)$	N_{ψ}	cw	$-\nu_k \le \beta_{k+1} \le \mu_k$						
$D_3 - D_4$	$(2\pi - \psi' - \psi)(1 - \sec \theta_k)$	P_{ψ}	ccw	$-\mu_k \le \beta_{k+1} \le \nu_k$						
$D_4 - D_5$	$(2\pi - \psi' + \psi)(1 - \sec \theta_k)$	N_{ψ}	ccw	$-\nu_k \le \beta_{k+1} \le \mu_k$						

Table 4.4. CRS maneuvers for different values of β_k for starting $N_{\psi'}$ configuration

is satisfied, then $(x_j, y_j, \theta_j, \beta_j) \to (0, 0, 0, 0)$ as $j \to \infty$ and the sphere is completely reconfigured.

Proof: We first note from Eqs.(3.20) and (3.21) and the third assertion in Theorem 3.1

$$\psi' \le \pi \quad \Longrightarrow \quad (3\pi - \psi') \ge (\pi + \psi') \tag{4.16}$$

$$\psi + \psi' \le \pi \implies 2\psi \le \pi \implies (\pi - \psi) \ge \psi$$
 (4.17)

Using the identities in Eqs.(4.16) and (4.17) we can deduce that Eq.(4.15) implies

$$\frac{(1 - \sec \theta_j)}{(1 - \sec \theta_{j+1})} \le \frac{(3\pi - \psi')}{(\pi - \psi)} \tag{4.18}$$

$$\frac{(1 - \sec \theta_j)}{(1 - \sec \theta_{j+1})} \le \frac{(\pi + \psi')}{\psi} \tag{4.19}$$

Using Eq.(4.12) we can show that Eqs.(4.18) and (4.19) imply

$$-\mu_i \ge (3\pi - \psi') (1 - \sec \theta_{i+1}) \tag{4.20}$$

$$-\nu_j \ge (\pi + \psi') (1 - \sec \theta_{j+1}) \tag{4.21}$$

We know that the k-th RS maneuver is a CRS maneuver. Also, $(x_k, y_k, \theta_k, \alpha_k, \beta_k)$

define a $P_{\psi'}$ configuration and satisfy Eq.(4.7) or define a $N_{\psi'}$ configuration and satisfy Eq.(4.11). Therefore, using Lemma 4.2 we claim that the CRS maneuver ends in a P_{ψ} configuration that satisfies Eq.(4.13) or an N_{ψ} configuration that satisfies Eq.(4.14). If the CRS maneuver ends in a P_{ψ} configuration, we can deduce the following from Eqs.(4.13) and (4.20)

$$-\mu_{k} \le \beta_{k+1} \le \nu_{k} \implies (3\pi - \psi') (1 - \sec \theta_{k+1}) \le \beta_{k+1} \le -(\pi + \psi') (1 - \sec \theta_{k+1})$$
(4.22)

The subsequent DPT maneuver, which results in a $P_{\psi'}$ configuration, therefore satisfies Eq.(4.7) for subscript k+1. If the CRS maneuver ends in a N_{ψ} configuration, we can deduce the following from Eqs.(4.14) and (4.21)

$$-\nu_{k} \le \beta_{k+1} \le \mu_{k} \implies (\pi + \psi') (1 - \sec \theta_{k+1}) \le \beta_{k+1} \le -(3\pi - \psi') (1 - \sec \theta_{k+1})$$
(4.23)

The subsequent DPT maneuver, which results in a $N_{\psi'}$ configuration , therefore satisfies Eq.(4.11) for subscript k+1.

Since the j-th RS maneuver is a CRS maneuver $\forall j \geq k+1$, Lemma 4.2 can be applied iteratively to the configuration variables $(x_j, y_j, \theta_j, \alpha_j, \beta_j)$, for integer values of $j = k+1, k+2, \cdots, \infty$. This implies that β_{j+1} will be bounded by one of the two relations

$$-\mu_{j} \leq \beta_{j+1} \leq \nu_{j}$$

$$-\nu_{j} \leq \beta_{j+1} \leq \mu_{j}$$

$$j = k+1, k+2, \cdots, \infty$$

$$(4.24)$$

From Corollary 3.1 we know that the Sweep-Tuck algorithm guarantees $\theta_j \to 0$ as $j \to \infty$. This implies $\mu_j, \nu_j \to 0$ and hence $\beta_j \to 0$ as $j \to \infty$. From Theorem 3.2 we already know that the Sweep-Tuck algorithm guarantees $(x_j, y_j, \theta_j) \to (0, 0, 0)$ as $j \to \infty$. This implies $(x_j, y_j, \theta_j, \beta_j) \to (0, 0, 0, 0)$ as $j \to \infty$ and the sphere is completely reconfigured. $\diamond \diamond \diamond$

4.5 Range of ψ for Inequality Condition

In this section we establish that the inequality condition in Eq.(4.15) is always satisfied for a subset of the range of ψ in Eq.(3.5) for $n \in (1, \infty)$. To this end, we first note from Eq.(3.20) that ψ and ψ' lie in the ranges $0 \le \psi < \cos^{-1}(1/n)$ and $\cos^{-1}(1/n) \le \psi' < \pi$, respectively. Using Eq.(3.19) we can readily show that $\psi' = \cos^{-1}(1/n)$ when $\psi = \cos^{-1}(1/n)$. Thus

$$\lim_{\psi \to \cos^{-1}(1/n)} \frac{(\pi + \psi')}{(\pi - \psi)} = \frac{\pi + \cos^{-1}(1/n)}{\pi - \cos^{-1}(1/n)} > 1$$
 (4.25)

Using Eq.(3.22) we can also show

$$\lim_{\psi \to \cos^{-1}(1/n)} \frac{C'F}{CF} = \lim_{\psi \to \cos^{-1}(1/n)} \frac{C'O}{CO} = \lim_{\psi \to \cos^{-1}(1/n)} \left[1 - 2(n\cos\psi - 1)/(n^2 - 1) \right] = 1$$
(4.26)

From Eqs.(3.3) and (4.26) we can therefore deduce that for $\psi \to \cos^{-1}(1/n)$,

$$\frac{\tan \theta_{j+1} - \theta_{j+1}}{\tan \theta_j - \theta_j} = 1 \qquad \Longrightarrow \qquad \theta_{j+1} = \theta_j \qquad \Longrightarrow \qquad \frac{1 - \sec \theta_{j+1}}{1 - \sec \theta_j} = 1 \tag{4.27}$$

From Eqs.(4.25) and (4.27) we conclude that there exists a Ψ , $0 \le \Psi < \cos^{-1}(1/n)$, such that Eq.(4.15) is always satisfied for $\Psi \le \psi < \cos^{-1}(1/n)$. We discuss the procedure for numerical computation of Ψ next.

To compute Ψ , we first determine the value of n from the initial conditions and choose ψ in conformity with Eq.(3.5). The value of ψ' is determined from Eq.(3.19) and we compute the ratio $(\pi + \psi')/(\pi - \psi)$. We determine the values to be assumed by θ in the sweep-tuck sequence and compute the ratios $(1 - \sec \theta_j)/(1 - \sec \theta_{j+1})$, $j = 1, 2, \dots, N$, where N is chosen based on the desired level of convergence. The

particular choice of ψ satisfies the inequality condition in Eq.(4.15) if

$$\max_{j \in [1, N]} \left\{ \frac{(1 - \sec \theta_j)}{(1 - \sec \theta_{j+1})} \right\} \le \frac{(\pi + \psi')}{(\pi - \psi)} \tag{4.28}$$

We start with an initial value of $\psi \approx \cos^{-1}(1/n)$ and verify the condition in Eq.(4.28) for each value of ψ as we reduce ψ in small increments. The value of Ψ is the smallest value of ψ for which Eq.(4.28) is satisfied. Since this procedure requires moderate computation and the exact value of Ψ is not critical, we determine an approximate value of Ψ using the analysis presented below.

Using Taylor's series expansion we can show $(\sec \theta - 1) \approx 1.5(\tan \theta - \theta)/\theta$. Thus, using Eqs.(3.3) and (3.22) and Corollary 3.1 we can write

$$\frac{(1 - \sec \theta_j)}{(1 - \sec \theta_{j+1})} \approx \frac{\theta_{j+1}}{\theta_j} \frac{(\tan \theta_j - \theta_j)}{(\tan \theta_{j+1} - \theta_{j+1})}$$

$$< \frac{(\tan \theta_j - \theta_j)}{(\tan \theta_{j+1} - \theta_{j+1})}$$

$$= \frac{CF}{C'F}$$

$$= \frac{1}{[1 - 2(n\cos \psi - 1)/(n^2 - 1)]}$$
(4.29)

Hence, Eq.(4.15) is satisfied if

$$\frac{1}{[1 - 2(n\cos\psi - 1)/(n^2 - 1)]} \le \frac{(\pi + \psi')}{(\pi - \psi)} \tag{4.30}$$

The value of Ψ can be computed easily from Eq.(4.30). Since θ does not appear in Eq.(4.30), Ψ can be computed apriori from the value of n alone and the data stored in a look-up table for quick reference. We have provided the value of Ψ in radians for specific values of n in Table 4.5 below.

We have also shown plots of the left-hand and right-hand sides of Eq. (4.15) for specific values of n in Figure 4.6. These results match well with the results in Table 4.5.

	1.1					l .		1			
Ψ	0.371	0.473	0.505	0.580	0.584	0.552	0.411	0.293	0.0	0.0	0.0

Table 4.5. Numerical values of Ψ for various $n \in (1, \infty)$

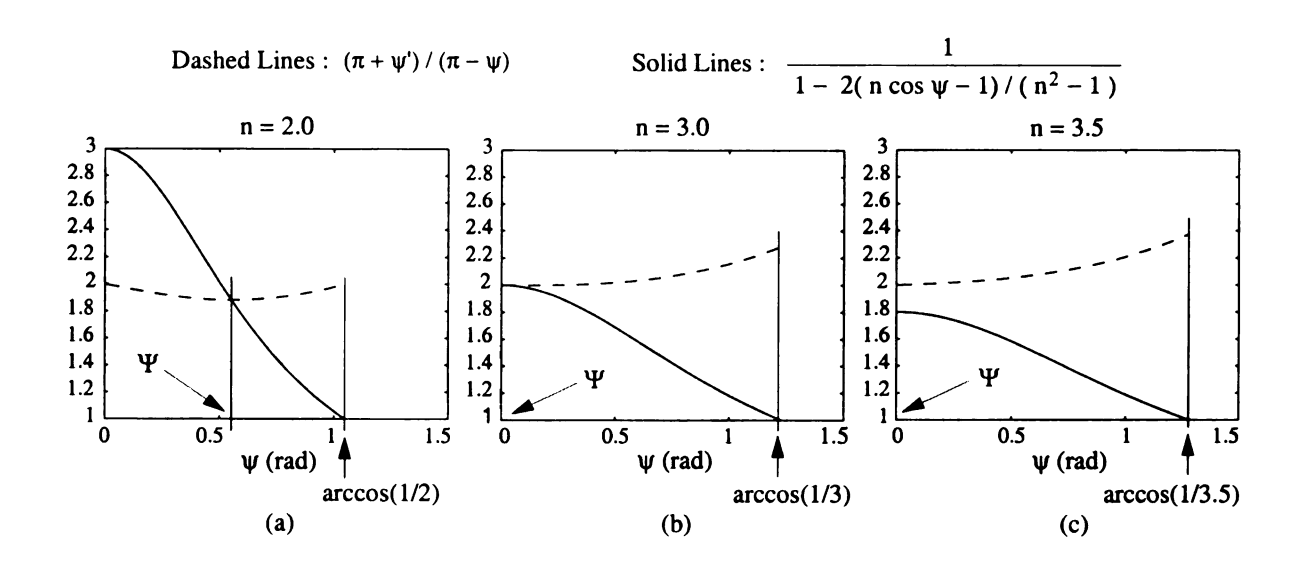


Figure 4.6. Angle Ψ for various values of $n \in (1, \infty)$

Based on the results above, we now state a corollary of Theorem 4.1:

Corollary 4.1 Consider the Sweep-Tuck algorithm for $n \in (1,\infty)$ and $\Psi \leq \psi \leq \cos^{-1}(1/n)$. At the initial time assume $0 < \theta < \pi/2$, as required by the Sweep-Tuck algorithm. Let $k, k \geq 1$, be any integer for which the configuration variables $(x_k, y_k, \theta_k, \alpha_k, \beta_k)$ define a $P_{\psi'}$ configuration and satisfy Eq.(4.7) or define a $N_{\psi'}$ configuration and satisfy Eq.(4.11). If for all integer values of $j, j \geq k$, the j-th RS maneuver is a CRS maneuver, then $(x_j, y_j, \theta_j, \beta_j) \rightarrow (0, 0, 0, 0)$ as $j \rightarrow \infty$ and the sphere is completely reconfigured.

Proof: The proof follows directly from Theorem 3 and the results above. $\diamond \diamond \diamond$

4.6 Preliminary Sweep Maneuver and Merging the Expanded Ranges

We assumed the initial configuration variables of the sphere to be $(x_0, y_0, \theta_0, \alpha_0, \beta_0)$ in section 4.3. We also assumed the configuration variables to be $(x_1, y_1, \theta_1, \alpha_1, \beta_1)$ after the PS maneuver which sets $\angle OCF = \psi'$. In this section we first investigate the change in β , $\Delta\beta = (\beta_1 - \beta_0)$, due to the PS maneuver.

Since the maximum angle of pre-sweep can be 2π , the maximum change in β due to the PS maneuver, $\Delta \beta_{max} = \max(\beta_1 - \beta_0)$, can be computed from Eq.(2.16) as follows

$$\Delta \beta_{max} = \pm 2\pi (1 - \sec \theta_0) \tag{4.31}$$

where the sign in Eq.(4.31) will be positive for ccw sweep and negative for cw sweep. The expanded range of β for subscript k = 0, for both Eqs.(4.7) and (4.11) is

$$W = \{(\pi + \psi') + (3\pi - \psi')\} (1 - \sec \theta_0) = 4\pi (1 - \sec \theta_0) \ge 2 |\Delta\beta|$$
 (4.32)

This implies that the direction of pre-sweep can be chosen suitably such that

$$(3\pi - \psi') (1 - \sec \theta_0) \le \beta_0 \le -(\pi + \psi') (1 - \sec \theta_0)$$

$$\implies (3\pi - \psi') (1 - \sec \theta_1) \le \beta_1 \le -(\pi + \psi') (1 - \sec \theta_1)$$
(4.33)

and

$$(\pi + \psi') (1 - \sec \theta_0) \le \beta_0 \le -(3\pi - \psi') (1 - \sec \theta_0)$$

$$\implies (\pi + \psi') (1 - \sec \theta_1) \le \beta_1 \le -(3\pi - \psi') (1 - \sec \theta_1)$$
(4.34)

Both Eqs.(4.33) and (4.34) are based on the fact that θ remains constant during a PS maneuver, that is, $\theta_1 = \theta_0$. We are now ready to define the "Proper Preliminary-

Sweep" (PPS) maneuver.

Definition 4.4 (PPS Manuever) A PS maneuver that satisfies Eq.(4.33) or Eq.(4.34) is said to be a "Proper Preliminary-Sweep" (PPS) maneuver.

We use the PPS maneuver to extend the results in Corollary 4.1 with Corollary 4.2 below.

Corollary 4.2 Consider the sphere in its initial configuration $(x_0, y_0, \theta_0, \alpha_0, \beta_0)$ with configuration variables satisfying $n \in (1, \infty)$, $0 < \theta_0 < \pi/2$, and β_0 in the range defined by Eq.(4.7) or (4.11) for subscript k = 0. The sphere can be completely reconfigured using a PPS maneuver followed by repeated application of CRS-DPT pairs with $\psi \in [\Psi, \cos^{-1}(1/n))$.

Proof: Since β_0 lies in the range given by Eq.(4.7) or (4.11), a PPS maneuver brings the sphere to a $P_{\psi'}$ configuration with β_1 satisfying Eq.(4.7) or a $N_{\psi'}$ configuration with β_1 satisfying Eq.(4.11). The complete reconfiguration of the sphere can now be proved using Corollary 4.1. $\diamond \diamond \diamond$

We conclude this section with Theorem 4.2, stated next.

Theorem 4.2 (Second Reconfiguration Theorem) Consider the sphere in its initial configuration $(x_0, y_0, \theta_0, \alpha_0, \beta_0)$ with the configuration variables satisfying $n \in (1, \infty)$, $0 < \theta_0 < \pi/2$, and β_0 in the range

$$(3\pi - \psi') (1 - \sec \theta_0) \le \beta_0 \le -(3\pi - \psi') (1 - \sec \theta_0)$$
(4.35)

The sphere can be completely reconfigured by a PPS maneuver followed by repeated application of CRS-DPT pairs with $\psi \in [\Psi, \cos^{-1}(1/n)]$.

Proof: From Eq.(3.20) we know $\psi' \leq \pi$. This implies $(\pi + \psi') \leq (3\pi - \psi')$ and $[-(3\pi - \psi'), (3\pi - \psi')] = [(\pi + \psi'), (3\pi - \psi')] \cup [-(3\pi - \psi'), (\pi + \psi')]$. Hence, satisfaction

of the condition in Eq.(4.35) guarantees β_0 lies in the range defined by Eq.(4.7) or (4.11) for subscript k = 0. The rest of the proof follows directly from Corollary 4.2. $\diamond \diamond \diamond$

The underlying idea for convergence of β can be understood with the help of the following illustration in Figure 4.7. Figure 4.7 is not an exact depiction of the conver-

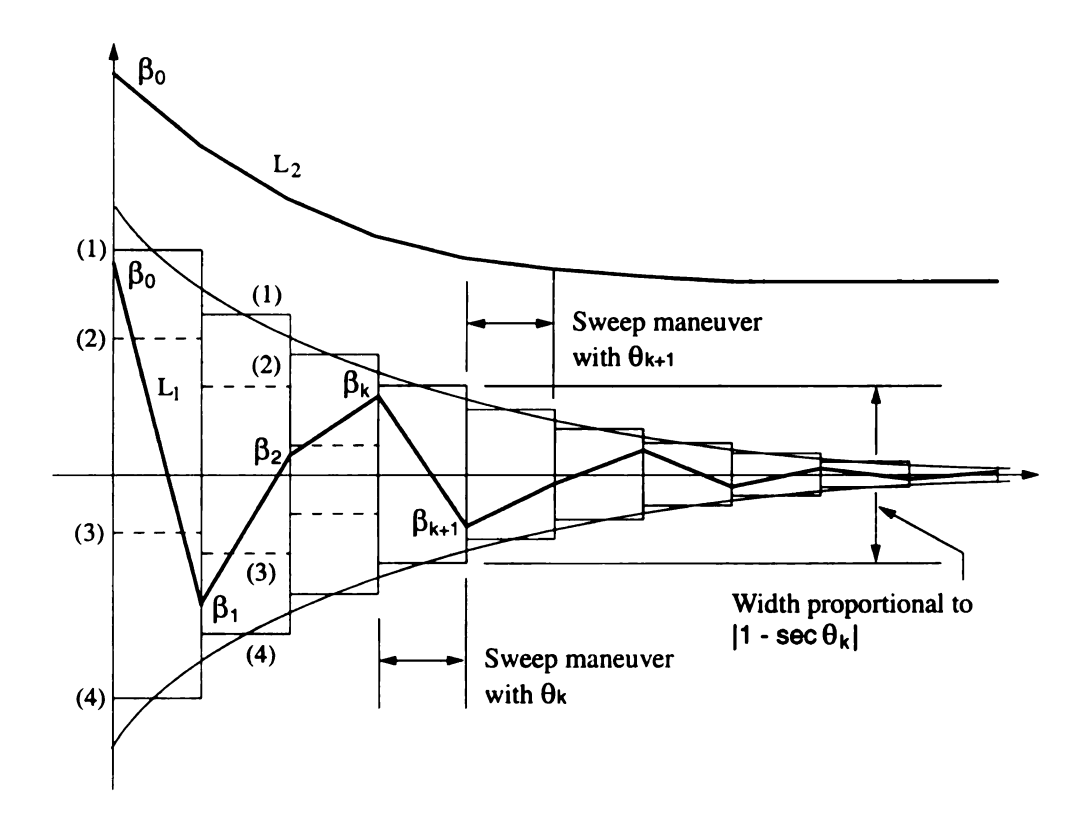


Figure 4.7. Convergence of β in Sweep-Tuck algorithm

gence of β but an approximate illustration of convergence of β . In figure 4.7 the steps represent successive sweeps. The four levels at each sweep given by (1), (2), (3), (4), represent the quadruple sweep options. The steps are diminishing in size since the Sweep-Tuck algorithm causes $\theta_{k+1} < \theta_k$. The diminishing steps form a diminishing envelope shown in figure 4.7. By imposing the range condition in Eq.(4.35) and by satisfying the inequality condition in Eq.(4.15), β is restricted to lie within this enve-

lope and eventually converge to zero. This shown by the trajectory L_1 . On the other hand if β does not satisfy Eq.(4.35), β converges to a non-zero value as shown in L_2 .

4.7 Simulation Results

We present simulation results for complete reconfiguration when $n \in (1, \infty)$. The initial configuration of the sphere is taken as follows:

$$x = -2.0$$
 $y = 0.5$ $\theta = 1.2$ $\alpha = 3.0$ $\beta = -3.0$ (4.36)

where the units are in meters and radians. From the definition of n in Theorem 3.1 and Eqs.(3.2) and (3.3) we obtain n=2.436. We choose ψ at 30% of the permissible range $\Psi \leq \psi < \cos^{-1}(1/n)$. The simulation results are given in Figure 4.8. Figure 4.8(a) shows the simultaneous convergence of C and F to the origin. Initially β satisfies Eq.(4.7) and hence a PPS maneuver sweeps F in a cw sense to the point F_1 whereby the sphere attains a $P_{\psi'}$ configuration. Subsequently, CRS-DPT maneuvers are successively applied. The point F is not clear in Figure 4.8(a) since the CRS manuever immediately after the PPS maneuver retraces the arc FF_1 in a ccw sense and goes beyond the point F. Figures 4.8(b), 4.8(c), and 4.8(d) show the convergence of x and y coordinates of x0, the convergence of x1, and that of x2 respectively, with time to origin. Hence, from Eq.(2.14), this leads to complete reconfiguration of the sphere.

In Figure 4.8(b), the linear and curved segments in the x and y plots are due to the DPT and CRS maneuvers respectively. Also, in Figure 4.8(d), the intervals when β remains constant correspond to DPT maneuvers. During CRS maneuvers θ remains constant, as shown in Figure 4.8(c), and β changes linearly which is consistent with Eq.(2.16). The PPS maneuver causes the change of β_0 to β_1 , however $\theta_1 = \theta_0$, which

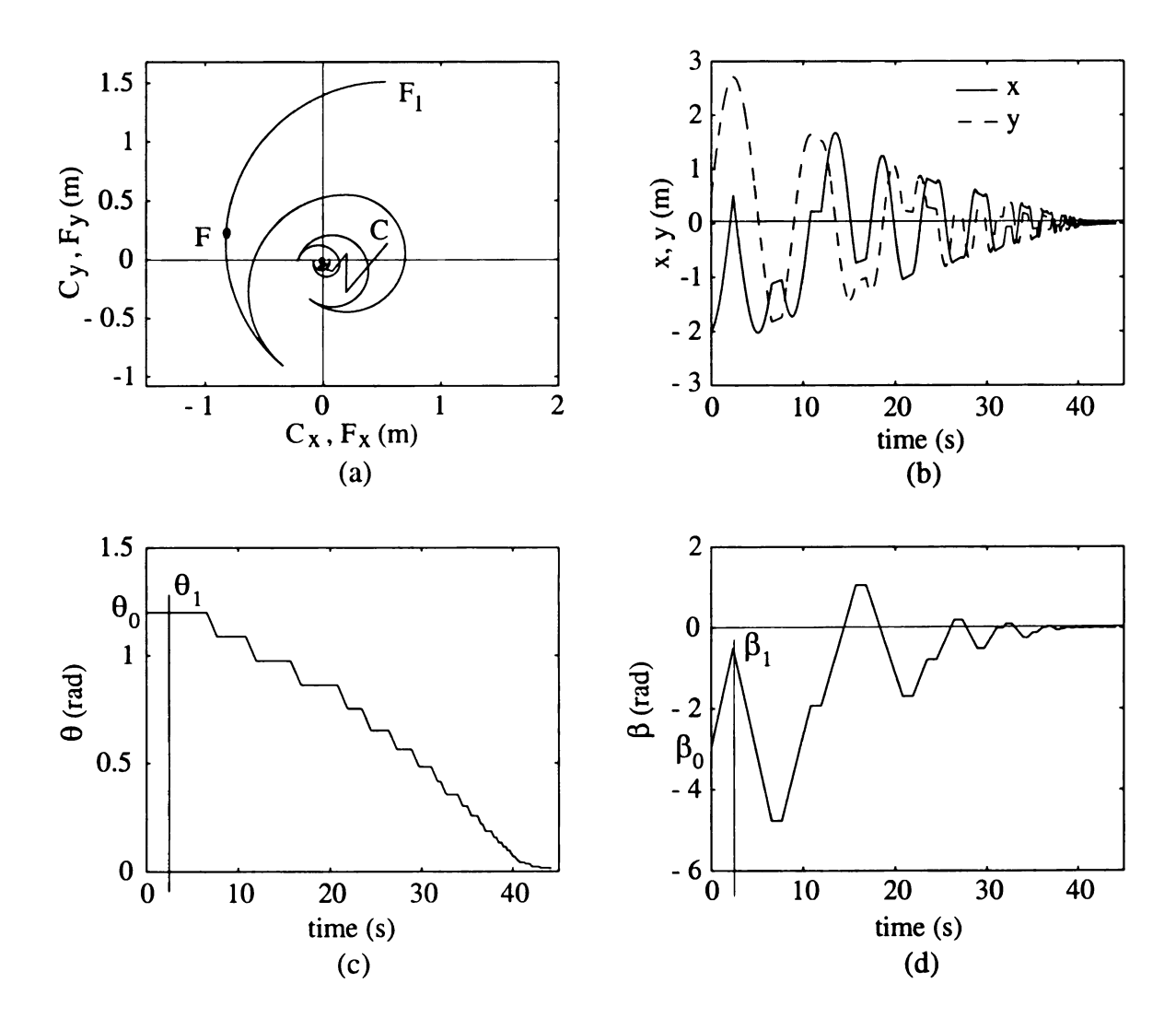


Figure 4.8. Complete reconfiguration: simulation results for $n \in (1, \infty)$

complies with the definition of PPS maneuver in Definition 4.4.

CHAPTER 5

Complete Reconfiguration:

Convergence Studies for $n \in (0,1)$

5.1 Quadruple Sweep Options

Similar to our investigation in section 4.2, we first investigate the change in β for the sweep options during an RS maneuver. For a $P_{\psi'}$: $\{C', F\}$ start configuration, as shown in Figure 5.1(a), the sweep options are

- 1. a cw sweep ending at P_{ψ} : $\{C', F_p\}$,
- 2. a cw sweep ending at N_{ψ} : $\{C', F_n\}$,
- 3. a ccw sweep ending at P_{ψ} : $\{C', F_p\}$, and
- 4. a ccw sweep ending at N_{ψ} : $\{C', F_n\}$

It can be verified that $\Delta\beta$ for these options are the same as the entries of Table 4.1, which pertains to the case $n \in (1, \infty)$. For a $N_{\psi'}$: $\{C', F\}$ start configuration, as shown in Figure 5.1(b), the values of $\Delta\beta$ are similarly identical to the entries of Table 4.2, which pertains to the case $n \in (1, \infty)$.

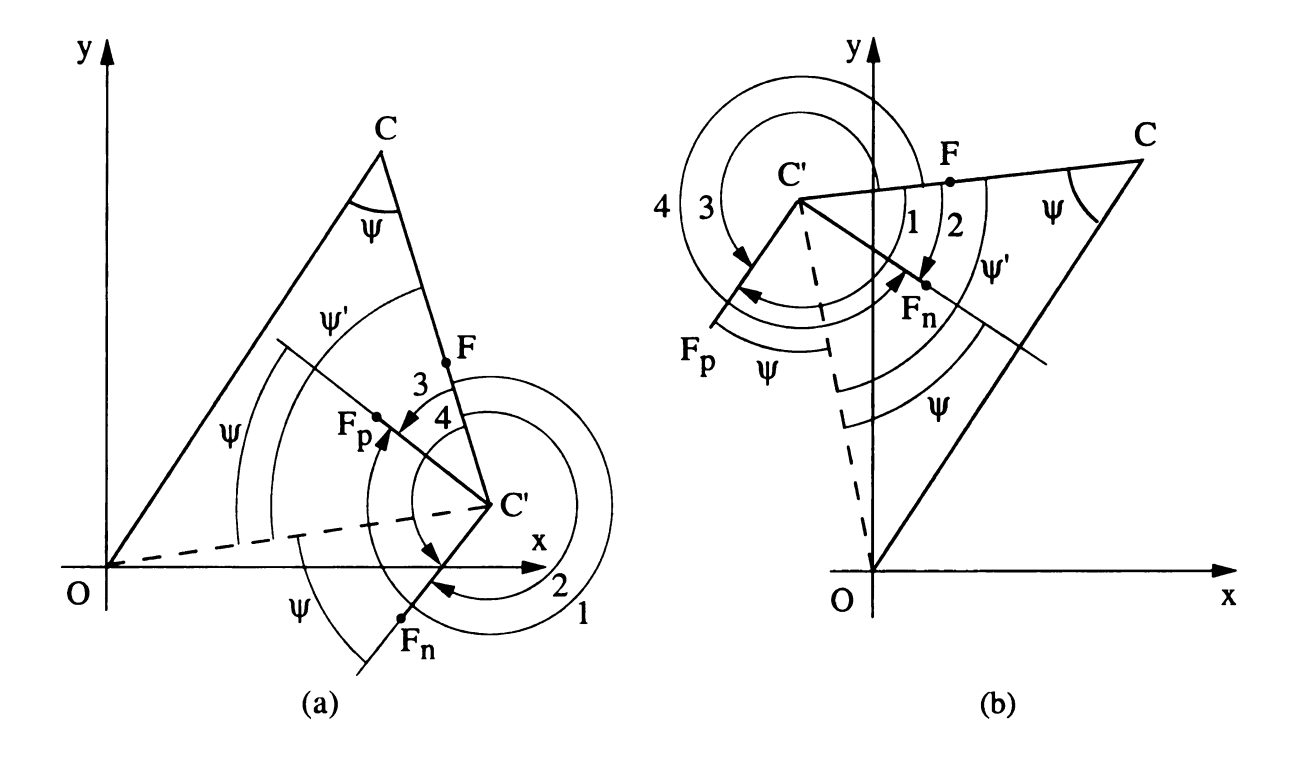


Figure 5.1. Quadruple sweep options: $n \in (0,1)$

5.2 CRS Maneuvers and Inequality Condition for Convergence

Since values of $\Delta\beta$ for the quadruple sweep options of an RS maneuver are the same for the cases $n \in (1, \infty)$ and $n \in (0, 1)$, for both $P_{\psi'}$ and $N_{\psi'}$ start configurations, the entire discussion in section 4.3 and part of the discussion in section 4.4 applies to the present case of $n \in (0, 1)$. By following the discussion in these sections it becomes clear that

- Lemmas 1 and 2 are applicable to both cases $n \in (1, \infty)$ and $n \in (0, 1)$.
- The statement of Theorem 3 is essentially applicable to the present case $n \in (0,1)$, but the proof needs to be modified.

Remark 5.1 The main difference between the cases $n \in (1, \infty)$ and $n \in (0, 1)$ arises from difference in their DPT maneuvers. From Eqs. (3.14) and (3.15) we know that CC' < CF for $n \in (1, \infty)$ and CC' > CF for $n \in (0, 1)$. This implies that DPT maneuvers change a P_{ψ} configuration into a $P_{\psi'}$ configuration and a N_{ψ} configuration for $n \in (1, \infty)$, but for $n \in (0, 1)$ it changes a P_{ψ} configuration into a $N_{\psi'}$ configuration and a N_{ψ} configuration into a $P_{\psi'}$ configuration. For the case $n \in (0, 1)$, the effect of a DPT maneuver can be verified from Figures 5.1(a) and 5.1(b) where N_{ψ} : $\{C, F\}$ changes to $P_{\psi'}$: $\{C', F\}$ and P_{ψ} : $\{C, F\}$ changes to $N_{\psi'}$: $\{C', F\}$, respectively.

We now state and prove the equivalent of Theorem 4.1 for the case $n \in (0,1)$.

Theorem 5.1 (Parallel of Theorem 4.1) Consider the Sweep-Tuck algorithm for $n \in (0,1)$ with ψ chosen to satisfy Eq.(3.5). Assume $0 < \theta < \pi/2$ at the initial time, as required by the Sweep-Tuck algorithm. Let $k, k \geq 1$, be any integer for which the configuration variables $(x_k, y_k, \theta_k, \alpha_k, \beta_k)$ define a $P_{\psi'}$ configuration and satisfy Eq.(4.7) or define a $N_{\psi'}$ configuration and satisfy Eq.(4.11). If for all integer values of $j, j \geq k$, the j-th RS maneuver is a CRS maneuver and the inequality

$$\frac{(1 - \sec \theta_j)}{(1 - \sec \theta_{j+1})} \le \frac{(\pi + \psi')}{(\pi - \psi)} \tag{5.1}$$

is satisfied, then $(x_j, y_j, \theta_j, \beta_j) \to (0, 0, 0, 0)$ as $j \to \infty$ and the sphere is completely reconfigured.

Proof: Using the identities in Eqs.(4.16) and (4.17) we can deduce that Eq.(5.1) implies

$$\frac{(1 - \sec \theta_j)}{(1 - \sec \theta_{j+1})} \le \frac{(\pi + \psi')}{(\pi - \psi)} \tag{5.2}$$

$$\frac{(1 - \sec \theta_j)}{(1 - \sec \theta_{j+1})} \le \frac{(3\pi - \psi')}{\psi} \tag{5.3}$$

From the definition of μ and ν in Eq.(4.12) we can show that Eqs.(5.2) and (5.3) imply

$$-\mu_{i} \ge (\pi + \psi') (1 - \sec \theta_{i+1}) \tag{5.4}$$

$$-\nu_j \ge (3\pi - \psi') (1 - \sec \theta_{j+1}) \tag{5.5}$$

We know that the k-th RS maneuver is a CRS maneuver. Also, $(x_k, y_k, \theta_k, \alpha_k, \beta_k)$ define a $P_{\psi'}$ configuration and satisfy Eq.(4.7) or define a $N_{\psi'}$ configuration and satisfy Eq.(4.11). Therefore, using Lemma 4.2 we claim that the CRS maneuver ends in a P_{ψ} configuration that satisfies Eq.(4.13) or an N_{ψ} configuration that satisfies Eq.(4.14). If the CRS maneuver ends in a P_{ψ} configuration, we can deduce from Eqs.(4.13) and (5.4)

$$-\mu_{k} \le \beta_{k+1} \le \nu_{k} \implies (\pi + \psi') (1 - \sec \theta_{k+1}) \le \beta_{k+1} \le -(3\pi - \psi') (1 - \sec \theta_{k+1})$$
(5.6)

The subsequent DPT maneuver, which results in a $N_{\psi'}$ configuration, therefore satisfies Eq.(4.11) for subscript k+1. If the CRS maneuver ends in an N_{ψ} configuration, we can deduce from Eqs.(4.14) and (5.5)

$$-\nu_{k} \le \beta_{k+1} \le \mu_{k} \implies (3\pi - \psi') (1 - \sec \theta_{k+1}) \le \beta_{k+1} \le -(\pi + \psi') (1 - \sec \theta_{k+1})$$
(5.7)

The subsequent DPT maneuver, which results in a $P_{\psi'}$ configuration, therefore satisfies Eq.(4.7) for subscript k + 1.

Since the j-th RS maneuver is a CRS maneuver $\forall j \geq k+1$, Lemma 4.2 can be applied iteratively to the configuration variables $(x_j, y_j, \theta_j, \alpha_j, \beta_j)$, for integer values of $j = k+1, k+2, \dots, \infty$. This implies that β_{j+1} will be bounded by one the two

relations

$$-\mu_j \le \beta_{j+1} \le \nu_j$$

$$-\nu_j \le \beta_{j+1} \le \mu_j$$

$$j = k+1, k+2, \dots, \infty$$

$$(5.8)$$

From Corollary 3.1 we know that the Sweep-Tuck algorithm guarantees $\theta_j \to 0$ as $j \to \infty$. This implies $\mu_j, \nu_j \to 0$ and hence $\beta_j \to 0$ as $j \to \infty$. From Theorem 3.2 we already know that the Sweep-Tuck algorithm guarantees $(x_j, y_j, \theta_j) \to (0, 0, 0)$ as $j \to \infty$. This implies $(x_j, y_j, \theta_j, \beta_j) \to (0, 0, 0, 0)$ as $j \to \infty$ and the sphere is completely reconfigured. $\diamond \diamond \diamond$

5.3 Range of ψ for Inequality Condition

Here we establish that the inequality condition in Eq.(5.1) is always satisfied for a subset of the range of ψ in Eq.(3.5) for $n \in (0,1)$. To this end, we first note from Eq.(3.20) that ψ and ψ' lie in the ranges $0 \le \psi < \cos^{-1}(1/n)$ and $\cos^{-1}(1/n) \le \psi' < \pi$, respectively. Using Eq.(3.19) we can readily show that $\psi' = \cos^{-1}(n)$ when $\psi = \cos^{-1}(n)$. Thus

$$\lim_{\psi \to \cos^{-1}(n)} \frac{(\pi + \psi')}{(\pi - \psi)} = \frac{\pi + \cos^{-1}(n)}{\pi - \cos^{-1}(n)} > 1$$
 (5.9)

Using Eqs. (3.16) and (3.22) we can also show

$$\lim_{\psi \to \cos^{-1}(n)} \frac{C'F}{CF} = \lim_{\psi \to \cos^{-1}(n)} \frac{C'O}{CO} = \lim_{\psi \to \cos^{-1}(n)} - \left[1 - 2(n\cos\psi - 1)/(n^2 - 1)\right] = 1$$
(5.10)

From Eqs.(3.3) and (5.10) we can therefore deduce that for $\psi \to \cos^{-1}(n)$,

$$\frac{\tan \theta_{j+1} - \theta_{j+1}}{\tan \theta_j - \theta_j} = 1 \qquad \Longrightarrow \qquad \theta_{j+1} = \theta_j \qquad \Longrightarrow \qquad \frac{1 - \sec \theta_{j+1}}{1 - \sec \theta_j} = 1 \quad (5.11)$$

From Eqs.(5.9) and (5.11) we conclude that there exists a Ψ , $0 \leq \Psi < \cos^{-1}(n)$, such

$\lceil n \rceil$	0.9	0.8	0.7	0.6	0.5	0.4	0.33	0.3	0.25	0.2	0.1
Ψ	0.387	0.505	0.569	0.588	0.552	0.411	0.0	0.0	0.0	0.0	0.0

Table 5.1. Numerical values of Ψ for various $n \in (0,1)$

that Eq.(5.1) is always satisfied for $\Psi \leq \psi < \cos^{-1}(n)$. Using the same procedure in section 4.5, Ψ can be numerically computed from the approximate relation

$$\frac{-1}{[1 - 2(n\cos\psi - 1)/(n^2 - 1)]} \le \frac{(\pi + \psi')}{(\pi - \psi)} \tag{5.12}$$

Equation (5.12) is very similar to Eq.(4.30) in section 4.5. The difference in sign can be explained with the help of Eqs.(3.16) and (3.22). As mentioned in section 4.5, the value of Ψ can be computed apriori from the value of n alone and the data stored in a look-up table for quick reference. We have provided the value of Ψ in radians for specific values of n in Table 5.1 below. We have also shown plots of the left-hand and right-hand sides of Eq.(5.1) for specific values of n in Figure 5.2. These results match well with the results in Table 5.1.

Based on the results above, we now state a corollary of Theorem 5.1:

Corollary 5.1 (Parallel of Corollary 4.1) Consider the Sweep-Tuck algorithm for $n \in (0,1)$ and $\Psi \leq \psi \leq \cos^{-1}(n)$. At the initial time assume $0 < \theta < \pi/2$, as required by the Sweep-Tuck algorithm. Let $k, k \geq 1$, be any integer for which the configuration variables $(x_k, y_k, \theta_k, \alpha_k, \beta_k)$ define a $P_{\psi'}$ configuration and satisfy Eq.(4.7) or define a $N_{\psi'}$ configuration and satisfy Eq.(4.11). If for all integer values of j, $j \geq k$, the j-th RS maneuver is a CRS maneuver, then $(x_j, y_j, \theta_j, \beta_j) \rightarrow (0, 0, 0, 0)$ as $j \rightarrow \infty$ and the sphere is completely reconfigured.

Proof: The proof follows directly from Theorem 5.1 and the results above. $\diamond \diamond \diamond$

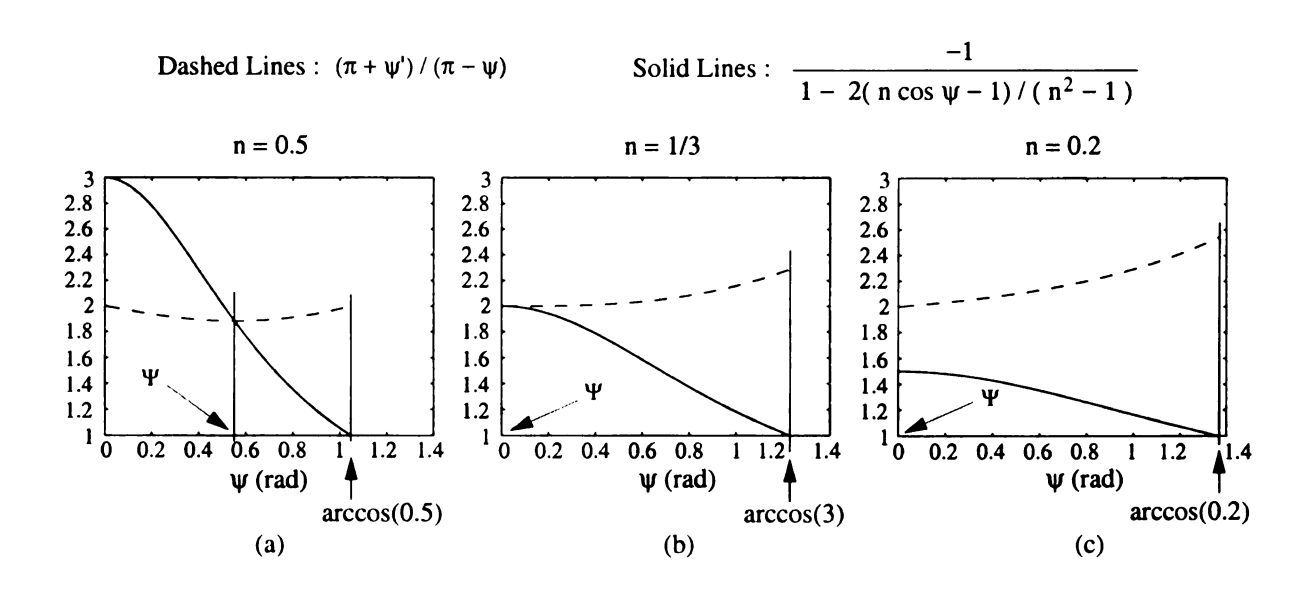


Figure 5.2. Angle Ψ for various values of $n \in (0,1)$

5.4 Preliminary Sweep Maneuver and Merging the Expanded Ranges

We use the PPS maneuver to extend the results in Corollary 5.1 with Corollary 5.2 below.

Corollary 5.2 (Parallel of Corollary 4.2) Consider $(x_0, y_0, \theta_0, \alpha_0, \beta_0)$ to be the initial configuration of the sphere satisfying $n \in (0,1)$, $0 < \theta_0 < \pi/2$, and β_0 in the range defined by Eq.(4.7) or (4.11) for subscript k = 0. The sphere can be completely reconfigured using a PPS maneuver followed by repeated application of CRS-DPT pairs with $\psi \in [\Psi, \cos^{-1}(n)]$.

Proof: Since β_0 satisfies lies in the range given by Eq.(4.7) or (4.11), a PPS maneuver brings the sphere to a $P_{\psi'}$ configuration with β_1 satisfying Eq.(4.7) or a $N_{\psi'}$ configuration with β_1 satisfying Eq.(4.11). The complete reconfiguration of the sphere can now be proved using Corollary 5.1. $\diamond \diamond \diamond$

We conclude this section with Theorem 5.2, stated next.

Theorem 5.2 (Parallel of Theorem 4.2) Consider $(x_0, y_0, \theta_0, \alpha_0, \beta_0)$ to be the initial configuration of the sphere satisfying $n \in (0,1)$, $0 < \theta_0 < \pi/2$, and β_0 in the range

$$(3\pi - \psi') (1 - \sec \theta_0) \le \beta_0 \le -(3\pi - \psi') (1 - \sec \theta_0)$$
 (5.13)

The sphere can be completely reconfigured by a PPS maneuver followed by repeated application of CRS-DPT pairs with $\psi \in [\Psi, \cos^{-1}(n)]$.

Proof: The proof is based on the results of Corollary 5.2 and is exactly similar to the proof of Theorem 4.2 which is based on the results of Corollary 4.2. $\diamond \diamond \diamond$

5.5 Simulations

We present simulation results for complete reconfiguration when $n \in (0,1)$. The initial configuration of the sphere is chosen as follows:

$$x = 5.5$$
 $y = 1.5$ $\theta = 1.2$ $\alpha = \pi/2$ $\beta = 2.5$ (5.14)

where the units are in meters and radians. From the definition of n in Theorem 3.1 and Eqs.(3.2) and (3.3) we obtain n = 0.244. We choose ψ at 50% of the permissible range $\Psi \leq \psi < \cos^{-1}(n)$. The simulation results are given in Figure 5.3. Figure 5.3(a) shows the simultaneous convergence of C and F to the origin. Initially β satisfies Eq.(4.7) and hence a PPS maneuver sweeps F in a cw sense to the point F_1 whereby the sphere attains a $P_{\psi'}$ configuration. Subsequently, CRS-DPT maneuvers are successively applied. Figures 5.3(b), 5.3(c), and 5.3(d) illustrate the convergence of x and y coordinates of x0, the convergence of x1, and that of x2 respectively, to the origin. Hence, from Eq.(2.14), this leads to complete reconfiguration of the sphere.

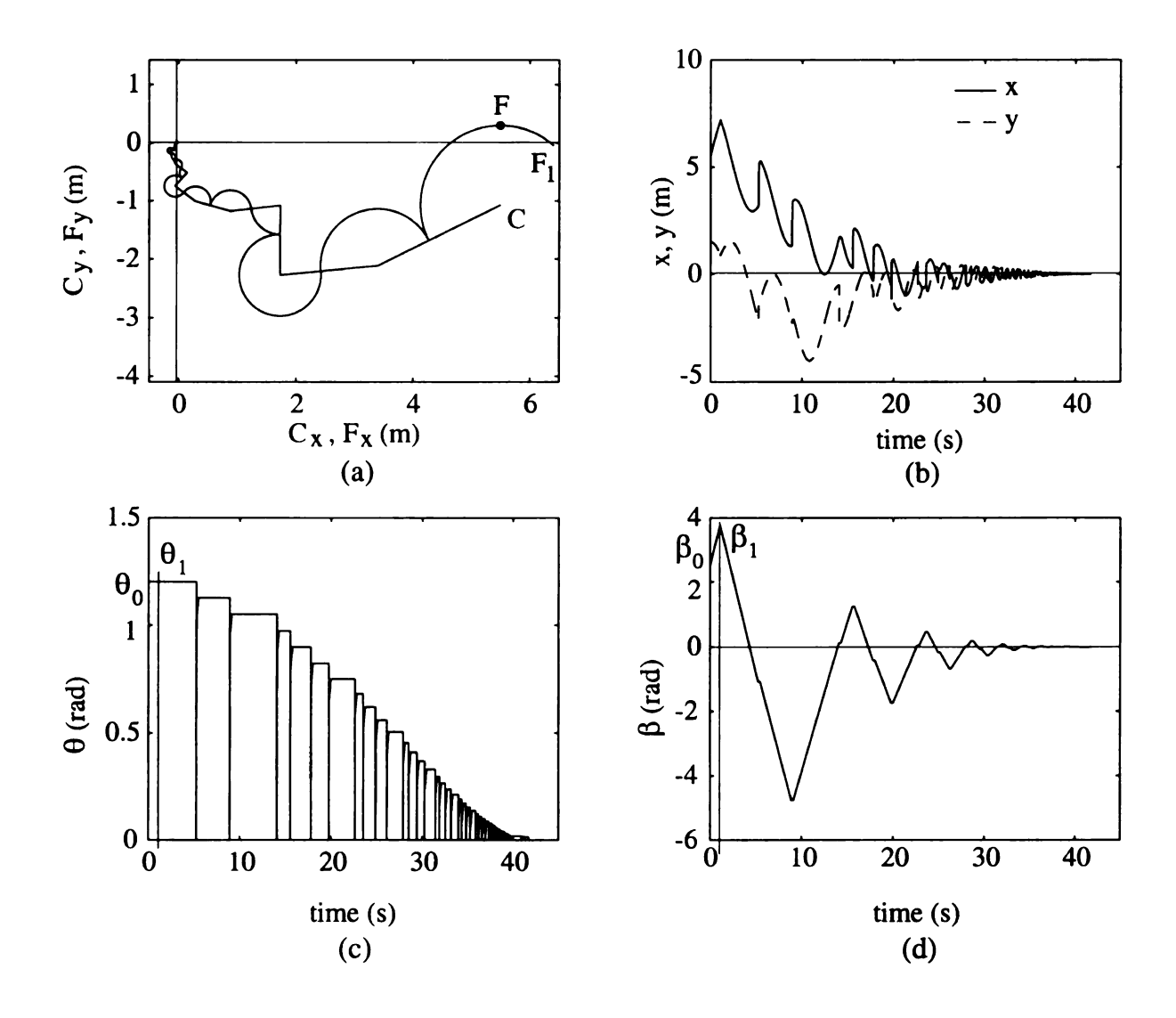


Figure 5.3. Complete reconfiguration: simulation results for $n \in (0,1)$

In Figure 5.3(b), the linear and curved segments in the x and y plots are due to the DPT and CRS maneuvers respectively. The linear segments are steeper and longer as compared to those in Figure 4.8(b). This is justified since, for $n \in (0,1)$, DPT maneuvers are longer (as can be inferred from Remark 3.2) and in the simulation we choose to apply a faster angular speed ω_1^y to execute them. In Figure 5.3(d), the intervals when β remains constant correspond to DPT maneuvers. The choice of higher angular speed for the DPT maneuver is again apparent from the small intervals. During CRS maneuvers θ remains constant, as shown in Figure 5.3(c), and

 β changes linearly which is consistent with Eq.(2.16). The PPS maneuver causes the change of β_0 to β_1 , however $\theta_1 = \theta_0$, which complies with the definition of PPS maneuver in Definition 4.4.

CHAPTER 6

Tuck-Out Maneuver and Special Cases

6.1 Tuck-Out Maneuver

From Theorem 4.2 and Theorem 5.2 we know that for completely reconfiguring the sphere by a PPS maneuver and repeated CRS-DPT pairs, Eq.(5.13) must be satisfied. Let us define ξ such that

$$\xi = \begin{cases} \cos^{-1}\left(\frac{1}{n}\right) & \text{for } n \in (1, \infty) \\ \cos^{-1}(n) & \text{for } n \in (0, 1) \end{cases}$$

$$(6.1)$$

The range in Eq.(5.13) is a function of ψ' , and is a maximum when ψ' is minimum. From Eq.(3.20), for a given n, ψ' is minimum when $\psi' = \xi$. Thus, the maximum range of β_0 , for a given n, is

$$(3\pi - \xi) (1 - \sec \theta_0) \le \beta_0 \le -(3\pi - \xi) (1 - \sec \theta_0)$$
(6.2)

If eta_0 lies in this range then there always exists a sub-range of ψ given by

$$\bar{\psi} \le \psi < \xi \tag{6.3}$$

 $\Psi \leq \bar{\psi}$, where Eq.(5.13) is satisfied. Hence if the initial configuration of the sphere satisfies Eq.(6.2) then the conditions for complete reconfiguration, in Theorem 4.2 or Theorem 5.2 are satisfied for $n \in (1, \infty)$ or $n \in (0, 1)$ cases respectively. However, if β_0 lies outside the range of Eq.(6.2), that is, if

$$|\beta_0| \ge (3\pi - \xi)(\sec \theta_0 - 1) \tag{6.4}$$

then Theorem 4.2 or Theorem 5.2 are not applicable.

Without any loss of generality we can assume that $|\beta_0| \leq \pi$. Let us define θ^* such that

$$|\beta_0| = (3\pi - \xi)(\sec \theta^* - 1) \tag{6.5}$$

Since $|\beta_0|$ satisfies Eq.(6.4), therefore $\theta^* > \theta_0$. Also, let us define $|\beta^*|$ such that

$$|\beta^*| = (3\pi - \xi)(\sec \theta_0 - 1)$$

From the expression of $|\beta^*|$ clearly $|\beta^*| \leq |\beta_0|$. In order to satisfy Eq.(6.2), we must either reduce $|\beta_0|$ to $|\beta^*|$ or increase θ_0 to θ^* . The former can be achieved by a control action (B). During the control action (B), recalling Eq.(2.16),

$$\Delta\beta = \Delta\alpha(1 - \sec\theta_0)$$

and if $\Delta\beta$ is finite, then

$$\lim_{\theta_0 \to 0} \frac{\Delta \beta}{1 - \sec \theta_0} = \pm \infty$$

We infer that for a given $\Delta\beta$, as θ_0 reduces $\Delta\alpha$ increases which leads to greater angular sweep of F about C. Further, if $\theta_0 = 0$, this control action becomes ineffective. On the other hand, a control action (A) can be applied to increase θ_0 to θ^* while maintaining β at β_0 . This is shown below in Figure 6.1. To increase θ , the point C moves away

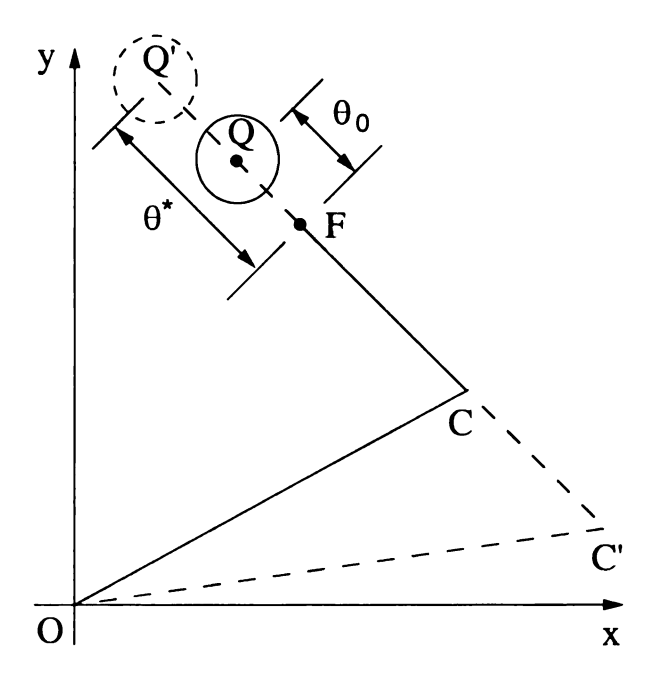


Figure 6.1. The tuck-out maneuver

from F. However, we observe in Figure 6.1 that $(CF/CO) \neq (C'F/C'O)$ and hence the value of n changes during this maneuver. It is therefore incorrect to determine θ^* using the relation in Eq.(6.5), where ξ is a function of n given by Eq.(6.1). However, we can choose a conservative value of θ^* such that

$$|\beta_0| \le (3\pi - \xi)(\sec \theta^* - 1) \quad \forall \ n$$

We set $\xi = \frac{\pi}{2}$, i.e, n = 0 or $n = \infty$. Then we have the maximum and the most

conservative value of θ^* for a given β_0 as follows

$$|\beta_0| = \left(3\pi - \frac{\pi}{2}\right)(\sec\theta^* - 1) \quad \Rightarrow \quad \theta^* = \cos^{-1}\left(\frac{2.5\pi}{2.5\pi + |\beta_0|}\right)$$
 (6.6)

If $\theta_0 \ge \theta^*$ then Eq.(6.2) is satisfied for any value of n. Note that $|\beta_0||_{max} = \pi$. Hence,

$$\theta^*_{max} = \cos^{-1}\left(\frac{2.5\pi}{2.5\pi + \pi}\right) = 0.7752 \text{ rad} \equiv 44.4153^{\circ}$$
 (6.7)

If $\theta_0 < \theta^*$, an initial control action (A) is required. If $\theta_0 \ge \theta^*$, the initial control action (A) is not required and if in addition $\theta_0 \ge \theta^*_{max}$, then Eq.(6.2) is satisfied for any β_0 and irrespective of the value of n. We observe that the maximum change in θ during this control action (A) can be $\Delta\theta = \theta^*_{max} - 0 = 44.4153^\circ$, which implies a finite motion and a relatively small distance of travel for the sphere. We define this special control action (A) below:

Definition 6.1 (Tuck-Out Maneuver) If at the initial time θ_0 and β_0 are such that $\theta_0 < \theta^*$, where θ^* is given by Eq.(6.6), a control action (A) is applied to increase the value of θ to θ^* . We define this control action as the "Tuck-Out" (TO) maneuver.

At the end of a TO maneuver, Eq.(6.2) is satisfied which ensures that the conditions on β_0 in Theorem 4.2 and Theorem 5.2 are satisfied and complete reconfiguration can be achieved. The effect of the TO maneuver can be understood clearly with the help of the following illustration in Figure 6.2 which is similar to Figure 4.7. In figure 6.2, β is initially outside the range V_1V_2 defined by Eq.(6.2) for the initial conditions. This will result in β converging to a non-zero value as shown by the trajectory in L_1 . A TO maneuver widens the range to W_1W_2 by increasing the value of θ to θ^* . This gives rise to a wider envelope and causes β_0 to lie within it. Further, a PPS maneuver followed by a sequence of CRS-DPT maneuver converges β to the origin, as shown in trajectory L_2 .

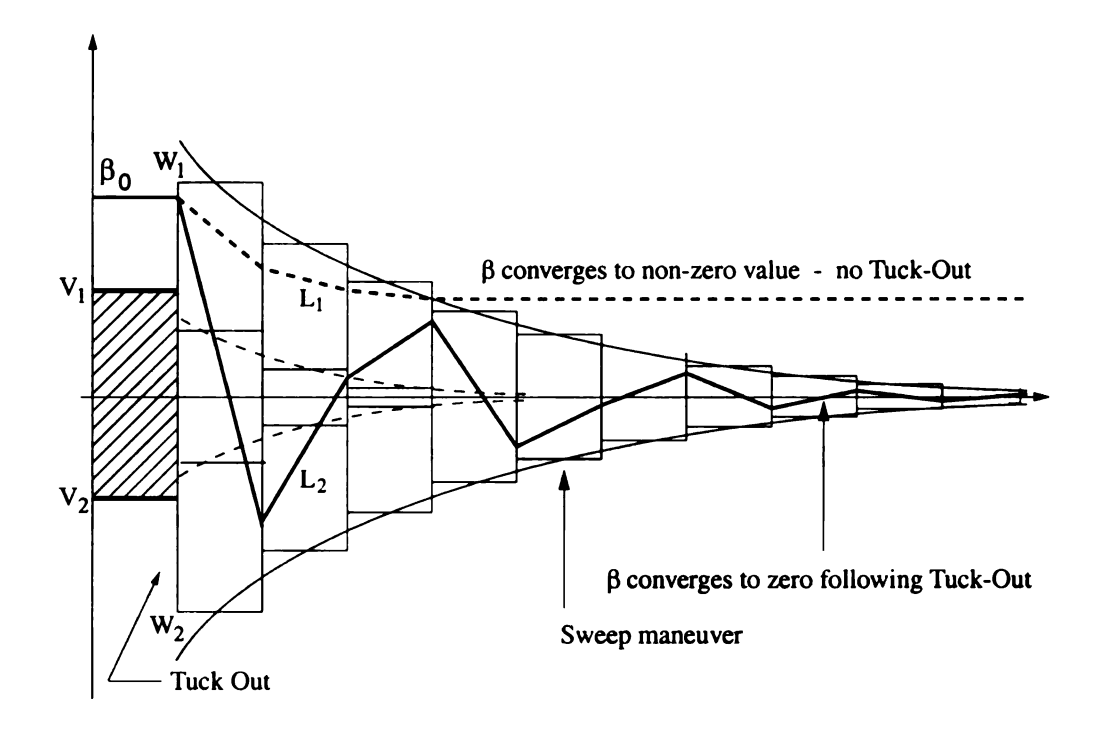


Figure 6.2. Convergence of β following the TO maneuver

We now state the third reconfiguration theorem which relaxes the condition on β_0 in Theorems 4.2 and 5.2 by incorporating the TO maneuver.

Theorem 6.1 (Third Reconfiguration Theorem) Consider the sphere in its initial configuration $(x_0, y_0, \theta_0, \alpha_0, \beta_0)$ with the configuration variables satisfying $n \in (0,1) \cup (1,\infty)$, $0 < \theta_0 < \pi/2$. If β_0 lies within the range

$$(3\pi - \xi) (1 - \sec \theta_0) \le \beta_0 \le -(3\pi - \xi) (1 - \sec \theta_0)$$
(6.8)

the sphere can be completely reconfigured by a PPS maneuver followed by repeated application of CRS-DPT pairs with $\psi \in [\Psi, \xi]$. If β_0 lies outside this range, the sphere can be completely reconfigured by first applying a TO maneuver followed by a PPS maneuver followed by repeated application of CRS-DPT pairs with $\psi \in [\max(\Psi, \bar{\psi}), \xi)$.

Proof: The proof follows directly from the discussion on the TO maneuver and from Theorems 4.2 and 5.2. $\diamond \diamond \diamond$

6.2 Special Cases

Until now we have considered the cases where the values of n due to initial conditions satisfy $n \in (0,1) \cup (1,\infty)$. The following special cases arising from initial conditions on the sphere require initial maneuvers that transform them to the general category of $n \in (0,1) \cup (1,\infty)$ whereby the result established in Theorem 6.1 can be applied for complete reconfiguration of the sphere. These initial maneuvers for the special cases are finite in number. The special cases are:

- (1) n = 1
- (2) $n=\infty$
- (3) n = 0
- (4) n: undefined
- (5) $\theta_0 > (\frac{\pi}{2} \epsilon)$ where ϵ is an arbitrarily small number.

6.2.1 Case: n = 1

We categorize our discussion of this special case into two sub-classes. They are:

- $\theta_0 < \theta^*$
- $\theta_0 \ge \theta^*$

If $\theta_0 < \theta^*$, we apply a TO maneuver. This increases the value of θ from θ_0 to θ^* . Although the value of n changes during this maneuver, Eq.(6.2) is satisfied for any

final value of n. Subsequently, with $n \neq 1$ and β_0 satisfying Eq.(6.2), complete reconfiguration can be achieved.

If $\theta_0 \geq \theta^*$, we do not require a TO maneuver. At the same time, from our discussion in section 3.3 we note that when n = 1, the Sweep-Tuck algorithm can not be applied for partial reconfiguration. We change the value of n using the following two steps:

- (1) Use control action (B) to make O, C, F co-linear and in that order.
- (2) Use control action (A) to change the value of n.

This is followed by application of the complete reconfiguration algorithm. Since $\theta_0 \geq \theta^*$, Eq.(6.2) is valid. It may be argued here that the action (B) can cause β_1 , the value of β after this control action, to go out of the range

$$(3\pi - \xi)(1 - \sec \theta_0) \le \beta_1 \le -(3\pi - \xi)(1 - \sec \theta_0) \tag{6.9}$$

However we note that the sweeping action (B) can be performed in a clockwise or counterclockwise sense giving rise to two options and hence two possible values of β_1 . This is shown in Figure 6.3. The control action ends with $\angle OCF = \pi$. The width of the permissible range of β_1 is

$$(6\pi - 2\xi)(\sec \theta_0 - 1) > (6\pi - 2\frac{\pi}{2})(\sec \theta_0 - 1)$$

> $5\pi(\sec \theta_0 - 1)$

The maximum change in β , $|\Delta\beta|_{max} = 2\pi(\sec\theta_0 - 1)$, since the maximum angle of sweep can be 2π . Hence we conclude that of the two options there exists at least one that keeps β_1 within the range in Eq.(6.9).

Next we apply a control action (A) to change the value of n. We consider the cases $\theta_0 > \theta^*$ and $\theta_0 = \theta^*$ separately. If $\theta_0 > \theta^*$ we choose to apply a control action

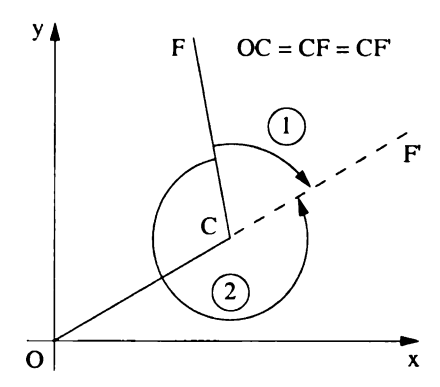


Figure 6.3. Preliminary control action (B) for n = 1

(A) to decrease θ from θ_0 to θ^* . This is because besides achieving $n \neq 1$ and $\theta_1 \geq \theta^*$ at the end of this control action, we also wish to impose an upper limit on the value of θ from where the reconfiguration algorithm is initiated. We impose

$$\theta_{lim} = \left(\frac{\pi}{2} - \epsilon\right)$$

where, we can choose ϵ to have an arbitrarily small value. As we shall see in our discussion on stability, the introduction of the upper bound θ_{lim} is especially helpful in proving stability of the equilibrium configuration. Thus, decreasing θ to θ^* ensures that $\theta_1 < \theta_{lim}$ since from Eq.(6.7), $\theta^*_{max} = 0.7752 < \pi/2$. On the other hand, if $\theta_0 = \theta^*$ we increase θ such that $\theta_1 \leq (\pi/2 - \epsilon)$. We choose θ_1 as follows

$$\theta_1 = k_1 \theta^* \quad \text{where} \quad 1 < k_1 \le k_{1max}, \quad k_{1max} = \frac{\pi/2 - \epsilon}{\theta^*_{max}} = \frac{\pi/2 - \epsilon}{0.7752}$$
 (6.10)

The choice of k_1 is done such that at the end of the control action (A) $n \neq \infty$.

6.2.2 Case: $n = \infty$

This case implies that initially the point C is coincident with the origin O so that CO = 0 and $CF \neq 0$. This is illustrated in Figure 6.4

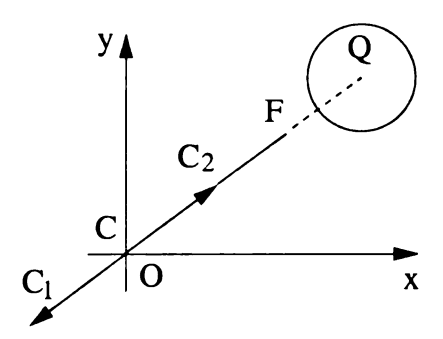


Figure 6.4. Preliminary control action (A) for $n = \infty$

As with n = 1, we categorize our discussion into two cases:

- $\theta_0 < \theta^*$
- $\theta_0 \geq \theta^*$

If $\theta_0 < \theta^*$, we apply the TO maneuver. This changes the value of n while increasing θ from θ_0 to θ^* . Subsequently the sphere can be completely reconfigured. On the other hand, if $\theta_0 \geq \theta^*$ we still require an action (A) to change the value of n. If, $\theta_0 > \theta^*$, the control action (A) decreases θ from θ_0 to θ^* and if $\theta_0 = \theta^*$, the control action (A) increase θ from θ_0 to θ_1 , where θ_1 is given by $\theta_1 = k_\infty \theta^*$. k_∞ is given by

$$k_{\infty} = \frac{\pi/2 - \epsilon}{\theta^*_{max}} = \frac{\pi/2 - \epsilon}{0.7752}$$
 (6.11)

which is the same as k_{1max} defined in the previous discussion on the special case of n=1.

6.2.3 Case: n = 0

This special case occurs when the points C and F are coincident, i.e. CF = 0, and $CO \neq 0$. This implies that $\theta_0 = 0$. If $|\beta_0| \neq 0$ then we require a TO maneuver to increase θ_0 to θ^* . Note that, here CF = 0, hence α can be chosen arbitrarily and the point C can move in any direction. We choose the direction along OF which makes C to move toward or away from the origin O. Consider Figure 6.5, which shows that C moves either to C_1 or to C_2 . We prefer C_1 since it ensures that the TO maneuver

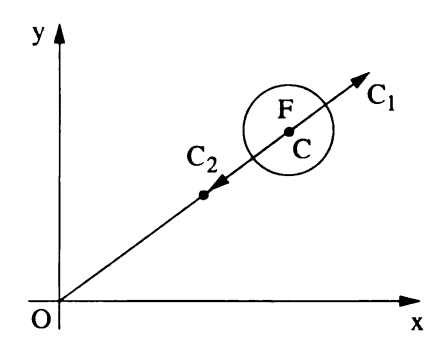


Figure 6.5. Preliminary control action (A) for n = 0

will not end with a special case of n = 1 or $n = \infty$.

If initially $\beta_0 = 0$, we still require a control action (A) to change the value of n since the Sweep-Tuck algorithm is not applicable to n = 0. This control action increases the value of θ from zero to θ_1 , where we choose θ_1 such that

$$\theta_{1} = \begin{cases} k_{0}|x_{0}, y_{0}| & \text{if } k_{0}|x_{0}, y_{0}| < \left(\frac{\pi}{2} - \epsilon\right) \\ \left(\frac{\pi}{2} - \epsilon\right) & \text{if } k_{0}|x_{0}, y_{0}| \ge \left(\frac{\pi}{2} - \epsilon\right) \end{cases}$$
(6.12)

where $|x_0, y_0| = \sqrt{x_0^2 + y_0^2}$ and k_0 is any chosen positive number. Choosing θ_1 and hence the control action in this way ensures that $\theta_1 \leq (\frac{\pi}{2} - \epsilon)$. Here again it is

preferred to move C to C_1 to prevent the final n from going to n=1 or $n=\infty$.

6.2.4 Case: n undefined

This case occurs when C, F and the origin O are coincident but $\beta_0 \neq 0$. We apply a TO maneuver to increase θ from zero to θ^* . Since α is arbitrary, C can move any arbitrary direction as shown in Figure 6.6. Also, note that after the TO maneuver,

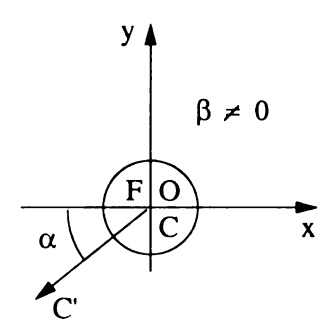


Figure 6.6. Preliminary control action (A) when n is undefined

we have n=1 and hence the steps described in subsection 6.2.1 are applied to change n from unity.

6.2.5 Case: $\theta_0 > (\frac{\pi}{2} - \epsilon)$

We have mentioned before that we restrict θ to $\theta \leq \left(\frac{\pi}{2} - \epsilon\right)$. Consider the case when $\theta_0 > \left(\frac{\pi}{2} - \epsilon\right)$. This shown in Figure 6.7 below. A preliminary control action (A) is applied that simply decreases θ from θ_0 to $\theta_m^* ax \leq \theta \leq \left(\frac{\pi}{2} - \epsilon\right)$. Since after the control action (A), $\theta \geq \theta^*_{max}$, hence we do not require a subsequent TO maneuver after this control action. The choice of final θ is made so that at the end of the preliminary control action, the special cases of n = 0, n = 1, $n = \infty$, and undefined

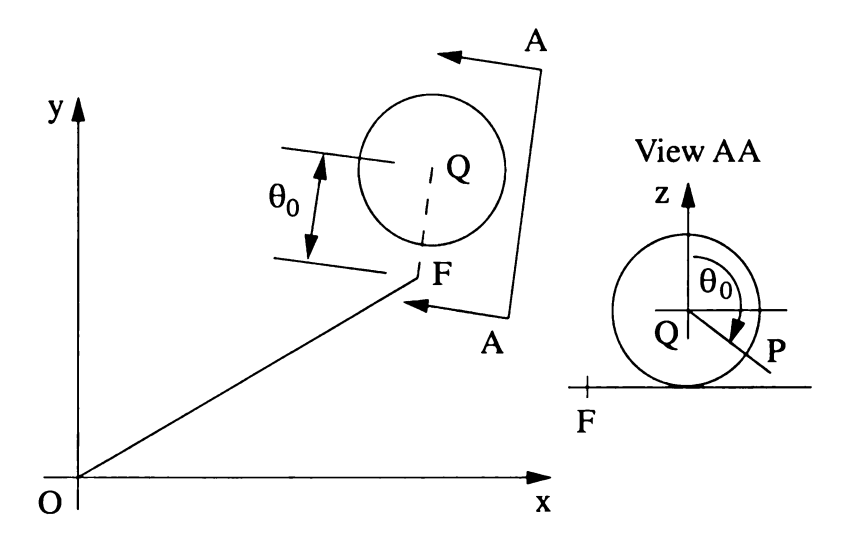


Figure 6.7. Configuration of sphere showing the case when $\theta_0 > (\frac{\pi}{2} - \epsilon)$

n are avoided.

6.3 Complete Reconfiguration Algorithm

In this section we assimilate the third reconfiguration theorem for $n \in (0,1) \cup (1,\infty)$ and the special cases in the form of a flow diagram as shown below. This flow diagram takes into account all possible initial conditions and gives a detailed illustration of how the complete reconfiguration algorithm functions. The preliminary maneuvers for the special cases are designed such that the special cases are transformed to the general category in finite number of control actions. The thicker lines in Figure 6.8 show the flow diagram for the general category of $n \in (0,1) \cup (1,\infty)$.

We now categorize all possible configurations of the sphere into finite number of "states" or configuration sets. We denote the vector of state variables by $\mathbb{X} = [x, y, \theta, \alpha, \beta]$, noting that $\mathbb{X} \in \mathbb{R}^5$. We categorize the configuration sets as follows:

(1) S_1 : $\{X \mid x=y=\theta=\beta=0\}$: Equilibrium configuration.

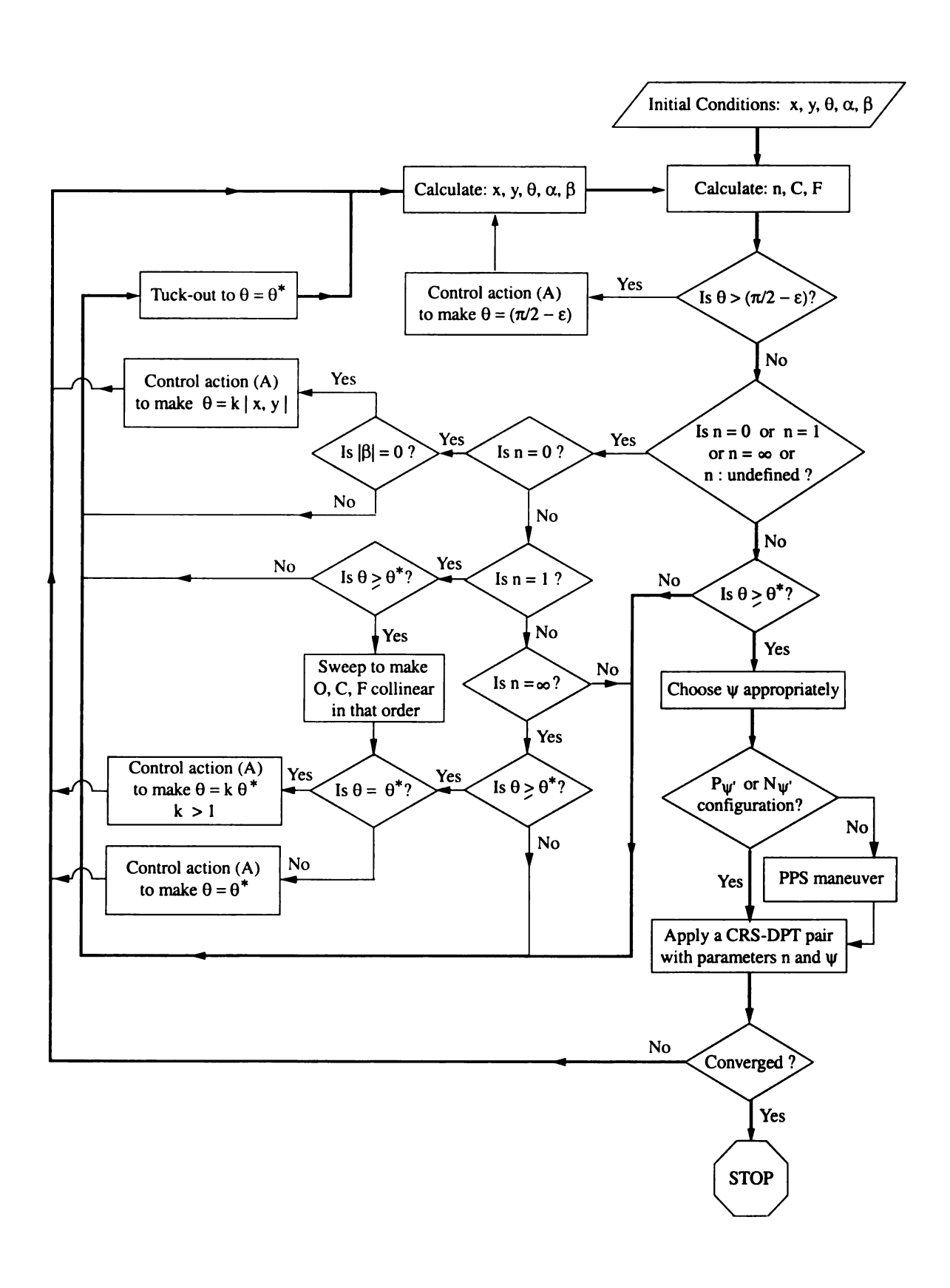


Figure 6.8. Flow diagram of the complete reconfiguration algorithm

(2)
$$S_2 : \{ X \mid \theta \ge \pi/2 \}$$

(3)
$$S_3 : \{ \mathbb{X} \mid \theta < \theta^* < \pi/2, \ n \in (0,1) \cup (1,\infty) \}$$

(4)
$$S_4$$
: $\{X \mid \theta^* \le \theta < \pi/2, n \in (0,1) \cup (1,\infty)\}$

(5)
$$S_5 : \{ \mathbb{X} \mid n = 0 \}$$

(6)
$$S_6$$
: {X | $n = 1$ }

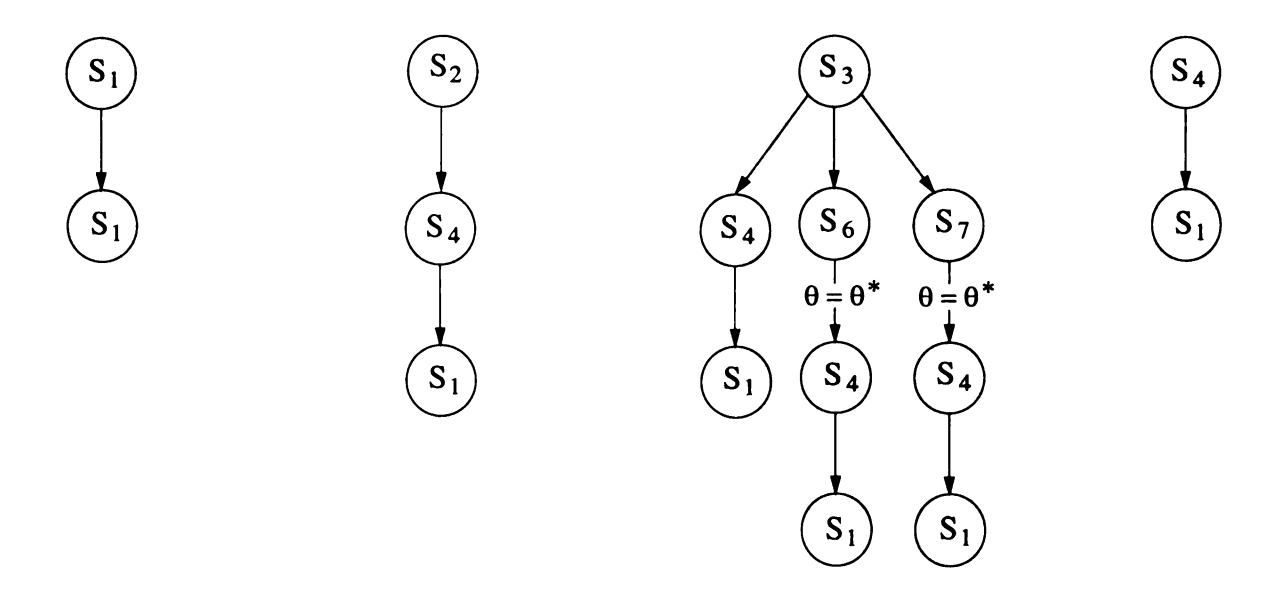
(7)
$$S_7 : \{X \mid n = \infty\}$$

(8)
$$S_8$$
: { $\mathbb{X} \mid n \text{ undefined}$ }

Based on the definitions of the configuration sets S_1 through S_8 we can readily infer that

$$S_1 \cup S_2 \cup S_3 \cup S_4 \cup S_5 \cup S_6 \cup S_7 \cup S_8 = R^5$$

The objective of complete reconfiguration is to drive the sphere from any on the configuration sets to S_1 . It can be verified by the reader that with finite and few transitions between the configuration sets S_2 through S_8 , the sphere achieves convergence to the equilibrium state given by S_1 . All possible transitions from individual states to the equilibrium configuration S_1 are illustrated in Figure 6.9. It is clear from Figure 6.9 that the intermediate states in transitions depend on the initial configuration set to which the sphere belongs. Moreover, the number of transitions to reach the equilibrium from any configuration set is finite and do not lead to any infinite loop. The expressions indicated between transitions are the conditions under which those transitions take place. For example, when the sphere is initially at state S_3 , the TO maneuver leads to either S_4 , S_6 , or S_7 with $\theta = \theta^*$ at the end of the transition. Whereas S_4 automatically leads to S_1 in the following transition, S_6 and S_7 first change to S_4 due to the condition $\theta = \theta^*$, which further transitions to S_1 .



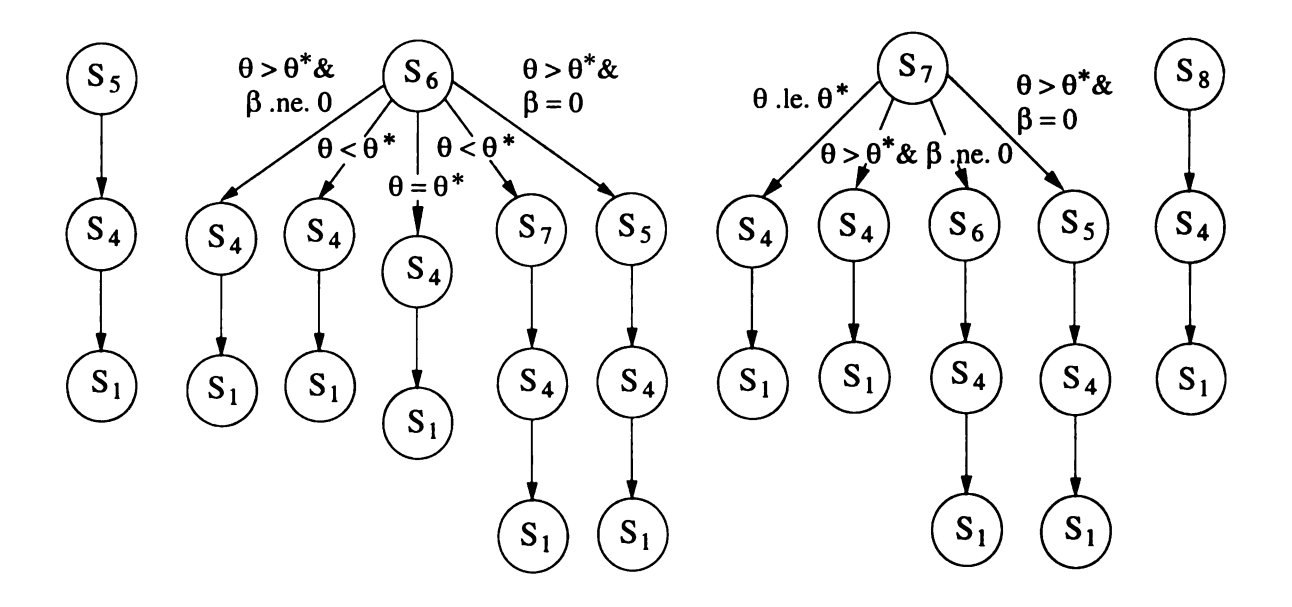


Figure 6.9. Diagram illustrating possible transitions from any initial configuration set to the equilibrium

6.4 Simulations

6.4.1 Tuck-Out Maneuver

We present simulation results to illustrate the TO maneuver followed by complete reconfiguration. The initial configuration of the sphere is chosen as

$$x = 1.0$$
 $y = 0.4$ $\theta = 0.7$ $\alpha = 0.5$ $\beta = -3.0$ (6.13)

where the units are in meters and radians. From the definition of n in Theorem 3.1 and Eqs.(3.2) and (3.3) we obtain n = 0.545. From Eq.(6.6), we obtain $\theta^* = 0.76$ and hence by Definition 6.1 an initial TO maneuver is necessary. The necessity of TO can also be confirmed by checking that Eq.(6.2) is not satisfied for the chosen initial conditions of this simulation. This is shown in the simulation results given in Figure 6.10.

In Figure 6.10(a) the TO maneuver can be identified as the motion of c to C_1 with F remaining unchanged during the maneuver. This is followed by the PPS maneuver when C is fixed and F sweeps to F_1 . Subsequently, the CRS-DPT pairs converge C and F simultaneously to the origin. Figure 6.10(b) shows the convergence of x and y coordinates of the center of the sphere Q to the origin. In Figure 6.10(c) the TO maneuver is best illustrated through the initial increase of θ to θ_1 . Although $\theta^* = 0.76$, we increase θ to $1.1\theta^* = 0.84$. The extra increment is to ensure that Eq.(6.2) is not satisfied just marginally and is helpful for computational purposes. β remains unaltered during the TO maneuver, as shown in Figure 6.10(d). At the end of the TO maneuver, the value of n changes to 2.111. With n = 2.111 and $\theta = 0.76$ we can verify that Eq.(6.2) is satisfied. We choose ψ at 20% of the permissible range $\Psi \leq \psi < \cos^{-1}(1/n)$ for completely reconfiguring the sphere.

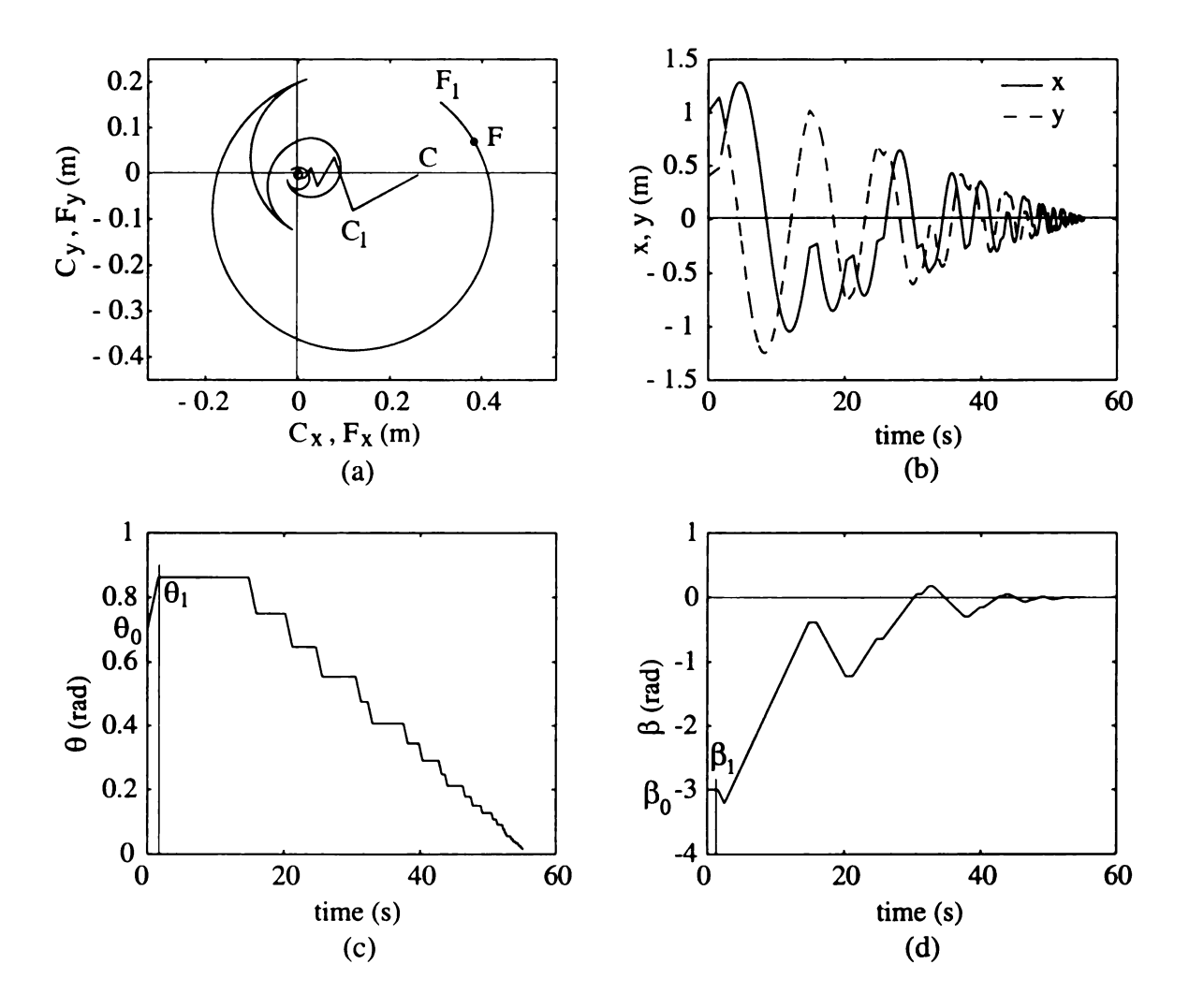


Figure 6.10. Tuck-Out maneuver and complete reconfiguration

6.4.2 Special Cases

We present simulation results to show complete reconfiguration from special cases. The first simulation has an undefined n as the initial condition. The initial configuration of the sphere is

$$x = 0.0$$
 $y = 0.0$ $\theta = 0.0$ $\alpha = arbitrary$ $\beta = 3.0$ (6.14)

where the units are in meters and radians. This configuration implies that initially C and F are at the origin but β is non-zero and hence the sphere is partially reconfigured. From Figure 2.2 we observe that α is the angle formed by the line CF with the x axis. In this special case since C and F are coincident, α is initially arbitrary. The simulation results are shown in Figure 6.11.

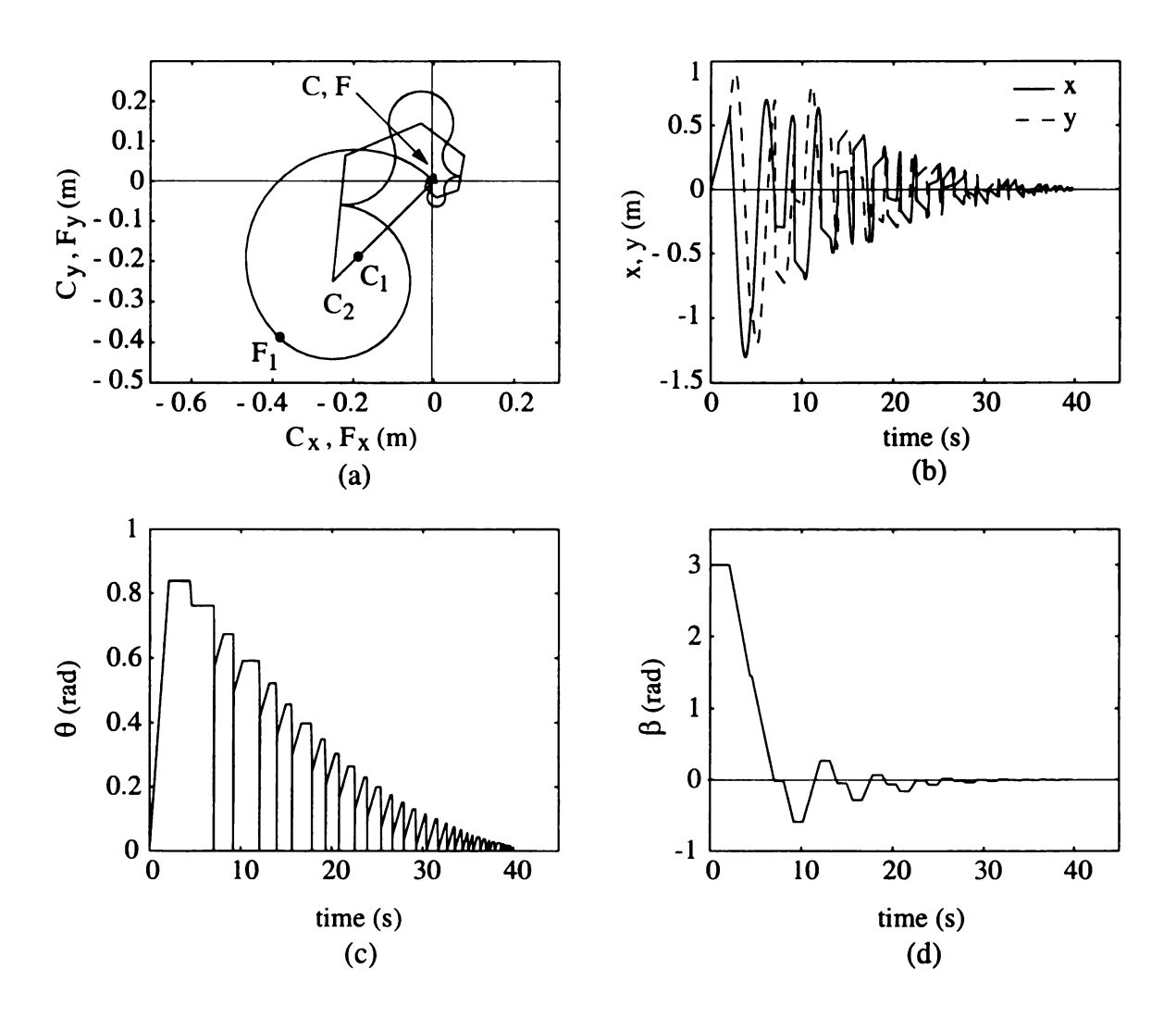


Figure 6.11. Complete reconfiguration from the special case of undefined n

In Figure 6.11(a) C and F are initially at the origin. α is arbitrarily chosen as

 $\pi/4$ and a control action (A) is applied which increases θ from zero to 0.84 and C moves to C_1 as shown in Figure 6.11(c) and Figure 6.11(a) respectively. For $|\beta| = 3.0$, the value of θ^* is 0.76 from Eq.(6.6). We modify the TO maneuver to increase θ to $1.1\,\theta^* = 0.84$ instead of θ^* . This helps in computation and maintains the stability of the equilibrium. At this stage the configuration of the sphere is transformed to the special case of n=1 with $\theta>\theta^*$ since F continues to lie at the origin and $\theta^*(=0.76) < 0.84$. Now O, C and F are made co-linear and in that order using a control action (B) as mentioned in section 6.2.1. This sweeps F about C_1 to the point F_1 . Since $\theta > \theta^*$, a control action (A) is applied that decreases θ to θ^* and the point C_1 goes to C_2 as shown in Figure 6.11(a). This changes the value of n from unity to 0.54. Now ψ is chosen as 0.7 which lies in the range $\psi \in [max(\Psi, \bar{\psi}), \xi)$. The rest of the simulation proceeds similar to the general category of $n \in (0,1) \cup (1,\infty)$ by applying a PPS maneuver followed by a series of CRS-DPT pairs. The convergence of x and y, θ , and β are shown in Figures 6.11(b), (c) and (d) respectively. x, y, and θ converge back to zero from their initial values of zero and in the process β is driven to zero resulting in complete reconfiguration from an initial partially reconfigured condition.

Next we present a simulation where initial conditions lead to the special case of n = 0. The initial configuration of the sphere is

$$x = 0.5$$
 $y = 0.5$ $\theta = 0.0$ $\alpha = \text{arbitrary}$ $\beta = -3.0$ (6.15)

where the units are in meters and radians. This configuration implies that initially C and F are coincident and hence, from Figure 2.2, α is initially arbitrary. The simulation results are shown in Figure 6.12.

In Figure 6.12(a), initially C and F are coincident. A control action (A) is applied that increases θ from zero to 0.84 as shown in Figure 6.12(b). Similar to the previous

simulation, the initial TO maneuver is modified to increase θ to $1.1\,\theta^*$ and hence the final value of θ after TO maneuver is 0.84 instead of 0.76 which is the value of θ^* for $|\beta| = 3$. The point C moves to C_1 during this control action, and results in n = 0.63. ψ is chosen as 0.667 which lies within the range $\psi \in [max(\Psi, \bar{\psi}), \xi)$ for n = 0.63. A PPS maneuver is applied that sweeps F to F_1 and subsequently a sequence of CRS-DPT pairs converges the states x, y, θ , and β to zero. This is shown in Figures 6.12(b), (c) and (d).

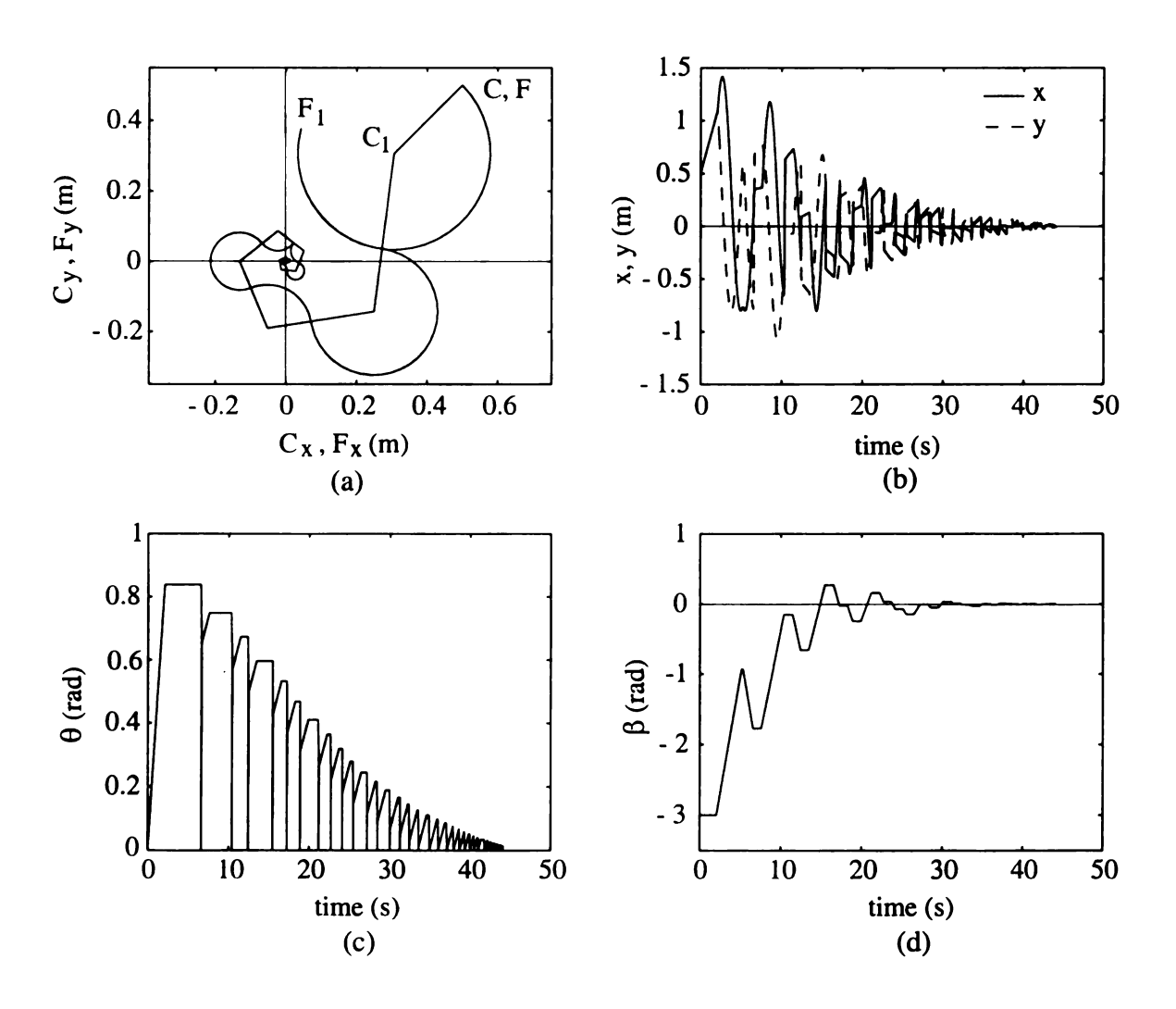


Figure 6.12. Complete reconfiguration from the special case of n=0

Finally we present a simulation where initial conditions lead to the special case of $n = \infty$. The initial configuration of the sphere is

$$x = 1.5$$
 $y = 0.0$ $\theta = 0.98$ $\alpha = 0.0$ $\beta = -3.0$ (6.16)

where the units are in meters and radians. The simulation results are given in Figure 6.13. With this initial configuration, the point C coincides with the origin as

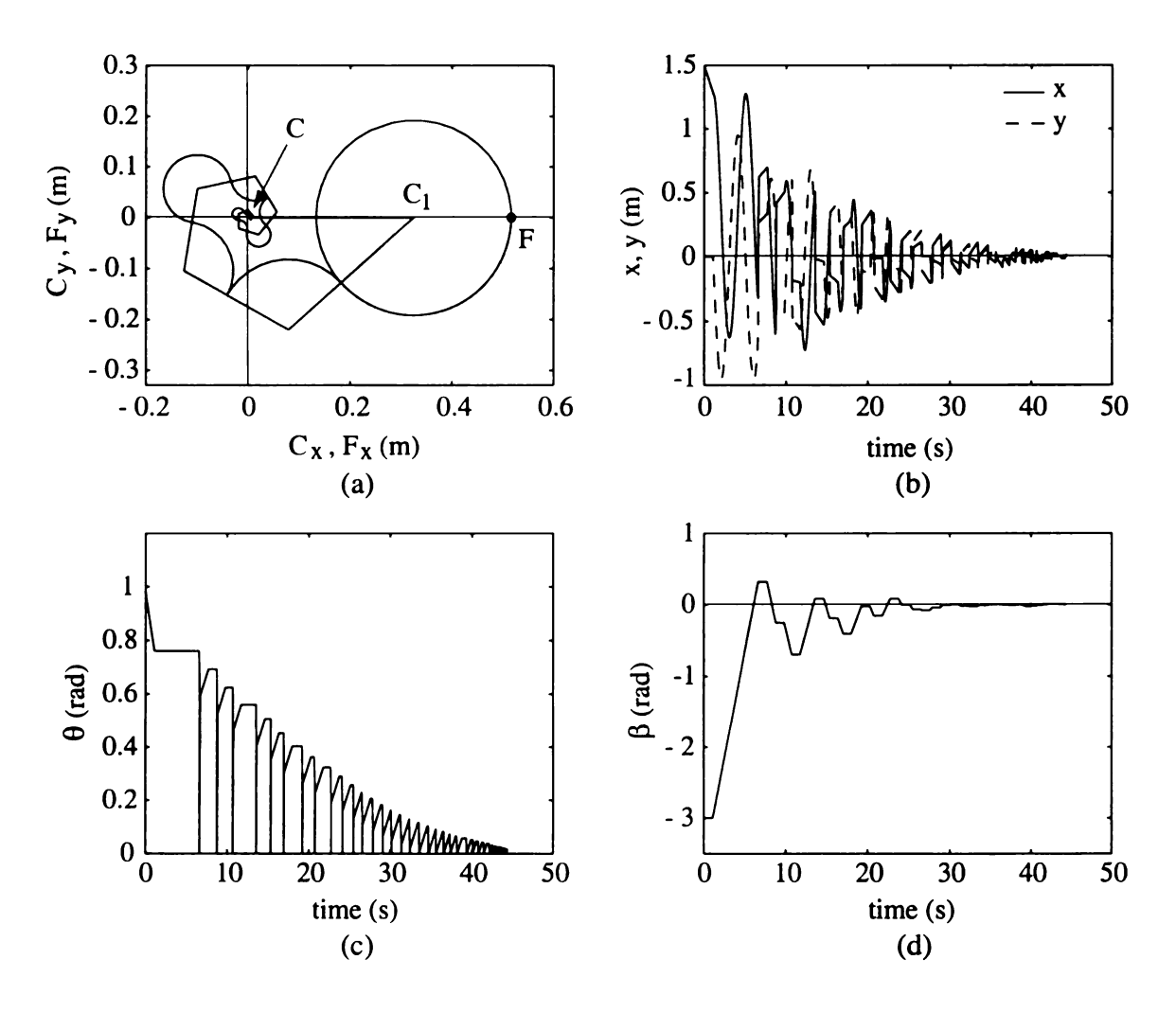


Figure 6.13. Complete reconfiguration from the special case of $n=\infty$

shown in Figure 6.13(a). The value of θ^* for $|\beta| = 3.0$ is 0.76 and hence initially $\theta > \theta^*$. Hence an initial TO maneuver is not necessary. Instead a control action (A) is applied that decreases θ to θ^* as shown in Figure 6.13(c). The point C moves to C_1 in Figure 6.13(a) and the value of n changes from infinity to 0.59. The angle ψ is chosen as 0.6 which lies within the range $\psi \in [max(\Psi, \bar{\psi}), \xi)$ for n = 0.59. With these values of n and ψ a PPS maneuver is first executed followed by a sequence of CRS-DPT pairs for complete reconfiguration of the sphere as shown in Figures 6.13(b), (c), and (d).

CHAPTER 7

Stability Analysis

7.1 Modified Governing Equations

In this chapter we shall prove that the equilibrium configuration given by Eq.(2.14) is stable under the complete reconfiguration algorithm developed in the previous chapters. The notion of stability adopted here is the following: The equilibrium configuration of the rolling sphere is considered stable if there exists a constant K such that

$$||X||_{2} \le K||X_{0}||_{2} \quad \forall \ t > 0$$
 (7.1)

where X is the state vector and in our case, from Eq.(2.14), we have

$$X = [x, y, \theta, \beta]^{T}$$
(7.2)

 X_0 is the arbitrary initial state vector, and $\parallel X \parallel_2$ represents the two-norm of X given as follows

$$\|X\|_{2} = \sqrt{x^{2} + y^{2} + \theta^{2} + \beta^{2}}$$
 (7.3)

The analysis of the stability of the equilibrium using the state vector given in Eq.(7.2) is complex and hence we propose a transformation to an equivalent system of equa-

tions. The modified governing equations, discussed below, greatly facilitate in proving stability of the equilibrium configuration.

From Eq.(2.14) we observe that both x and y are simultaneously driven to the origin under the repeated sequence of CRS-DPT maneuvers and the preliminary control actions discussed before. Hence effectively, the distance of the sphere center from the origin given by

$$r = \sqrt{(x^2 + y^2)}$$

is driven to zero. In the modified system we replace x and y by their polar coordinate counterparts r and σ , where

$$x = r\cos\sigma, \quad y = r\sin\sigma \tag{7.4}$$

However, instead of considering the states r and σ in place of x and y we consider the states $R (= r^2), \sigma$. This can be done without any loss of generality since $r \geq 0$. Moreover, in the new governing equation we consider the states $\Theta (= \theta^2), \alpha, \beta$ instead of θ, α, β . Again, this is done without any loss of generality since in our Euler angle representation of the sphere orientation, $0 \leq \theta \leq \pi$, as mentioned in section 2.1. This leads us to the following states for the modified system of equations

$$R, \sigma, \Theta, \alpha, \beta$$

We now show the derivation of the modified system equations from the original equations of motion given in Eqs. (2.9), (2.10), (2.11), (2.12), (2.13). Multiplying Eqs. (2.9) and (2.10) by x and y respectively and adding, we have:

$$\frac{1}{2}\frac{d}{dt}\left(x^2+y^2\right) = \frac{1}{2}\frac{d}{dt}(r^2) = (x\sin\alpha - y\cos\alpha)\omega_x^1 + (x\cos\alpha + y\sin\alpha)\omega_y^1 \qquad (7.5)$$

Hence using Eq.(7.4), Eq.(7.5) can be written as

$$\frac{d}{dt}(r^2) = 2r\left(\sin(\alpha - \sigma)\omega_x^1 + \cos(\alpha - \sigma)\omega_y^1\right) \tag{7.6}$$

To write the equation of motion in σ we have

$$x = r \cos \sigma \implies \dot{x} = \dot{r} \cos \alpha - r \sin \sigma \dot{\sigma}$$

which upon simplifying, results in

$$r\dot{\sigma} = -\cos(\alpha - \sigma)\omega_x^1 + \sin(\alpha - \sigma)\omega_y^1 \tag{7.7}$$

The modified governing equations are as follows:

$$\dot{R} = 2\sqrt{R} \left\{ \sin(\alpha - \sigma)\omega_x^1 + \cos(\alpha - \sigma)\omega_y^1 \right\}$$
 (7.8)

$$\dot{\sigma} = \frac{1}{\sqrt{R}} \left\{ -\cos(\alpha - \sigma)\omega_x^1 + \sin(\alpha - \sigma)\omega_y^1 \right\}$$
 (7.9)

$$\dot{\Theta} = 2\sqrt{\Theta}\omega_y^1 \tag{7.10}$$

$$\dot{\alpha} = -\omega_x^1 \cot \sqrt{\Theta} \tag{7.11}$$

$$\dot{\beta} = \omega_x^1 \tan \sqrt{\frac{\Theta}{2}} \tag{7.12}$$

From Eq.(2.14), the equilibrium configuration for the transformed system is

$$R = 0, \Theta = 0, \beta = 0 \tag{7.13}$$

and retaining the notion of stability in Eq.(7.1), the resulting state vector for stability analysis is

$$X = [R, \Theta, \beta]^T \tag{7.14}$$

7.2 Stability of Equilibrium under PPS followed by CRS-DPT sequence

We first prove stability of the equilibrium configuration in Eq.(7.13 under the Sweep-Tuck algorithm consisting of a PPS maneuver followed by CRS-DPT pairs. We assume that the parameters n and ψ are such that β_0 and θ_0 satisfy Eq.(6.2) and ψ satisfies $\psi \in [\Psi, \xi) \cap [\bar{\psi}, \xi)$. This is when the TO maneuver, if necessary, is already performed and $n \in (0, 1) \cup (1, \infty)$. Considering Figure 7.1, applying triangle inequality

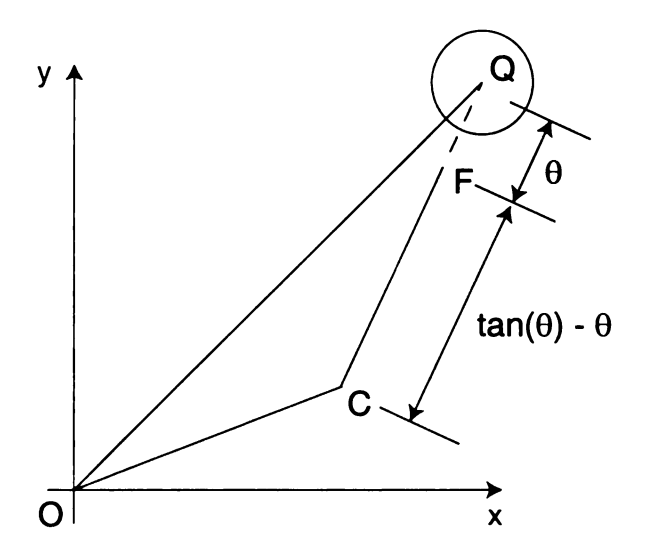


Figure 7.1. Typical configuration of sphere used to illustrate the triangle inequality for $\triangle OCQ$

we have

$$OQ \le OC + CQ \tag{7.15}$$

Let us consider a CRS-DPT pair in which the DPT maneuver causes the point C to move to C', as shown in Figure 7.2. Let us consider an intermediate point C_1

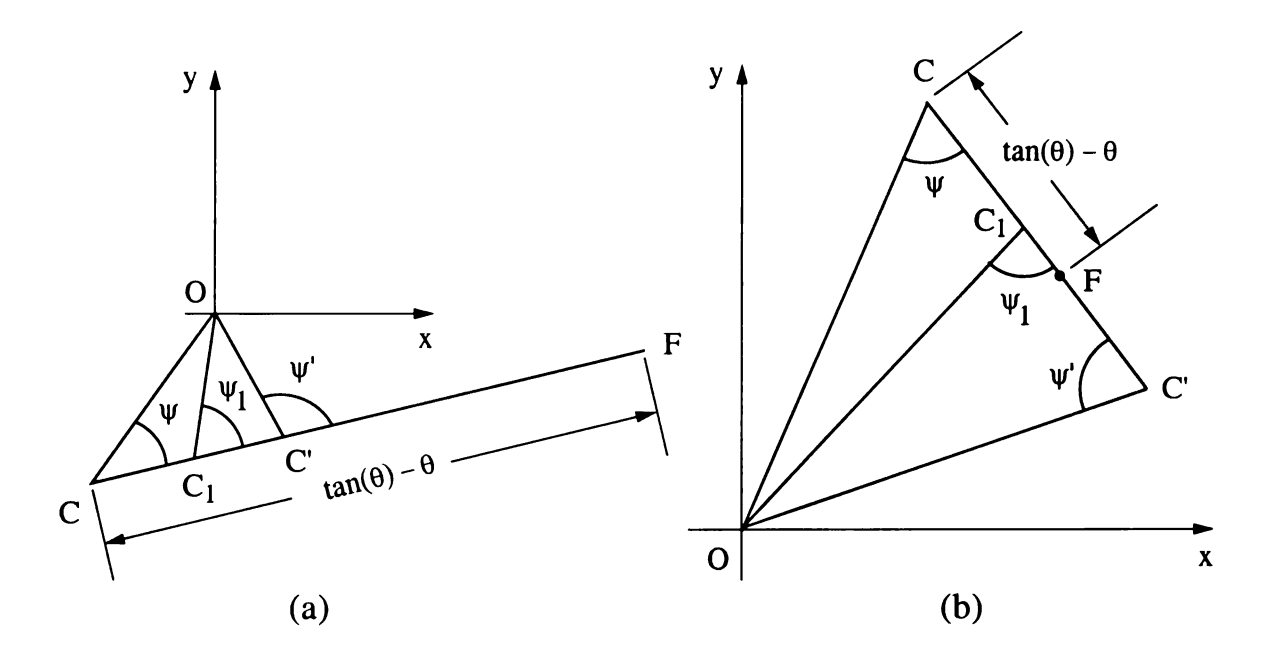


Figure 7.2. Variation of OC during a DPT maneuver

between C and C' during the DPT maneuver where $\angle OCC_1 = \psi_1$. In Theorem 3.1 we have established that $\psi' > \psi$. Hence we infer that

$$\psi \prime > \psi_1 > \psi \tag{7.16}$$

Also, from Eq.(3.17) we have

$$\sin \psi \prime > \sin \psi \tag{7.17}$$

since OC' < OC. From Eqs. (7.16) and (7.17 we conclude that that

$$\sin \psi_1 > \sin \psi \tag{7.18}$$

From Figure 7.2 we can write

$$OC_1\sin\psi_1 = OC\sin\psi$$

Hence we conclude from Eq.(7.18) that $OC_1 < OC$. Thus, during a DPT maneuver, OC continuously decreases. During a CRS or a PPS maneuver OC remains constant. Moreover, in a sequence of CRS-DPT maneuvers, the distance OC at the beginning of each CRS-DPT pair decreases in a geometric progression as established in section 3.2. Hence we infer that at any time during a PPS maneuver followed by a CRS-DPT sequence

$$OC < OC|_{t=0} \tag{7.19}$$

where t=0 represents the initiation of the PPS maneuver. Consider the distance CQ given by $CQ = \tan \theta$. At any arbitrary point C_1 between C and C', as shown in Figure 7.2,

$$C'F < CF \implies C_1F < CF$$

Therefore, upon denoting the angle θ at C and C_1 as θ and θ_1 respectively, we infer that at any arbitrary C_1 , $\theta_1 < \theta$. Hence,

$$\tan \theta_1 < \tan \theta \quad \Rightarrow \quad C_1 Q < CQ$$

Moreover, θ remains constant during a CRS or a PPS maneuver and hence we infer that during a PPS maneuver followed by a sequence of CRS-DPT pairs,

$$CQ < CQ|_{t=0} (7.20)$$

Hence, combining Eqs.(7.15), (7.19), and (7.20) we have,

$$OQ \le OC|_{t=0} + CQ|_{t=0} \tag{7.21}$$

From triangle inequality we also have

$$|OC|_{t=0} \le |OQ|_{t=0} + |CQ|_{t=0}$$
 (7.22)

Combining Eqs. (7.21) and (7.22) we have:

$$OQ \le OQ|_{t=0} + 2 CQ|_{t=0} \tag{7.23}$$

Now,

$$OQ = |x, y| \left(= \sqrt{x^2 + y^2} \right), \quad OQ|_{t=0} = |x_0, y_0|, \quad \text{and} \quad CQ|_{t=0} = \tan \theta_0$$

Hence from Eq.(7.23) we have

$$|x,y| \le |x_0, y_0| + 2\tan\theta_0 \tag{7.24}$$

As mentioned before, we invoke the reconfiguration algorithm only when $\theta \leq \left(\frac{\pi}{2} - \epsilon\right)$. Also, considering that θ never increases during a Sweep-Tuck algorithm, we write the following

$$2 \tan \theta_0 \le k_{max} \theta_0$$
 where $k_{max} = 2 \frac{\tan (\pi/2 - \epsilon)}{(\pi/2 - \epsilon)}$

Therefore,

$$|x, y| \le |x_0, y_0| + k_{max}\theta_0 \tag{7.25}$$

Also,

$$\theta \le \theta_0 \tag{7.26}$$

During a PPS maneuver or a sequence consisting of CRS-DPT pairs, change of β

occurs only during a PPS or a CRS maneuver. During a PPS maneuver we have,

$$|\beta| \le (3\pi - \psi)(\sec \theta_0 - 1) \quad \Rightarrow \quad |\beta| \le 3\pi(\sec \theta_0 - 1) \tag{7.27}$$

and considering the k-th CRS maneuver we can write

$$|\beta| \le (3\pi - \psi)(\sec \theta_k - 1) \quad \Rightarrow \quad |\beta| \le 3\pi(\sec \theta_k - 1) \tag{7.28}$$

Since $\theta_k < \theta_0$ we can combine Eqs.(7.27) and (7.28) to write

$$|\beta| \leq 3\pi(\sec\theta_0 - 1)$$

from which write the following

$$|\beta| \le c_{max}\theta_0^2 \tag{7.29}$$

where,

$$c_{max} = 3\pi \left. \frac{\sec \theta - 1}{\theta^2} \right|_{\theta = \pi/2 - \epsilon}$$
$$= 3\pi \left. \left(\frac{1}{2} + \frac{5}{24} \theta^2 + \dots \right) \right|_{\theta = \pi/2 - \epsilon}$$

From Eq.(7.25) we write

$$(x^{2} + y^{2}) \leq 2(x_{0}^{2} + y_{0}^{2}) + 2k_{max}^{2}\theta_{0}^{2}$$

$$\Rightarrow (x^{2} + y^{2})^{2} \leq 8(x_{0}^{2} + y_{0}^{2})^{2} + 8k_{max}^{4}\theta_{0}^{4}$$

$$\Rightarrow r^{4} \leq 8r_{0}^{4} + 8k_{max}^{4}\theta_{0}^{4}$$
(7.30)

Combining Eqs. (7.26), (7.29) and (7.30) we have

$$r^{4} + \theta^{4} + \beta^{2} \leq \left(8k_{max}^{4} + c_{max}^{2} + 9\right) \left[r_{0}^{4} + \theta_{0}^{4} + \beta^{2}\right]$$

$$\Rightarrow \left|r^{2}, \theta^{2}, \beta\right| \leq \sqrt{8k_{max}^{4} + c_{max}^{2} + 9} \left|r_{0}^{2}, \theta_{0}^{2}, \beta_{0}\right|$$

$$\Rightarrow \left|R, \Theta, \beta\right| \leq \sqrt{8k_{max}^{4} + c_{max}^{2} + 9} \left|R_{0}, \Theta_{0}, \beta_{0}\right|$$
(7.31)

We write the following for a PPS maneuver followed by a sequence of CRS-DPT pairs

$$|R, \Theta, \beta| \le K_{seq} |R_0, \Theta_0, \beta_0| \tag{7.32}$$

This proves the stability of the equlibrium under the Sweep-Tuck algorithm consisting of the PPS maneuver and a sequence of CRS-DPT pairs where the sphere motion is represented by the modified system of equations in Eqs. (7.8) through (7.12).

7.3 Stability of Equilibrium under TO Maneuver

Next we consider the stability of the equlibrium under the TO maneuver. The TO maneuver is a preliminary maneuver that is applied before the Sweep-Tuck sequence if $\theta_0 < \theta^*$. The maneuver increases θ from θ_0 to θ^* as shown in Figure 7.3. From triangle inequality,

$$|OQ'| \le |OQ| + |QQ'| \quad \Rightarrow \quad |x,y| \le |x_0,y_0| + \theta^* - \theta_0 \quad \Rightarrow \quad |x,y| \le |x_0,y_0| + \theta^*$$
(7.33)

Also, during a TO maneuver,

$$\theta \le \theta^*$$
 and $\beta = \beta_0$ (7.34)

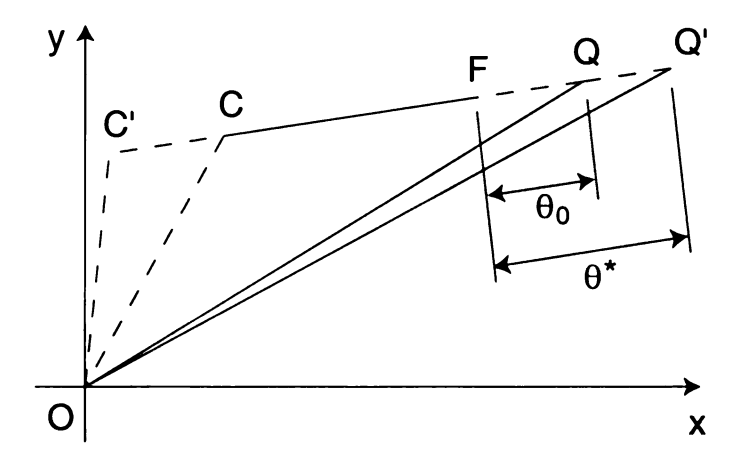


Figure 7.3. Triangle inequality on $\triangle OQQ'$: TO maneuver

Now, from Eq.(6.6)

$$|\beta_0| = 2.5\pi \left(\sec \theta^* - 1\right) \Rightarrow \frac{|\beta_0|}{2.5\pi} = \frac{1}{2}\theta^{*2} + \frac{5}{24}\theta^{*4} + \dots \Rightarrow \theta^{*2} \le \frac{4}{5\pi}|\beta_0|$$

Hence, from Eq.(7.34) we can write

$$\theta^2 \le \frac{4}{5\pi} |\beta_0| \tag{7.35}$$

From Eq.(7.33) we have

$$r^4 \le 8r_0^4 + 8\left(\frac{4}{5\pi}\right)^2 \beta_0^2 \tag{7.36}$$

Combining Eqs. (7.34), (7.35), and (7.36), we have the following

$$|r^2, \theta^2, \beta| \le 3\sqrt{1 + \left(\frac{4}{5\pi}\right)^2} |r_0^2, \theta_0^2, \beta_0| \Rightarrow |R, \Theta, \beta| \le 3\sqrt{1 + \left(\frac{4}{5\pi}\right)^2} |R_0, \Theta_0, \beta_0|$$

Thus the equilibrium configuration is stable under the application of a TO maneuver. We write the following for a TO maneuver

$$|R,\Theta,\beta| \le K_{TO} |R_0,\Theta_0,\beta_0| \tag{7.37}$$

7.4 Stability Analysis for the Special Cases

The special cases described in section 6.2 involve preliminary maneuvers that change the value of n. We now prove the stability of the system under the application of the initial maneuvers when $\theta_0 \geq \theta^*$ for the special cases.

7.4.1 Case: n = 1

When $\theta_0 \geq \theta^*$, we initially apply a control action (B) to align the points O, C and F as discussed in section 6.2.1. For this control action we can write Eq.(7.25) which can be simplified to Eq.(7.30). Also, during control action (B)

$$\theta = \theta_0 \tag{7.38}$$

Here we consider $\theta_0 \ge \theta^*$ and hence

$$|\beta_0| \leq 3\pi(\sec\theta_0 - 1)$$

as shown in section 7.2. We have shown in section 6.2.1 that this control action (B) maintains β within the same range, that is, for any β during the control action (B) we can write

$$|\beta| \le 3\pi(\sec\theta_0 - 1) \Rightarrow |\beta| \le c_{max}\theta_0^2 \tag{7.39}$$

from Eq.(7.29). Combining Eqs.(7.30), (7.38), and (7.39), we have the following

$$|R, \Theta, \beta| \le \sqrt{8k_{max}^4 + c_{max}^2 + 9} |R_0, \Theta_0, \beta_0|$$

Thus, the equilibrium is stable under the initial control action (B) when n = 1. Next a control action (A) is applied to change the value of n. As discussed in section 6.2.1, if $\theta_0 > \theta^*$ we decrease θ from θ_0 to θ^* . Applying triangle inequality we have

$$r \le r_0 + \theta_0 - \theta^* \Rightarrow r \le r_0 + \theta_0 \Rightarrow r^4 \le 8r_0^4 + 8\theta_0^4$$
 (7.40)

Also since θ decreases and β remains unchanged, we write

$$\theta \le \theta_0 \quad \text{and} \quad \beta = \beta_0 \tag{7.41}$$

Combining Eqs. (7.40) and (7.41) we can show that

$$|R,\Theta,\beta| \le 3 |R_0,\Theta_0,\beta_0| \tag{7.42}$$

Thus the equilibrium is stable under the preliminary control action (A).

Now we consider the case when $\theta_0 = \theta^*$. In this case the control action (A) increases θ from θ^* to $k_1\theta^*$ as mentioned in section 6.2.1. Applying triangle inequality we have

$$r \le r_0 + k_1 \theta^* - \theta^* \Rightarrow r \le r_0 + (k_1 - 1)\theta_0 \Rightarrow r^4 \le 8r_0^4 + 8(k_1 - 1)^4 \theta_0^4$$
 (7.43)

Also since θ reaches a maximum of $k_1\theta_0$ and β remains unchanged, we have

$$\theta \le k_1 \theta_0 \quad \text{and} \quad \beta = \beta_0 \tag{7.44}$$

Combining Eqs. (7.43) and (7.44) we have

$$|R, \Theta, \beta| \le \sqrt{8(k_1 - 1)^4 + k_1^4 + 9} |R_0, \Theta_0, \beta_0|$$
 (7.45)

Thus, the equilibrium is stable under the preliminary control actions required for the special case of n = 1. We observe that there can be two pairs of preliminary control actions:

(1) Sweep followed by a decrease in θ (if $\theta > \theta^*$): For this pair, we can write

$$|R, \Theta, \beta| \le 3\sqrt{8k_{max}^4 + c_{max}^2 + 9} |R_0, \Theta_0, \beta_0|$$
 (7.46)

which is written as

$$|R,\Theta,\beta| < K_{dec1} |R_0,\Theta_0,\beta_0| \tag{7.47}$$

(2) Sweep followed by an increase in θ (if $\theta = \theta^*$): For this pair, we can write

$$|R,\Theta,\beta| \le \sqrt{8(k_1-1)^4 + k_1^4 + 9} \sqrt{8k_{max}^4 + c_{max}^2 + 9} |R_0,\Theta_0,\beta_0|$$
 (7.48)

which we write as

$$|R,\Theta,\beta| \le K_{inc1} |R_0,\Theta_0,\beta_0| \tag{7.49}$$

7.4.2 Case: $n = \infty$

This special case involves a single control action (A) that either decreases θ from θ_0 to θ^* if $\theta_0 > \theta^*$ or increases θ from θ^* to $k_1\theta^*$ if $\theta_0 = \theta^*$. The proof stability of the equilibrium under these control actions are similar to those for the n = 1 case and hence are not repeated here.

During the control action (A) that decreases θ , we obtain Eq.(7.42). Denoting

 $K_{dec\infty} = 3$, we have

$$|R, \Theta, \beta| \le K_{dec\infty} |R_0, \Theta_0, \beta_0| \tag{7.50}$$

Similarly during the control action (A) that increases θ , we obtain Eq.(7.45). Denoting $K_{inc\infty} = \sqrt{8(k_1 - 1)^4 + k_1^4 + 9}$, we have

$$|R, \Theta, \beta| \le K_{inc\infty} |R_0, \Theta_0, \beta_0| \tag{7.51}$$

7.4.3 Case: n = 0

In this case $|x_0, y_0| \neq 0$ and $\theta_0 = 0$. When $\beta_0 \neq 0$, a preliminary TO maneuver is applied and the stability of the equilibrium under this maneuver has already proved in section 7.3. Here we consider the case when $\beta_0 = 0$. The change in θ due to the initial control action (A) is based on the value of r_0 as explained in section 6.2.3. We have the following relations

$$\theta \le k_0 r_0$$
 and $\beta = \beta_0$ (7.52)

where k_0 is defined in section 6.2.3. Also, from triangle inequality we have

$$r \le r_0 + k_0 r_0 - \theta_0 \Rightarrow r \le (k_0 + 1) r_0 \quad \text{(since } \theta_0 = 0\text{)}$$
 (7.53)

Combining Eqs. (7.52) and (7.53) we can write the following

$$|R, \Theta, \beta| \le \sqrt{(k_0 + 1)^2 + k_0^2} |R_0, \Theta_0, \beta_0|$$
 (7.54)

This proves the stability of the equilibrium under the preliminary control action (A) in case of n = 0. Denoting $K_0 = \sqrt{(k_0 + 1)^2 + k_0^2}$ we have from Eq.(7.54)

$$|R,\Theta,\beta| \le K_0 |R_0,\Theta_0,\beta_0| \tag{7.55}$$

7.4.4 Case: n = undefined

The initial control action (A) for this case is a TO maneuver that takes θ from zero to θ^* . The stability of equilibrium under this TO maneuver is discussed in section 7.3 and is not repeated here. This TO maneuver leads to an n=1 case which has been discussed above.

7.4.5 Case: $\theta_0 > (\frac{\pi}{2} - \epsilon)$

In this case we apply a control action (A) to decrease θ from θ_0 to $\theta_f \leq (\pi/2 - \epsilon)$. From triangle inequality we have

$$r \le r_0 + (\theta_0 - \theta_f) \Rightarrow r \le r_0 + \theta_0 \tag{7.56}$$

Also, since θ decreases and β remains constant during the control action (A), we have

$$\theta \le \theta_0 \quad \text{and} \quad \beta = \beta_0 \tag{7.57}$$

Hence, from Eqs.(7.56) and (7.57) we can write

$$|R, \Theta, \beta| \le 3 |R_0, \Theta_0, \beta_0| \quad \Rightarrow \quad |R, \Theta, \beta| \le K_\theta |R_0, \Theta_0, \beta_0| \tag{7.58}$$

This proves the stability of the equilibrium under the initial control action (A) applied when $\theta_0 > (\pi/2 - \epsilon)$.

7.5 Stability of Equilibrium under Complete Reconfiguration Algorithm

In Figure 6.9 we have shown all possible state transitions of the sphere to the equilibrium from arbitrary initial conditions, where the states S_1 through S_8 are explained in section 6.3. In the sections above we have established stability of the equilibrium for each of the elementary transitions. This was done by deriving the expressions of the constant K, given in Eq.(7.1), for each transition. In this section, we first associate each transition with their corresponding values of K. This is shown with the help of Figure 7.4. In the process of complete reconfiguration the sphere undergoes a series of transitions to different configuration sets before it ends at the equilibrium configuration. Consider the case in Figure 6.9 when the sphere initially belongs to the configuration set S_3 and transitions through S_6 , S_4 and finally reaches the equilibrium configuration S_1 . For this series of transitions we have from Figure 7.4

$$|R, \Theta, \beta| \leq K_{TO} K_{incl} K_{seg} |R_0, \Theta_0, \beta_0|$$

We denote

$$K_{32} = K_{TO} K_{inc1} K_{seq}$$

since the starting configuration is S_3 and it is the second series of transitions for S_3 . Proceeding similarly, we determine the constants K's for all series in Figure 7.4 as follows

$$S_1: K_{11} = 1$$
 $S_2: K_{21} = K_{\theta} K_{seq}$ $S_3: \begin{cases} K_{31} = K_{TO} K_{seq} \\ K_{32} = K_{TO} K_{inc1} K_{seq} \\ K_{33} = K_{TO} K_{inc\infty} K_{seq} \end{cases}$ $S_4: K_{41} = K_{seq}$

$$S_{5}: \begin{cases} K_{51} = K_{TO} K_{seq} \\ K_{52} = K_{0} K_{seq} \end{cases} \qquad S_{6}: \begin{cases} K_{61} = K_{dec1} K_{seq} \\ K_{62} = K_{TO} K_{seq} \\ K_{63} = K_{inc1} K_{seq} \\ K_{64} = K_{TO} K_{inc\infty} K_{seq} \\ K_{65} = K_{dec1} K_{0} K_{seq} \end{cases}$$

$$S_{7}: \begin{cases} K_{71} = K_{TO} K_{seq} \\ K_{72} = K_{inc\infty} K_{seq} \\ K_{73} = K_{dec\infty} K_{seq} \end{cases} \qquad S_{8}: K_{81} = K_{TO} K_{seq}$$

$$K_{74} = K_{dec\infty} K_{inc1} K_{seq} \\ K_{75} = K_{dec\infty} K_{0} K_{seq} \end{cases}$$

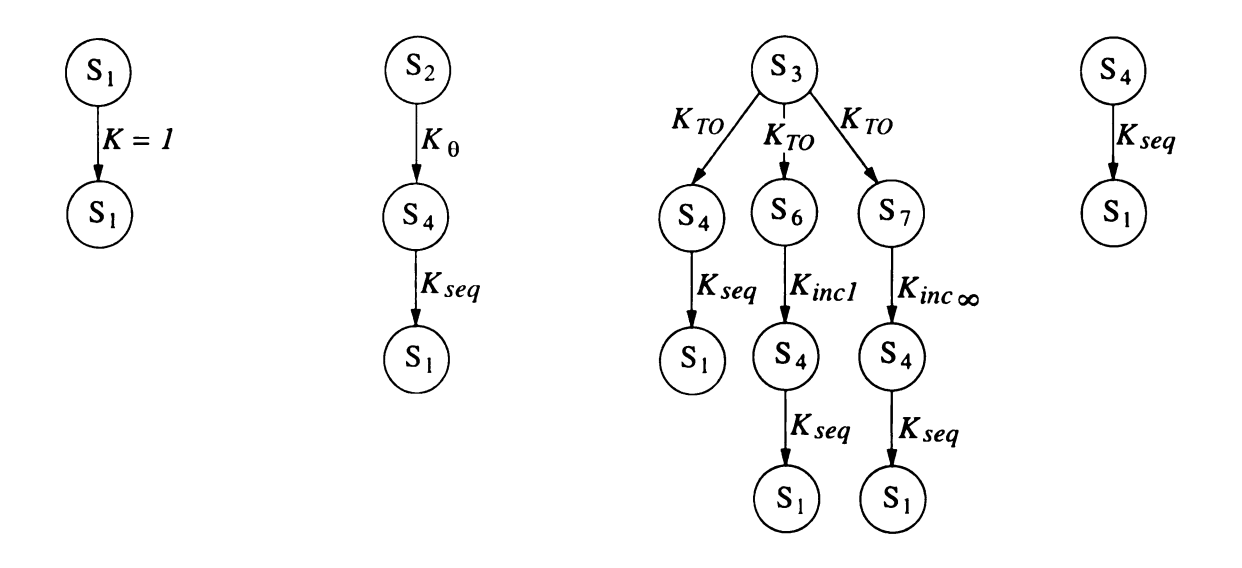
Let us denote

$$K_{max} = \frac{max\{K_{11}, K_{21}, K_{31}, K_{32}, K_{33}, K_{41}, K_{51}, K_{52}, K_{61}, K_{62}, K_{63}, K_{64}, K_{65}, K_{71}, K_{72}, K_{73}, K_{74}, K_{75}, K_{81}\}}$$

Thus, for the complete algorithm we have

$$|R, \Theta, \beta| \le K_{max}|R_0, \Theta_0, \beta_0| \tag{7.59}$$

This implies that for any arbitrary initial condition of the sphere the equilibrium configuration is stable under the complete reconfiguration algorithm by satisfying the Eq. (7.59).



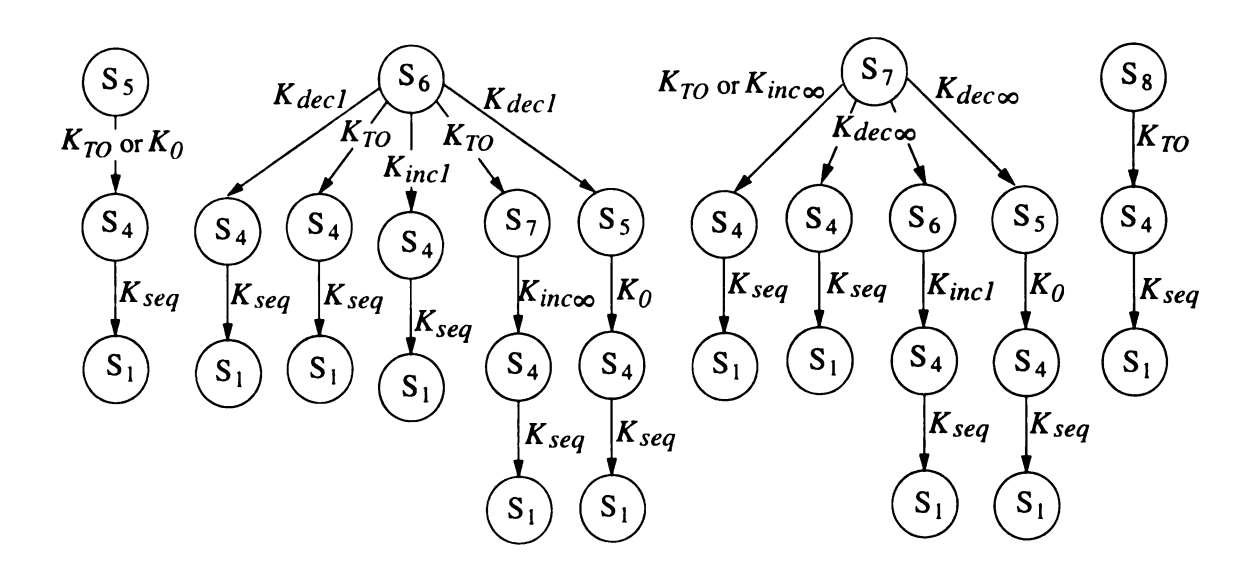


Figure 7.4. The constant K's associated with each transition

CHAPTER 8

Conclusion

Research on the feedback stabilization of nonholonomic systems has gained popularity over the recent years. Although, nonholonomic systems cannot be stabilized by smooth static state feedback, alternative control strategies have been implemented for systems that can be reduced to the chained form. These control strategies fail for nonholonomic systems that cannot be reduced to the chained form. The rolling sphere belongs to this category of nonholonomic systems. The problem has been addressed by few researchers without much success. A feedback law for stabilizing the sphere to an equilibrium has remained elusive from literature.

In this dissertation we address the problem of reconfiguring a rolling sphere to an equilibrium configuration from arbitrary initial conditions using state feedback. The kinematic model of the sphere consists of two Cartesian coordinates and three Euler angles representing the position and orientation of the sphere respectively. Within this choice of coordinates we define two control inputs that are mutually perpendicular angular speeds. The control inputs are defined in the moving coordinate frame of the sphere. The control inputs individually lead to two control actions that cause the sphere to move in linear or circular segments. These control actions form the basis of our proposed feedback control strategy. The feedback law essentially applies these control actions alternately in a sequence for stabilization to the equilibrium.

We identify two points C and F based on the geometry of motion under these control actions. The points C and F defines the configuration of the sphere partially. The individual control actions either cause C to move rectilinearly or F to move in a circular arc about the center C.

We first address the problem of partial reconfiguration of the sphere. In partial reconfiguration, convergence of one of the orientation coordinates is ignored. Partial reconfiguration is shown to be equivalent to converging the points C and F simultaneously to the origin. Based on the geometry of the motion of the sphere under the two control actions, we define the DPT and RS maneuvers. Repeated application of an RS-DPT pair leads to partial reconfiguration and this forms the Sweep-Tuck algorithm. The ratio n = CF/CO, is an important element in the development of the Sweep-Tuck algorithm. Our analysis categorizes the $n \in (0,1)$ and $n \in (1,\infty)$ cases in the general category. Cases such as n = 0, n = 1, $n = \infty$ are treated separately. The special cases require certain preliminary control actions that transform them into the general category of $n \in (0,1)$ and $n \in (1,\infty)$.

Complete reconfiguration also requires convergence of β to the origin and we wish to utilize the Sweep-Tuck algorithm to attain this additional objective. The Sweep-Tuck algorithm allows multiple trajectories of the sphere between its initial and final configurations. This is due to the flexibility of executing the RS maneuver in each RS-DPT pair. The RS maneuver provides quadruple options each of which leads to a different change in the value of β . We propose a method of choosing among the four RS options such that the selected RS maneuver leads to the minimum magnitude of β . We call this the CRS maneuver. Thus the complete reconfiguration algorithm consists of a series of CRS-DPT pairs. We deduce two conditions that must be satisfied for complete reconfiguration, of which one is a range condition that must be satisfied by the initial value of β and the other is an inequality condition that must be satisfied at each CRS-DPT pair. We further show that the inequality condition is not restrictive

and can be satisfied for any value of $n \in (0,1) \cup (1,\infty)$.

If the range condition on β is not satisfied initially, we propose to perform the TO maneuver, at the end of which the range condition is satisfied. Subsequently the sphere can be completely reconfigured using CRS-DPT pairs. The TO maneuver and certain other preliminary maneuvers are required to transform the special cases to the general category. These preliminary control actions maintain the stability of the equilibrium. The reconfiguration algorithm, consisting of the preliminary maneuvers and the main sequence of CRS-DPT pairs, is shown to stabilize the equilibrium under the proposed feedback law.

APPENDIX

APPENDIX A

Proof of Inequality 3.21

First consider the case $n \in (1, \infty)$. Using Eq.(3.19) and the trigonometric identity $\tan(A+B) = [\tan(A) + \tan(B)]/[1 - \tan(A) \tan(B)]$, we obtain

$$\tan(\psi + \psi') = \frac{\sin(2\psi) - 2n\sin\psi}{n^2 + \cos(2\psi) - 2n\cos\psi} \tag{A.1}$$

Taking derivative with respect to ψ , we get

$$\frac{d}{d\psi}(\psi + \psi') = \frac{2\left[1 + 2n^2 - n(3 + n^2)\cos\psi + n^2\cos(2\psi)\right]}{\left[n^2 + \cos(2\psi) - 2n\cos\psi\right]^2}\cos^2(\psi + \psi') \tag{A.2}$$

We show that the right hand side of the above equation is negative as follows

$$1 + 2n^{2} + n^{2} \cos(2\psi) < n(3 + n^{2}) \cos\psi \iff 2(n^{2} \cos^{2} \psi - 1) < (3 + n^{2})(n \cos \psi - 1)$$

$$\iff 2(n \cos \psi + 1) < (3 + n^{2})$$

$$\iff 2n \cos \psi < 1 + n^{2}$$

$$\iff (1 - n)^{2} > 0 \tag{A.3}$$

In the above derivation we used the inequality $(n\cos\psi - 1) \neq 0$ from Eq.(3.5). For $n \in (0,1)$ we have

$$\tan(\psi + \psi') = \frac{n^2 \sin(2\psi) - 2n \sin\psi}{n^2 \cos(2\psi) - 2n \cos\psi + 1} \tag{A.4}$$

and the following expression for the derivative

$$\frac{d}{d\psi}(\psi + \psi') = \frac{2n\left[-(1+3n^2)\cos\psi + n\left(\cos(2\psi) + 2 + n^2\right)\right]}{\left[n^2\cos(2\psi) - 2n\cos\psi + 1\right]^2}\cos^2(\psi + \psi') \tag{A.5}$$

Using the inequality $(\cos \psi - n) \neq 0$ from Eq.(3.5), the right hand side of the above equation is shown to be negative as follows

$$n\left(\cos\left(2\psi\right) + 2 + n^2\right) < (1 + 3n^2)\cos\psi \iff 2n\left(\cos^2\psi - n^2\right) < (1 + 3n^2)(\cos\psi - n)$$

$$\iff 2n\left(\cos\psi + n\right) < (1 + 3n^2)$$

$$\iff 2n\cos\psi < 1 + n^2$$

$$\iff (1 - n)^2 > 0 \tag{A.6}$$

Clearly, the function $(\psi + \psi')$ is a monotonically decreasing function of ψ for $n \in (1,\infty) \cup (0,1)$. Furthermore, from Eq.(3.19) we can show that $\psi' = \pi$ when $\psi = 0$ and hence the function $(\psi + \psi')$ has a maximum value of π at $\psi = 0$. This proves the inequality in Eq.(3.21).

BIBLIOGRAPHY

BIBLIOGRAPHY

- [1] M. Aicardi, G. Casalino, A. Balestrino, and A. Bicchi. Closed-loop smooth steering of unicycle-like vehicles. *Proc. 33rd IEEE International Conference on Decision and Control*, pages 2455–2458, 1994.
- [2] A. Astolfi. On the stabilization of nonholonomic systems. *Proc. 33rd IEEE International Conference on Decision and Control*, pages 3481–3486, 1994.
- [3] S. Bhattacharya and S. K. Agrawal. Spherical rolling robot: A design and motion planning studies. *IEEE transactions on Robotics and Automation*, 16(6):835–839, 2000.
- [4] A. Bicchi, A. Balluchi, D. Prattichizzo, and A. Gorelli. Introducing the sphericle: An experimental testbed for research and teaching in nonholonomy. *Proceedings of the IEEE International Conference on Robotics and Automation*, pages 2620–2625, 1997.
- [5] A. Bicchi, D. Prattichizzo, and S. S. Sastry. Planning motions of rolling surfaces. Proc. 34th IEEE International Conference on Decision and Control, pages 2812–2817, 1995.
- [6] A. M. Bloch and S. Drakunov. Stabilization of a nonholonomic system via sliding modes. Proc. 33rd IEEE International Conference on Decision and Control, pages 2961-2963, 1994.
- [7] A. M. Bloch, N. H. McClamroch, and M. Reyhanoglu. Controllability and stabilizability properties of a nonholonomic control system. *Proc. 29th IEEE International Conference on Decision and Control*, pages 1312–1314, 1990.
- [8] A. M. Bloch, M. Reyhanoglu, and N. H. McClamroch. Control and stabilization of nonholonomic dynamical systems. *IEEE Transactions on Automatic Control*, 37(11):1746-1757, 1992.
- [9] R. W. Brockett. *Differential Geometric Control Theory*, chapter Asymptotic Stability and Feedback Stabilization, pages 181–191. Brikhauser, 1982.
- [10] H. B. Brown and Y. Xu. A single-wheeled gyroscopically stabilized robot. *IEEE Robotics and Automation Magazine*, 4(3):39-44, 1997.

- [11] L. Bushnell, D. Tilbury, and S. S. Sastry. Steering three-input chained-form nonholonomic systems using sinusoids: The fire-truck example. *Proc. European Control Conference*, pages 1432–1437, 1993.
- [12] C. Camicia, F. Conticelli, and A. Bicchi. Nonholonomic kinematics and dynamics of the sphericle. *Proceedings of the IEEE/RSJ International Conference on Intelligent Robots and Systems*, 1:805–810, 2000.
- [13] C. Canudas de Wit and O. J. Sordalen. Exponential stabilization of mobile robots with nonholonomic constraints. *IEEE Transactions on Automatic Control*, 37(11):1791-1797, 1992.
- [14] T. Das. Dynamics of self-propulsion with rolling constraints. Master's thesis, Michigan State University, 2000.
- [15] T. Das and R. Mukherjee. Dynamic analysis of rectilinear motion of a self-propelling disk with unbalance masses. ASME Journal of Applied Mechanics, pages 58-66, 2000.
- [16] H. Date, M. Sampei, D. Yamada, M. Ishikawa, and M. Koga. Manipulation problem of a ball between two parallel plates based on time-state control form. Proc. 38th IEEE International Conference on Decision and Control, pages 2120– 2125, 1999.
- [17] M. Fleiss, J. Levine, P. Martin, and P. Rouchon. Flatness and defect of nonlinear systems: Introductory theory and examples. *International Journal of Control*, 61(6):1327-1361, 1995.
- [18] D. T. Greenwood. *Principles of Dynamics*. Prentice Hall, Englewood Cliffs, NJ, 2 edition, 1988.
- [19] J. Guldner and V. I. Utkin. Stabilization of nonholonomic mobile robots using lyapunov functions for navigation and sliding mode control. *Proc. 33rd IEEE International Conference on Decision and Control*, pages 2967–2972, 1994.
- [20] L. Gurvits and Z. X. Li. *Progress in Nonholonomic Motion Planning*, chapter Smooth Time-Periodic Feedback Solutions for Nonholonomic Motion Planning, pages 53–108. Kluwer Academic Press, 1992.
- [21] A. Halme, T. Schonberg, and Y. Wang. Motion control of a spherical mobile robot. *Proceedings of AMC'96-MIE*, 1996.

- [22] D. Hristu-Varsekelis. The dynamics of a forced sphere-plate mechanical system. *IEEE Transactions on Automatic Control*, 46(5):678-686, 2001.
- [23] J. Jurdjevic. The geometry of the plate-ball problem. Archives for Rational Mechanics and Analysis, 124:305-328, 1993.
- [24] I. Kolmanovsky and N. H. McClamroch. Developments in nonholonomic control problems. *IEEE Control Systems Magazine*, 15(6):20-36, 1995.
- [25] A. Koshiyama and K. Yamafuji. Design and control of all-direction steering type mobile robot. *International Journal of Robotics Research*, 12(5):411–419, 1993.
- [26] M. Levi. Geometric phases in the motion of rigid bodies. Archive for Rational Mechanics and Analysis, 122(3):213–229, 1993.
- [27] Z. Li and J. Canny. Motion of two rigid bodies with rolling constraint. *IEEE Transactions on Robotics and Automation*, 6(1):62-72, 1990.
- [28] A. Marigo and A. Bicchi. Rolling bodies with regular surface: Controllability theory and applications. *IEEE Transactions on Automatic Control*, 45(9):1586–1599, 2000.
- [29] R. Mukherjee and M. Kamon. Almost-smooth time-invariant control of planar space multibody systems. *IEEE Transactions on Robotics and Automation*, 15(2):264-276, 1999.
- [30] R. Mukherjee, M. A. Minor, and J. T. Pukrushpan. Motion planning for a spherical mobile robot: Revisiting the classical ball-plate problem. ASME Journal of Dynamic Systems, Measurement, and Control (to appear), 2002.
- [31] R. Mukherjee and J. T. Pukrushpan. Class of rotations induced by spherical polygons. AIAA Journal of Guidance, Control and Dynamics, 23(4):746-749, 2000.
- [32] R. M. Murray. Nilpotent bases for a class of nonintegrable distributions with applications to trajectory generation for nonholonomic systems. *Mathematics of Control, Signals, and Systems*, 7(1):58-75, 1995.
- [33] R. M. Murray and S. S. Sastry. Nonholonomic motion planning: Steering using sinusoids. *IEEE Transactions on Automatic Control*, 38(5):700-713, 1993.
- [34] G. Oriolo and M. Vendittelli. Robust stabilization of the plate-ball manipulation system. *Proc. IEEE Conference on Robotics and Automation*, 1:91–96, 2001.

- [35] J. B. Pomet. Explicit design of time-varying stabilizing control laws for a class of controllable systems without drift. *Systems and Control Letters*, 18:147–158, 1992.
- [36] P. Rouchon, M. Fleiss, J. Levine, and P. Martin. Flatness, motion planning, and trailer systems. *Proc. 32nd IEEE International Conference on Decision and Control*, pages 2700–2705, 1993.
- [37] M. Sampei, K. Hiromitsu, and M. Ishikawa. Control strategies of mechanical systems with various constraints control of non-holonomic systems. *Proc. IEEE Conference on System, Man and Cybernetics*, 3:III-158 III-165, 1999.
- [38] C. Samson. Time-varying feedback stabilization of a car-like wheeled mobile robot. *International Journal of Robotics Research*, 12(1):55–66, 1993.
- [39] N. Sarkar, X. Yun, and V. Kumar. Control of contact interactions with acatastatic nonholonomic constraints. *International Journal of Robotics Research*, 16(3):357-374, 1997.
- [40] O. J. Sordalen, O. Egeland, and C. Canudas de Wit. Attitude stabilization with a nonholonomic constraint. Proc. 31st IEEE International Conference on Decision and Control, pages 1610–1611, 1992.
- [41] O. J. Sordalen and K. Y. Wichlund. Exponential stabilization of a car with n trailers. Proc. 32nd IEEE International Conference on Decision and Control, pages 978-983, 1993.
- [42] H. J. Sussmann. Subanalytic sets and feedback control. *Journal of Differential Equations*, 31:31–52, 1979.
- [43] D. Tilbury, R. M. Murray, and S. S. Sastry. Trajectory generation for the n-tralier problem using goursat normal form. *Proc. 32nd IEEE International Conference on Decision and Control*, pages 971–977, 1993.
- [44] G. Walsh and L. Bushnell. Stabilization of multiple input chained form control systems. Systems and Control Letters, 25:227-234, 1995.

